

INFORMATION TO USERS

This manuscript has been reproduced from the microfilm master. UMI films the text directly from the original or copy submitted. Thus, some thesis and dissertation copies are in typewriter face, while others may be from any type of computer printer.

The quality of this reproduction is dependent upon the quality of the copy submitted. Broken or indistinct print, colored or poor quality illustrations and photographs, print bleedthrough, substandard margins, and improper alignment can adversely affect reproduction.

In the unlikely event that the author did not send UMI a complete manuscript and there are missing pages, these will be noted. Also, if unauthorized copyright material had to be removed, a note will indicate the deletion.

Oversize materials (e.g., maps, drawings, charts) are reproduced by sectioning the original, beginning at the upper left-hand corner and continuing from left to right in equal sections with small overlaps.

Photographs included in the original manuscript have been reproduced xerographically in this copy. Higher quality 6" x 9" black and white photographic prints are available for any photographs or illustrations appearing in this copy for an additional charge. Contact UMI directly to order.

ProQuest Information and Learning
300 North Zeeb Road, Ann Arbor, MI 48106-1346 USA
800-521-0600

UMI[®]

NOTE TO USERS

This reproduction is the best copy available.

UMI[®]

UNIVERSITY OF OKLAHOMA
GRADUATE COLLEGE

OPTIMAL DESIGN OF CRUDE OIL DISTILLATION PLANTS

A DISSERTATION
SUBMITTED TO THE GRADUATE FACULTY
In partial fulfillment of the requirements for the
degree of
DOCTOR OF PHILOSOPHY

By

SHUNCHENG JI

Norman, Oklahoma

2001

UMI Number: 3029622

UMI[®]

UMI Microform 3029622

Copyright 2002 by Bell & Howell Information and Learning Company.

All rights reserved. This microform edition is protected against
unauthorized copying under Title 17, United States Code.

Bell & Howell Information and Learning Company
300 North Zeeb Road
P.O. Box 1346
Ann Arbor, MI 48106-1346

OPTIMAL DESIGN OF CRUDE OIL DISTILLATION PLANTS

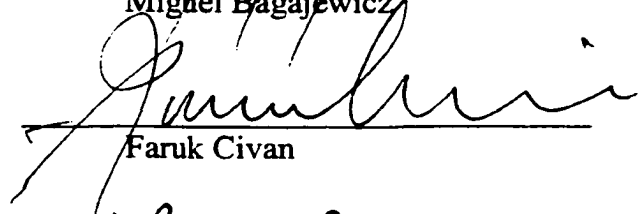
A DISSERTATION

**APPROVED FOR THE
SCHOOL OF CHEMICAL ENGINEERING AND MATERIALS SCIENCE**

By:



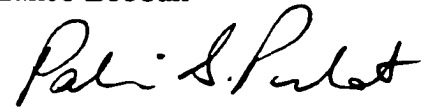
Miguel Bagajewicz



Faruk Civan



Lance Lobban



Pakize Pulat



Daniel Resasco

**c Copyright by Shuncheng Ji 2001
All Rights Reserved.**

ACKNOWLEDGEMENTS

I would like to thank all of the Chemical Engineering Faculty and Staff at the University of Oklahoma for their support and friendship, especially Dr. Richard Mallinson, who provided me partial support for one and a half years, and Mr. Rick Wheeler who helped me consistently with computer trouble shootings. I appreciate my classmates, Fernando Cancino and Jose Soto for helpful discussions.

I would like to thank Dr. Faruk Civan, Dr. Lance Lobban, Dr. Pakize Pulat and Dr. Daniel Resasco for their participation on my dissertation committee. I will be very grateful to Dr. Bagajewicz for his guidance and patience through the entire dissertation work.

Finally, I would like to thank my wife, Shufang; and my daughter, Mengmeng (Mary) for their support, encouragement and love.

TABLE OF CONTENTS

Chapter 1

Introduction.....	1
1.1 Description of the problem.....	6
1.2 Crude oil properties.....	7
1.2.1 Boiling range.....	8
1.2.2 Gravity, API.....	11
1.2.3 Salt Content.....	11
1.3 Crude distillation products.....	11
1.4 State of the art in the design.....	14
1.5 Topics in this dissertation.....	17
1.6 References.....	18

Chapter 2 Rigorous Targeting Procedure for the Design of Conventional Atmospheric

Crude Fractionation Units.....	20
2.1 Overview.....	20
2.2 Introduction.....	20
2.3 Heat demand-supply diagram.....	26
2.4 Pump-around circuits and heat recovery.....	30
2.5 Design procedure.....	33
2.6 Illustration.....	35
2.7 Effect of minimum temperature approach.....	53
2.8 Flexibility.....	55
2.9 Reboiler.....	55

2.10 Applicability to other crudes.....	57
2.11 Conclusion.....	58
2.12 Nomenclature.....	58
2.13 References.....	60
Chapter 3 Rigorous Targeting Procedure for the Design of Crude Fractionation with Pre-flashing.....	63
3.1 Overview.....	63
3.2 Introduction.....	63
3.3 Effect of pre-flashing on products.....	67
3.4 Carrier effects.....	71
3.5 Steam Stripping: Effect of the temperature.....	80
3.6 Steam Injection.....	83
Energy requirements for stripping agents.....	84
3.8 Effect of pressure.....	85
3.9 Comparison for lower AGO yield.....	87
3.10 Effect of pre-flash temperature	90
3.11 Feed location of pre-flash drum Vapors.....	91
3.12 Conclusion.....	95
3.13 Nomenclature.....	96
3.14 References.....	97
Chapter 4 On the Energy Efficiency of Stripping-Type Crude Distillation.....	99
4.1 Overview.....	99
4.2 Introduction.....	99

4.3 Crude vaporization patterns and heat demand.....	103
4.4 Features of Stripping type design.....	108
4.5 Energy Targeting.....	109
4.6 Comparison with the conventional design.....	115
4.7 Conclusions.....	121
4.8 References.....	114
4.9 Appendix.....	122
Chapter 5 Design of Crude Distillation Plants with Vacuum Units. I. Targeting.....	126
5.1 Overview.....	126
5.2 Introduction.....	126
5.3 Alternatives for atmospheric-vacuum distillation.....	130
5.4 Vacuum oil distillation.....	134
5.5 Vacuum tower specifications.....	140
5.6 Targeting procedures.....	141
5.7 Results for the light crude.....	144
5.8 Heavy crude.....	153
5.9 Conclusion.....	154
5.10 References.....	157
5.11 Appendix.....	158
Chapter 6 Design of Crude Distillation Plants with Vacuum Units. II. HEN Design....	161
6.1 Overview.....	161
6.2 Introduction.....	161
6.3 Energy Targets.....	164

6.4 Heat exchanger network.....	170
6.5 Stream matching pattern and its representation.....	171
6.6 Multi-period model.....	178
6.7 Results and Discussion.....	181
6.8 Conclusion.....	184
6.9 Nomenclature.....	188
6.10 References.....	189
Chapter 7 New flowsheets.....	192
7.1 Introduction.....	192
7.2 Use of the heat demand-supply diagram.....	192
7.3 Distillation sequencing.....	197
7.4 Vacuum distillation.....	202
7.5 References.....	204

ABSTRACT

Crude distillation is the first processing unit in the refinery. It separates the crude into distillates, which are either intermediate products further processed or raw materials for the chemical industry. Crude distillation consumes fuel in the equivalent of 2% of the crude processed. This dissertation proposes a rigorous procedure that uses simulators that are able to rigorously represent the column operating conditions as a function of the design parameters and complements it with heat exchanger network design methods. Targeting procedures for both atmospheric distillations and complete distillations are presented. These procedures use a heat demand-supply diagram and commercial software to determine the energy targets for a plant processing several crude oils. These procedures allow each crude to be processed at optimal conditions. Two important alternative designs, the preflash design and stripping-type design have been studied in detail. A rigorous definition for “carrier effect” is provided and the role of light components in the crude distillation is analyzed. The impact of the different heating pattern in the stripping-type design is analyzed and compared with the conventional design. It is concluded that that a stripping-type distillation is less competitive than the conventional design in terms of energy consumption and investment cost. The problem of designing a multi-period heat exchanger network for a complete distillation plant is addressed. The plant has a preflash drum to facilitate the processing of light crudes. A new concept, matching pattern, is proposed to capture the heat exchange topology features. The dissertation also proposes a methodology to develop new designs and provides some examples that are proven promising.

Chapter 1 Introduction

Crude distillation is the first processing unit in the refinery. It separates the crude into distillates, which are either intermediate products further processed or raw materials for the chemical industry. Crude distillation consumes fuel in the equivalent of 2% of the crude processed. Because of its large scale, even a small percentage of energy reduction is economically significant. In spite of its importance, procedures for its optimal design are rather scarce compared with other large-scale chemical processes.

A schematic diagram for crude distillation is shown in Figure 1.1. The crude oil is split in the atmospheric tower into fuel gas, naphtha, kerosene, diesel, gas oil and atmospheric residue (topped crude). The atmospheric residue is sent to the vacuum tower to be further separated into light vacuum gas oil, heavy vacuum gas oil and vacuum residue.

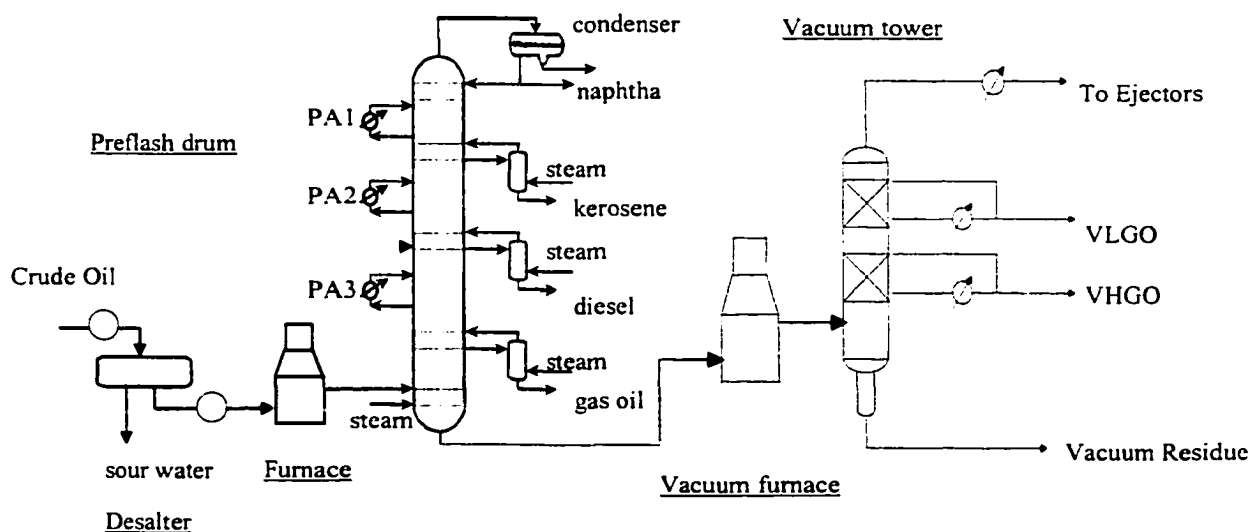


Figure 1.1 A schematic diagram for crude distillation

The crude distillation designs evolved in many years of practice. Figure 1.2 shows a simplified version of the atmospheric column. There are five products coming out from this column: naphtha from the top, residue from the bottom, kerosene, diesel and gas oil from the intermediate trays. The three products (kerosene, diesel and gas oil) withdrawn from the side of the column are also called side withdrawals.

The side withdrawals can not meet their specifications because they contain substantial amount of light components. The light components are removed in side strippers (Figure 1.3).

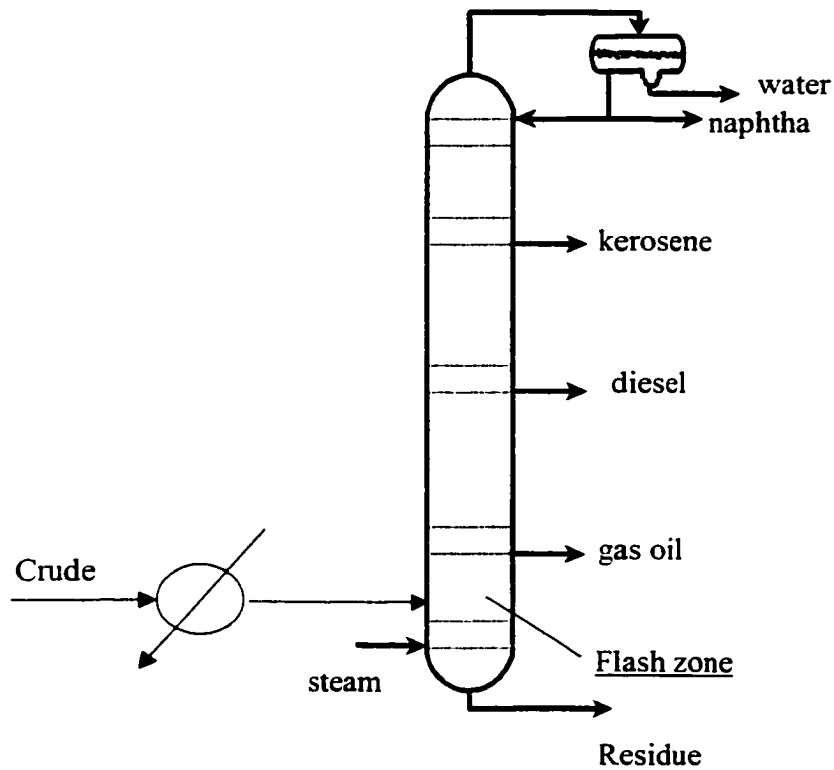


Figure 1.2 The atmospheric distillation column (design A)

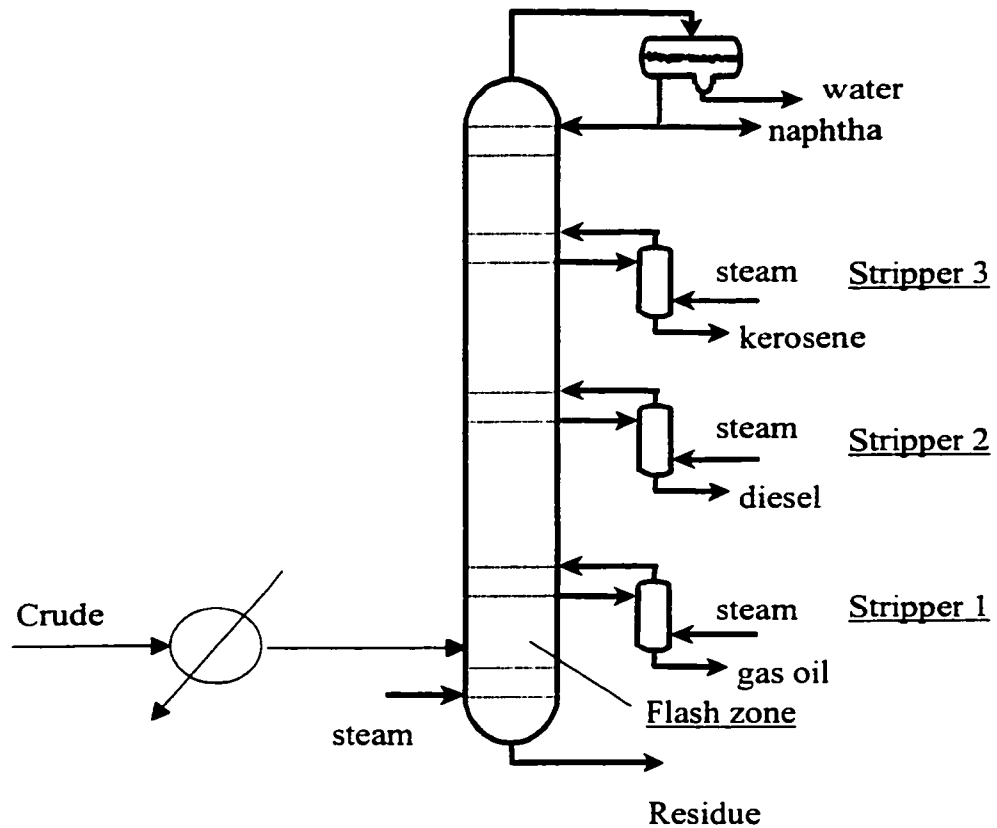


Figure 1.3 The atmospheric distillation column with side strippers (design B)

Design B is a feasible scheme but not a good one. In this design, all heat is removed from the condenser. This results in vapor and liquid traffic increasing throughout the tower from the bottom to the top. The diameter of the top section of the column has to be large to accommodate the high traffic (Watkins, 1979). This scheme of heat removal is also not appropriate for heat recovery because heat from the condenser at a low temperature level (Watkins, 1979, Bagajewicz, 1998).

Design B can be improved by removing part of the heat somewhere below the top tray. There are two types of schemes (Watkins, 1979): pump-around reflux and pump-back reflux.

The pump-back scheme (Figure 1.4) withdraws the liquid from a tray, cool it down and pumps it back to the column at a point several trays below the withdrawal point. Note the amount of heat that can be removed by the pump-back scheme is limited by the liquid entering the withdraw tray.

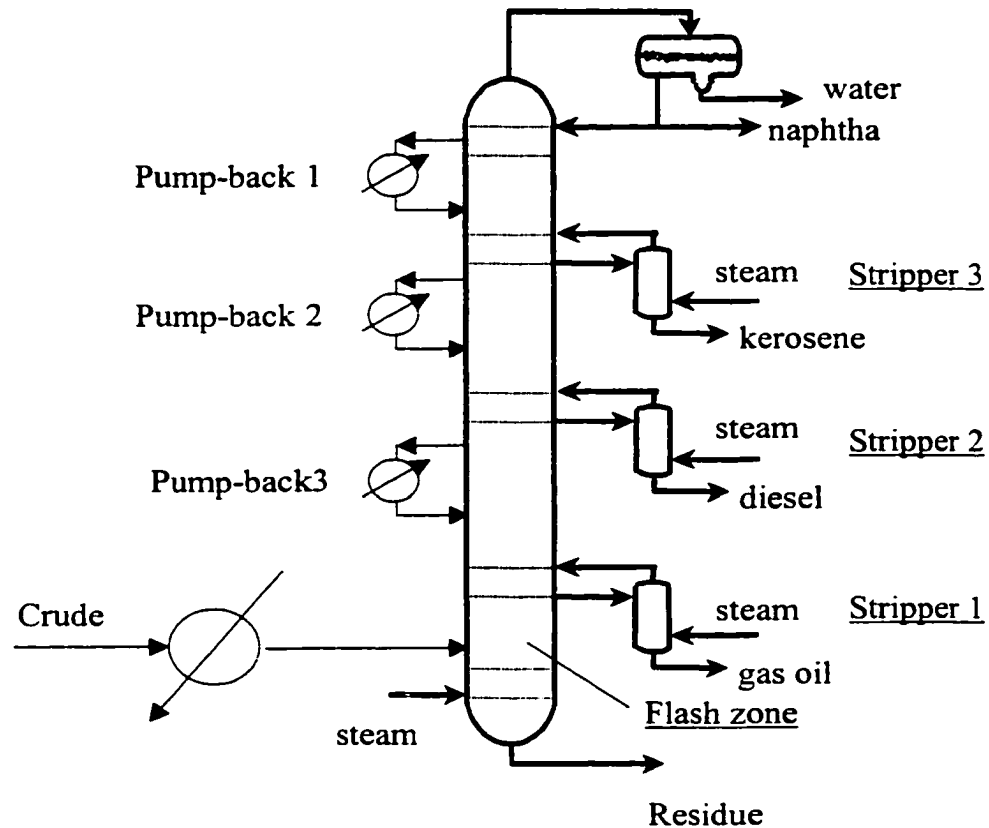


Figure 1.4 Pump-back reflux

The pump-around scheme (Figure 1.5) uses an externally circulated and cooled stream for partial heat removal. Because the liquid is recycled in the pump-around zone, the amount of liquid withdrawn can be several times larger than the liquid reflux entering the pump-around zone. The pump-around scheme is the design used in the refineries.

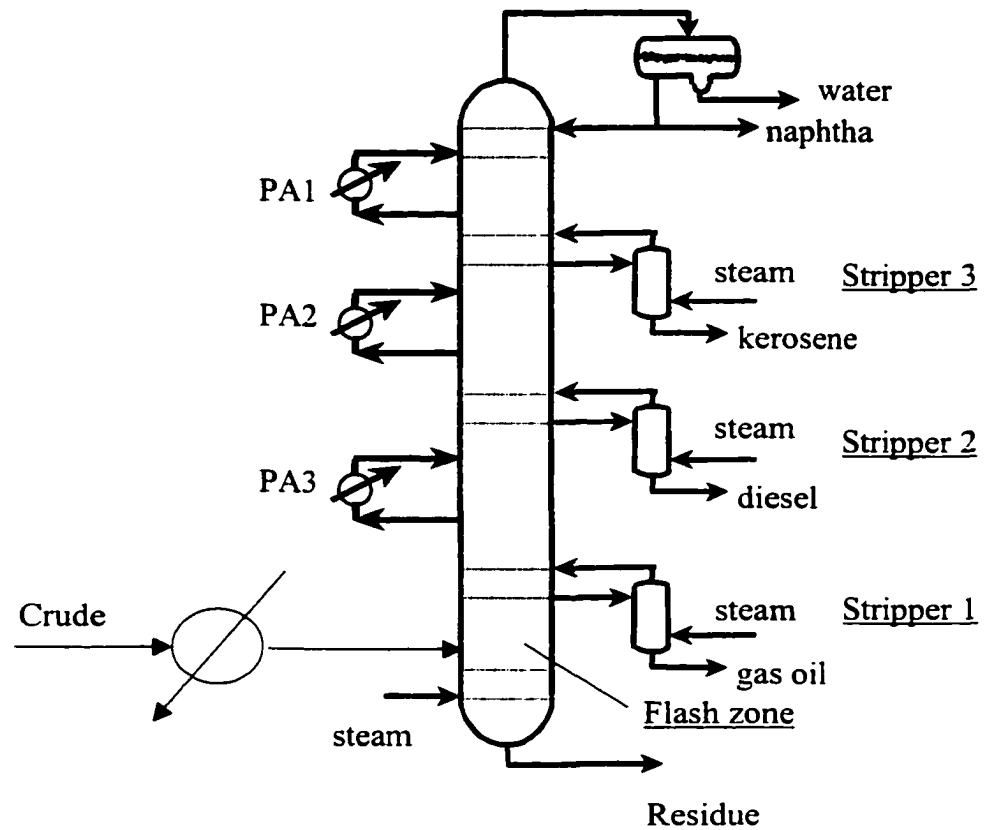


Figure 1.5 Pump-around reflux --- some heat removed from the pump-around circuits

Thus, the conventional design using side strippers and pump-arounds (Figure 1.5) appeared 70 years ago and still the dominant design. Because the trade-off between energy cost and capital cost has changed profoundly in the past 70 years, it is necessary to check whether the assumptions used to design this process are still valid and propose an updated procedure. Existing procedures (Watkins, 1979) are not accurate in nature because they rely on empirical charts. Another problem is that these procedures do not take into account the impact of heat integration and are therefore energy inefficient. In

addition, new methodologies are available for tackling certain design problems that did not exist at the time these procedures were developed.

Another motivation for this thesis is to study some interesting design alternatives. For example, the addition of pre-fractionation columns to this conventional design (Figure 1.6) is practiced sometimes. There have always been disputes as to whether these designs could lead to smaller energy consumption. This thesis evaluates these designs in a systematic way.

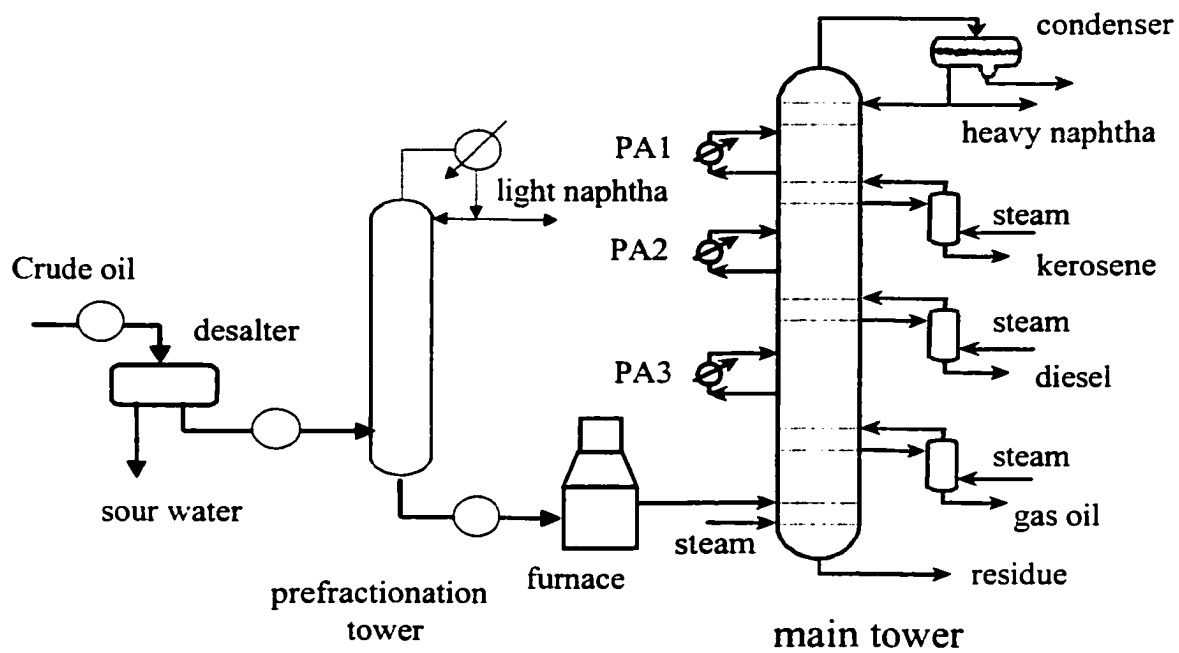


Figure 1.6 Pre-fractionation Design

1.1 Description of the problem

The crude distillation problem is the following. Given:

- A set of crude oils to be processed and their properties
- A set of specifications for products
- Maximal allowable processing temperatures of the crudes

- Final temperatures of products
- Available utilities, their temperatures, and their costs

determine the distillation column(s) and the associated heat exchanger network that will minimize the annualized cost of the equipment plus the annual cost of utilities.

1.2 Crude oil properties

Crude oil is very complex. The compounds in crude oils can be grouped into 3 major categories: Paraffinic hydrocarbons, naphthenic hydrocarbons and aromatic hydrocarbons. Paraffinic hydrocarbons are saturated compounds. Naphthenic hydrocarbons are saturated cyclic hydrocarbons. Aromatic hydrocarbons contain unsaturated cyclic compounds.

With gas chromatographic methods, more than 70 different components have been identified from very light hydrocarbons (less than 10 carbon atoms) to very heavy large hydrocarbon molecules. The relevant properties to crude distillation are boiling ranges, density and salt content. Boiling ranges are used because of the large amount of compounds which are very expensive to identify. Density helps characterize the crude because it tells about its proportion of light hydrocarbons. Finally salt comes with the crude and it is harmful. So it needs to be removed.

1.2.1 Boiling range

The boiling range of the crude oil provides information about the quantities of the various products present. The commonly used distillations are true boiling point (TBP) distillation (TBP) and ASTM distillation.

True Boiling Point (TBP) distillation is a batch distillation using a large number of trays and a high reflux ratio. The temperature-volumetric yield curve is constructed representing the actual boiling point of the hydrocarbon material present at the volume percentage point (Watkins, 1979). Most commonly the column has 15 theoretical trays and is operated at a reflux ratio of 5. TBP distillations are usually reported at 760 mm Hg, even though the highest boiling portion of the mixture is distilled out at reduced pressures (30 to 40 mm Hg). The TBP data (Figure 1.7) can be used to define the average normal boiling points for pseudocomponents. The pseudocomponent concept is very useful for simulations. During the TBP distillation, if the distillates are collected over a small temperature range, the whole crude is then divided in fractions. Each fraction is still a mixture of many unknown components, but the components in one fraction have a similar boiling point. It would be convenient for distillation calculations to treat these fractions as if they were pure components. They are called pseudocomponents.

In practice, it is not necessary to collect those narrow fractions experimentally. The pseudocomponents can be obtained by setting up cutting points on a smooth TBP distillation curve. Figure 1.8 shows the first three pseudocomponents. It can be seen that a pseudocomponent is defined by the interval between two adjacent cut points and its percentage in the crude is the differences between values at adjacent cut points. The normal boiling point (NBP) of each fraction is determined as a volume-fraction average

by integrating across the cut range. These average boiling points are used to calculate other thermophysical properties for each pseudocomponent (PRO/II Workbook, 1996).

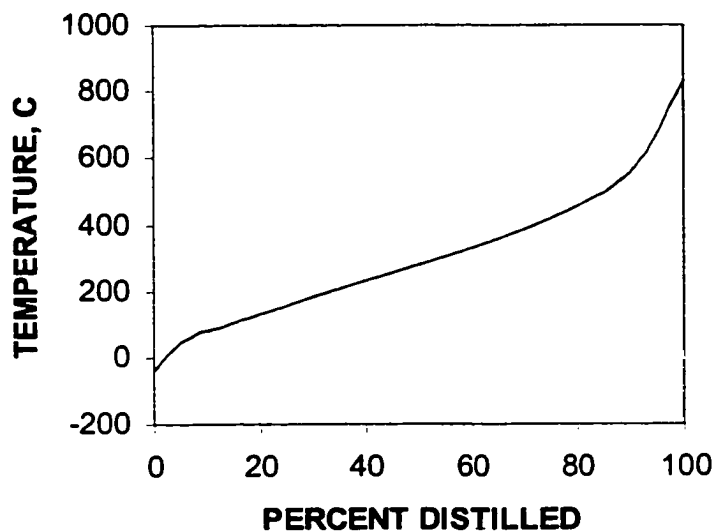


Figure 1.7 Typical TBP curve

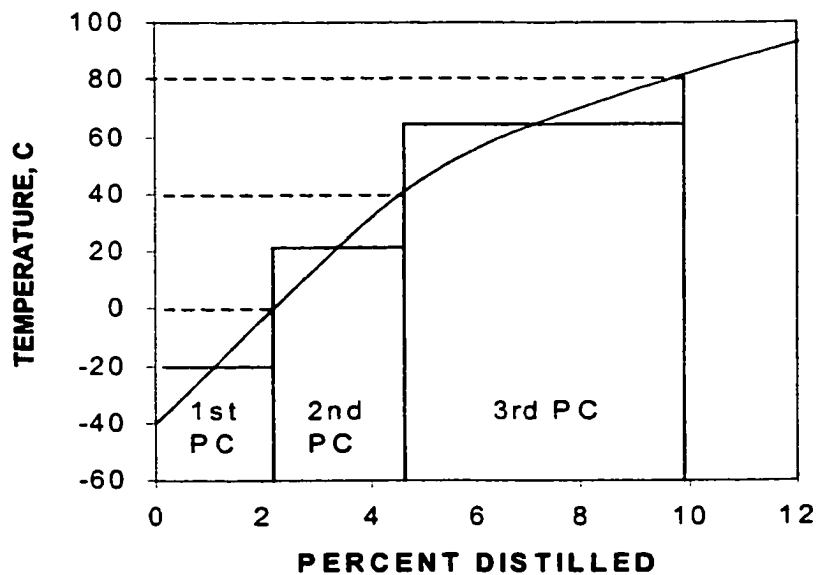


Figure 1.8 Definition of pseudo-components based on TBP curve

PC: pseudo-component

The disadvantage of TBP distillation is that the equipment is expensive and the test takes a long time to carry out. An easier method is ASTM D-86 distillation. ASTM D86 distillation is carried out in a glass flask equipped with an electric heater and a water cooler. The oil sample is heated in the flask and the resultant vapor is condensed and collected in a receiver at laboratory pressure. The temperature versus volumetric amount collected is recorded. Virtually no fractionation occurs in this distillation. The initial boiling point (IBP) is defined as the temperature at which the first drop of liquid is collected. The final boiling point or end point is defined as the maximum temperature reached during the distillation. ASTM D86 distillation is typically used for light and medium petroleum products and is carried out at atmospheric pressure. ASTM D1160 distillation (PROII manual, 1996) is similar to ASTM D86 distillation, but is used for heavier petroleum products and is often carried out under vacuum, sometimes at absolute pressures as low as 1 mm Hg.

One can convert these curves to TBP using correlation (Nelson, 1958, API handbook, 1970).

Equilibrium flash vaporization (EFV) is a test used to determine the vaporization ratios of crude oils as a function of temperature. In this test, the crude oil is continuously heated without separating the vapor from the remaining liquid (Nelson, 1958). The temperature versus liquid amount is recorded. To obtain the EFV curve, a series of runs at different temperatures are carried out, and each run constitutes one point (of temperature and percentage vaporized) on the flash curve.

1.2.2 Gravity, API

API is a density scale used in the petroleum industry. It can be calculated from specific gravity is the following (Gray, 1994):

$$\circ API = (145.5 / spgr) - 131.5 \quad (1)$$

In the above equation, specific gravity refers to the weight per unit volume as compared to water at 60 °F. Most crude have a gravity in the range of 20 to 45 API. 20 corresponds to heavy crudes and 45 to lighter crudes.

1.2.3 Salt Content

The salts in crude oil are primarily chlorides, sulfates and carbonates of sodium, calcium and magnesium. The salt may deposit on heat transfer surfaces and cause fouling. Chloride salts may also decompose to form acids and cause corrosion. The salt content of the crude oil is required to be less than 10 lb/1000 bbl for crude distillation (Gray, 1994).

Desalting is performed by mixing the crude oil with 3 to 10 volume per cent water at temperatures from 90 to 150 °C (200-300 °F). Both the water/oil ratio and the temperature of operation are functions of the density of the crude oil. Typical operating conditions are shown in Table 1.1 (Gray, 1994).

1.3 Crude distillation products

Typical fraction cut points and boiling ranges for atmospheric and vacuum tower fractions are given in Table 1.2.

Table 1.1 Typical Operating Condition for Desalting

API	Water Wash, vol %	Temperature °C (°F)
API>40	3-4	115-125 (240-260)
30<API<40	4-7	125-140 (260-280)
API<30	7-10	140-150 (280-300)

Table 1.2 Typical distillates and its use

Fraction	Boiling ranges		Processing use
	ASTM (°F)	TBP (°F)	
Naphtha (heavy straight-run gasoline)	180-400	190-380	Reforming stock
Kerosene	330-540	380-520	Kerosene, jet-50 cut
Light gas oil (LGO)	420-640	520-610	Diesel fuel
Heavy gas oil (HGO)	550-830	610-800	Catalytic cracker or hydrocracker feed
Vacuum gas oil (VGO)	750-1050	800-1050	Deasphalter, catalytic cracker feed or hydrocracker feed
Vacuum reduced crude	1000+	1050+	fuel oil, asphalt or feed to visbreaker or coker.

The main products from a typical crude distillation unit are listed below in the order of increasing boiling points (Gary, 1994).

Fuel gas. The fuel gas consists of methane and ethane. The fuel gas is mainly used as fuel for refinery furnaces. Sometimes it is also used as feedstocks for ammonia production.

Wet gas. The wet gas consists of propane and butane as well as methane and ethane. The mixture of propane and butane can be sold as LPG and butanes are raw material for gasoline blending and some alkylation unit feed.

Naphtha. Most naphtha is used in gasoline production, either directly or as catalytic reformat. Naphtha is also used as petrochemical feedstock, mainly for thermal cracking to olefins or for reforming and extraction of aromatics.

Gas oils. The light, atmospheric, and vacuum gas oils are used as feedstock for a hydrocracker or catalytic cracker to produce gasoline, jet, and diesel fuels. The heavy vacuum gas oils can also be used as feedstock for lubricating oil units.

Residue. The vacuum bottoms can be sent to a visbreaker, coker, or deasphalting unit to produce heavy fuel oil or cracking and/or lube base stocks. For asphalt crude oils, the residue can be used to produce road or roofing asphalt.

The relevant specifications of these products are the following:

- ASTM D86 temperatures or D1186 temperatures (for vacuum gas oils)
- Flash point (for kerosene)
- Products 5-95 gap

The flash point of a product is the temperature at which vapor given off will ignite when an external flame is applied under specified test conditions. A flash point is defined to minimize fire risk during normal storage and handling.

The term **gap** refers to the difference between the 5% ASTM D86 distillation temperature of a heavier product and the 95% ASTM D86 distillation temperature of an adjacent lighter product. When the distillation curves of the two products overlap, a negative gap appears.

1.4 State of the art in the design

One of the most important early publications is “Petroleum Refinery Engineering” by Nelson (1936). This book discusses the crude distillation in detail. It contains many charts and experimental data. The 4th edition was published in 1958. In the design procedure presented in this book, the amount of products is estimated from the crude distillation curve, then the number of trays between side withdraws are picked. Next, the temperature and pressure in each tray are calculated using empirical charts. Heat balance is then carried out and the reflux is determined. The design procedure ends with the design of the preheat train.

Another early publication is a paper by Packie (1941). In his method, 5-95 gaps and 50% distillation temperature differences are used as separation criteria. Packie used empirical charts to express the relation among the 5-95 gap, the reflux ratio, and the number of trays in the section under consideration. However, the empirical nature of these charts results in inaccuracies in the amount of heat removal and tray temperatures. Furthermore, as in the case of Nelson (1936), Packie considered column design and heat integration separately, that is, heat integration does not start until the column design is finished.

Much later, another book on crude distillation was published by Watkins (1979). This procedure provided in this book is similar to the one proposed by Nelson (1958). It uses empirical charts and iterations are required to compute heat and material balances. However, departing from Nelson and Packie's criterion regarding heat integration, Watkins pointed out that "optimizing the crude preheat-tower cooling heat-exchange train is the heart of crude unit design, and each case must be studied on an individual basis in order to arrive at the most economical processing scheme." The statement reflects the times the book was written (1979) right after the first energy crisis (1973). However, he did not present a specific methodology to perform this integrated design.

Bagajewicz (1998a) studied the flexibility of atmospheric crude distillation units. He found that pump-around circuits are only effective to remove heat at higher temperature. Main steam injection was found beneficial from the point of view of energy integration. The combined usage of large steam injection with smaller overflash was shown to have large energy savings. In another paper (1998b), he presented a technique to calculate energy retrofit horizons in process plants. The methodology takes advantage of two facts: (a) Pinch-type calculations can be performed using operator type representations and (b) Processes like crude fractionation offer large flexibility in the operating/design parameters. The simulation package Pro/II (SimSci) was used to perform these studies.

Recently, Liebmann *et al.* (1995, 1998) proposed an integrated design procedure. The design procedure starts with a sequence of simple columns that are generated by decomposing the crude main tower. The total number of trays is assumed to be the same as that of Watkins' design, and the number of trays for each column is calculated with the

assumption that the R/R_{\min} values are approximately the same for all columns. There is no thermal coupling between these initial columns. Next, reboilers and thermal coupling are introduced in order to reduce utility consumption. To assess the proposed modifications, a tool from Pinch Technology (developed in the eighties), namely, the grand composite curve, is used. After all the possible design modifications have been explored, these columns are merged into a single complex column.

The major advantage of the procedure presented by Liebmann *et al.* (1998) is that it couples the column performance with heat recovery goals. However, the procedure is not able to assess the trade off between steam injection and distribution of heat removal in pump-around circuits. Finally, addressing the column as a whole, which is the alternative we present in this paper, is more convenient and straightforward. It does not rely on any special rules of thumbs for reflux ratios, and it helps determine better the relationships with column variables and heat integration.

Sharma *et al.* (1999) proposed a method for calculating the maximum pump-around heat removal. First, a practical minimum reflux ratio for each column section is determined using Packie's empirical diagram. Then, the heat removal in the upper part of the column is calculated using a heat balance. The upper part may start from an arbitrary tray and end with the condenser. Following, the upper part is extended tray by tray and heat surplus is calculated for each tray. The resultant heat surplus data are used to construct a column grand composite curve. Finally, the maximum heat removal for each section is determined using the column grand composite curve. A major advantage of this method is that the maximum heat removal can be estimated quickly without the need of

simulation. However, because Packie's diagram is empirical and the effect of the stripping steam is not included, the heat removal calculated is not accurate.

To address all the aforementioned inaccuracies, it seems natural to think of simulator and heat integration procedures as means of developing a new design procedure that would capture rigorously the column behavior, the effect of steam and refluxes and the relationship with heat integration. Bagajewicz (1998b) suggested the use of rigorous simulation for crude distillation design/retrofit.

The major features of such procedure are:

- The plant should be able to process several crudes at optimal conditions.
- It should operate at maximum efficiency possible in all cases.
- The trade-off between energy and capital expenditure should be clear.

1.5 Topics in this dissertation

This dissertation discusses a rigorous procedure that uses simulators that are able to rigorously represent the column operating conditions as a function of the design parameters and complements it with state of the art heat exchanger network design methods. In Chapter 2, a targeting procedure for conventional distillation will be presented. This procedure uses a heat demand-supply diagram and commercial software to determine the energy target for a plant processing several crude oils. This procedure allows each crude to be processed at optimal conditions. Chapter 3 addresses the problem of designing a crude distillation with a pre-flash unit. A rigorous definition for "carrier effect" is provided and the role of light components in the crude distillation is analyzed in detail. Then a rigorous procedure for energy targeting in the design of crude distillation with preflashing is provided. Chapter 4 is devoted to the study of the stripping-type

distillation which was claimed by Liebmann and Dhole (1995) to be more energy-efficient than the conventional design. The impact of the different heating patterns in the stripping-type design is therefore analyzed and compared with the conventional design. Chapter 5 addresses the energy targeting for the design of complete distillation plants, that is, including both the atmospheric tower and the vacuum tower. Chapter 6 focuses on the design of a multi-period heat exchanger network for a complete distillation plant. The plant has a preflash drum to facilitate the processing of light crudes. The last chapter (Chapter 7) discusses the possible alternative designs and presents preliminary results.

1.6 References

1. American Petroleum Institute, 1970, Technical Data Book - Petroleum Refining, 2nd Ed., Procedure 7B3.1, 7-29 - 7-286.
2. American Petroleum Institute, 1970, Technical Data Book - Petroleum Refining, 2nd Ed., Procedure 7H2.1, 7-201 - 7-202.
3. Bagajewicz, M., On the design flexibility of atmospheric crude fractionation units, Chem. Eng. Comm., 166, 111-136, 1998a
4. Bagajewicz, M. J., Energy savings horizons for the retrofit of chemical processes. Application to crude fractionation units. Computers & Chemical Engineering, 1-9, 23 (1), 1998b
5. Gary, James H., Petroleum refining : technology and economics, 3rd ed. M. Dekker, New York, 1994
6. Hans-Joachim Neumann, Petroleum Refining, Ferdinand Enke Publishers Stuttgart, 1984

7. Liebmann, K., Integrated crude oil distillation design, Ph. D. dissertation, University of Manchester Institute of Science & Technology, 1996.
8. Miller, W., Osborne, H., The science of petroleum, Volume II, Oxford University Press, London, 1938.
9. Nelson, W. L., Petroleum Refinery Engineering, 1th edition, McGraw-Hill, New York, 1936.
10. Nelson, W. L., Petroleum Refinery Engineering, 4th edition, Chapter 4, McGraw-Hill, New York, 1958.
11. Packie, J.W. Distillation Equipment in the Oil Refining Industry. *AIChE Transactions*. 1941, 37, 51.
12. PRO/II Workbook, Hydrocarbon Distillation, Simulation Sciences Inc., 1996.
13. Rhodes, A. K., Worldwide refining report, Oil & Gas Journal, December, 37-86, 1993.
14. Watkins, R. N. Petroleum refinery distillation. Gulf Publishing Company: Houston, 1979.

Chapter 2 Rigorous Targeting Procedure for the Design of Conventional Atmospheric Crude Fractionation Units

2.1 Overview

The problem of designing crude fractionation units is not only a distillation design. It has the added complexity that these units should be able to process different types of crude, sometimes from heavy to light. Important heat exchange also takes place, and the energy efficiency is related to the column design parameters. Part I of this two-part paper presents a rigorous targeting methodology to design this multipurpose plant, which can be implemented using a commercial simulator. Part II deals with the heat exchanger network design.

2.2 Introduction

Crude distillation is energy intensive. It consumes fuel in the equivalent of 2% of the crude processed. The conventional design (Figure 2.1), consisting of a column with side strippers and pump-around circuits, appeared 70 years ago (Miller, 1938), and is still the design used in the refining industry. Watkins (1979) proposed a design procedure for this system and discussed a few variants such as pump-back reflux and stripping using reboilers. A few alternative designs can be found in the literature. For example, the addition of pre-fractionation columns to this conventional design was proposed by Brugma (1941) and is being used in several industrial sites. Another old design, the carrier design, was proposed as early as the 1920s. This design makes use of light components to enhance the separation in the stripping section of the column. Nelson

(1958) also mentioned some other alternative designs. All these old designs have been abandoned for reasons that are not completely known or understood. One important fact is that they were abandoned before the seventies, when energy consumption started to play an important role in process economics. Because energy efficiency is now desired, all these designs merit reevaluations. Nevertheless, the conventional design is widespread and popular.

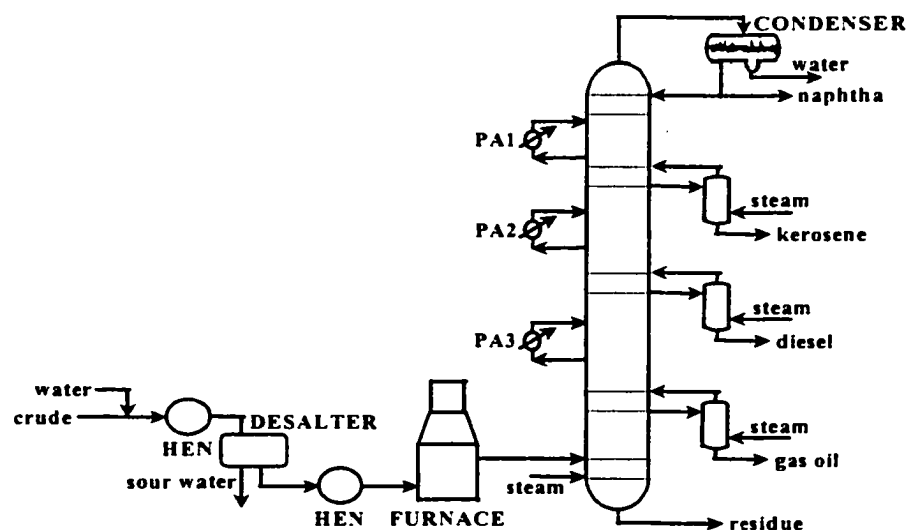


Figure 2.1 Conventional Crude Distillation

Crude is mixed with water and heated in a heat exchanger network before entering a desalter where most of the water containing the salt is removed. The desalted crude enters another heat exchanger network and receives heat from hot streams. Both heat exchanger networks make use of the vapors of the main column condenser, the pump-around circuit streams, and the products that need to be cooled. The preheated crude then enters the furnace, where it is heated to about 340-370 °C. The partially

vaporized crude is fed into the flash zone of the atmospheric column, where the vapor and liquid separate. The vapor includes all the components that comprise the products, while the liquid is the residue with a small amount of relatively light components in the range of gas oil. These components are removed from the residue by steam stripping at the bottom of the column. In addition to the overhead condenser, there are several pump-around circuits along the column, where liquid streams are withdrawn, cooled, and sent back to upper trays. Products are withdrawn in liquid state from different trays and then stripped by steam in side strippers to remove light components. Bagajewicz (1998) offered a detailed discussion of the effect of the different variables on the energy efficiency of this conventional design.

Crude oil is a complex mixture. There exist about one thousand distinguishable components with boiling temperatures varying from room temperature to over 550 °C. Crude distillation yields mixtures called naphtha, kerosene, diesel, and gas oil. These products are specified by ASTM D86 distillation temperatures.

Compared to common distillation of discrete components, crude distillation has the following specific features:

- *Large processing quantity:* The charge rate is the largest among all petroleum or chemical processing units. The typical processing capability is around 15,000 m³ per day (100,000 bbl/day). In such a large-scale process, energy cost accounts for a larger part of manufacturing cost than in other processes.
- *Large temperature variation throughout the column:* The temperature difference between the top tray and the flash zone is about 250°C, which means large heat degradation throughout the column.

- *Absence of a reboiler:* The main column functions as a rectifying section for products, while side columns act as stripping sections.
- *Low separation sharpness:* Product quality is specified by ASTM boiling points rather than component fractions as in the discrete component separation case. The former is a more relaxed requirement.
- *Components in a lighter product can be found in any of heavier products:* This is because all components constituting the light product have to travel through trays where heavier products are withdrawn.

The major objective in the design of crude distillation units is to find the most energy efficient separation structure. Although some ideas exist for the design of energy integrated distillation schemes (Agrawal, 1996), they are not directly applicable to crude fractionation for the following reasons:

- The number of components in the crude is too large to handle. Usually around 30 to 40 pseudo components are used, while available studies on sequencing seldom addressed systems containing over 5 components.
- Previous separation sequencing studies assumed the products are pure, however products in crude distillation are mixtures.

Packie (1941) pioneered the field of crude fractionation design. In his method, 5-95 gaps and 50% distillation temperature differences are used as separation criteria. The term gap refers to the difference between the 5% ASTM D86 distillation temperature of a heavier product and the 95% ASTM D86 distillation temperature of an adjacent lighter product. When the distillation curves of the two products overlap, a negative gap appears. Packie used empirical charts to express the relation among the 5-95 gap, the reflux ratio,

and the number of trays in the section under consideration. However, the empirical nature of these charts results in inaccuracy and prevents optimal designs. Furthermore, in his design procedure, Packie considered column design and heat integration separately. Heat integration does not start until the column design is finished.

Watkins (1979) pointed out that “optimizing the crude preheat-tower cooling heat-exchange train is the heart of crude unit design, and each case must be studied on an individual basis in order to arrive at the most economical processing scheme.” However, Watkins did not present a specific methodology to perform this design.

Recently, Liebmann *et al.* (1995, 1998) proposed an integrated design procedure. The design procedure starts with a sequence of simple columns that are generated by decomposing the crude main tower. The total number of trays is assumed to be the same as that of Watkins’ design, and the number of trays for each column is calculated with the assumption that the R/R_{\min} values are approximately the same for all columns. There is no thermal coupling between these initial columns. Next, reboilers and thermal coupling are introduced in order to reduce utility consumption. The grand composite curve is used to assess the proposed modifications. After all the possible design modifications have been explored, these columns are merged into a single complex column.

The major advantage of the procedure presented by Liebmann *et al.* (1998) is that it couples the column performance with heat recovery goals. However, the procedure is not able to assess the trade off between steam injection and distribution of heat removal in pump-around circuits. Finally, addressing the column as a whole, which is the alternative we present in this paper, is more convenient and straightforward. It does not

rely on any special rules of thumbs for reflux ratios, and it helps determine better the relationships with column variables and heat integration.

Sharma et al. (1999) proposed a method for calculating the maximum pump-around heat removal. First, a practical minimum reflux ratio for each column section is determined using Packie's empirical diagram. Then, the heat removal in the upper part of the column is calculated using a heat balance. The upper part may start from an arbitrary tray and end with the condenser. Following, the upper part is extended tray by tray and heat surplus is calculated for each tray. The resultant heat surplus data are used to construct a column grand composite curve. Finally, the maximum heat removal for each section is determined using the column grand composite curve. A major advantage of this method is that the maximum heat removal can be estimated quickly without the need of simulation. However, as Packie's diagram is empirical and the effect of the stripping steam is not included, the heat removal calculated is not accurate. In contrast, the procedure presented in this paper is based on rigorous simulations and can capture the relationships between the column variables and the heat integration opportunities.

In this paper we present a new procedure for crude distillation design. The major features of this procedure are:

- The design objective is to process several crudes at optimal conditions.
- The design calculations are rigorous.

Heat demand-supply diagrams are used as a tool guiding the design. The major advantage of the heat demand-supply diagram is that the contribution of each process stream or pump-around to the total utility consumption is shown explicitly. This feature helps determine necessary changes leading to lower energy consumption.

- The interaction between steam stripping and pump-around duties is taken into consideration.
- The starting point of the column design is a complex column without pump-around circuits.

While general procedures that would render globally optimal solutions are a desirable goal, there is also interest in determining the optimal parameters for the subset of conventional units. This choice is made because practitioners are not always willing to make radical departures from this design. In addition, the knowledge of such optimal designs provides a useful horizon for retrofit procedures. In addition, the heat exchanger network design procedure presented in part II renders a structure suitable for the processing of different crudes at maximum energy efficiency. A short version of this procedure was presented by Bagajewicz et al. (1999).

The paper is organized as follows: The heat demand-supply diagram, an important tool, is presented first and the roles of the different column design variables in this diagram are discussed. Next, limitations in the pump-around circuit heat load are described. Finally, the design targeting procedure is presented. This rigorous procedure is based on the use of commercial simulators, departing from the use of charts, rules of thumb, and other approximations.

2.3 Heat demand-supply diagram

Heat demand-supply diagrams are an extension of the concept of temperature-enthalpy diagrams (Hohmann, 1971; Huang and Elshout, 1976; Naka et. al., 1980; Andrecovich and Westerberg, 1985; Terranova and Westerberg, 1989; Dhole and

Linnhoff, 1993). In the demand-supply diagram, a stream is represented by a curve. This curve represents the product of mass flowrate and specific heat capacity (true or apparent in the case of phase changing streams) as a function of temperature. A schematic heat demand-supply diagram for typical crude fractionation units, like the one of Figure 2.1, is shown in Figure 2.2.

In setting up the diagram, a heat demand line is first drawn and used as a background. The crude is the only cold stream. In some cases, as proposed by Liebmann *et al.* (1998), water at room temperature to produce steam is also considered a cold stream. However, in many refineries, low-pressure steam is in surplus, and it can be considered as a cheap or even free heat source. To locate the hot streams (heat supply), the usual minimum temperature difference is used. Thus the temperatures of hot streams are shifted to the left by this minimum difference, which has been traditionally named heat recovery minimum approximation temperature (HRAT). The area below the heat demand line represents the total heat demand of the unit without heat recovery.

In Figure 2.2, we see two different regions:

- Regions where heat supplies are larger than demands
- Regions where heat supplies are smaller than demands

When the supply exceeds the demand, one can move the surplus part of the supply to a lower temperature region where the supply is deficient. Figure 2.2 shows two areas where the supply is in deficit (gray areas). The left gray area can be covered by the heat surplus from the condenser or from PA1. The right one can be covered using the excess of PA2. This illustration is omitted throughout the paper, assuming that this area matching is implicit.

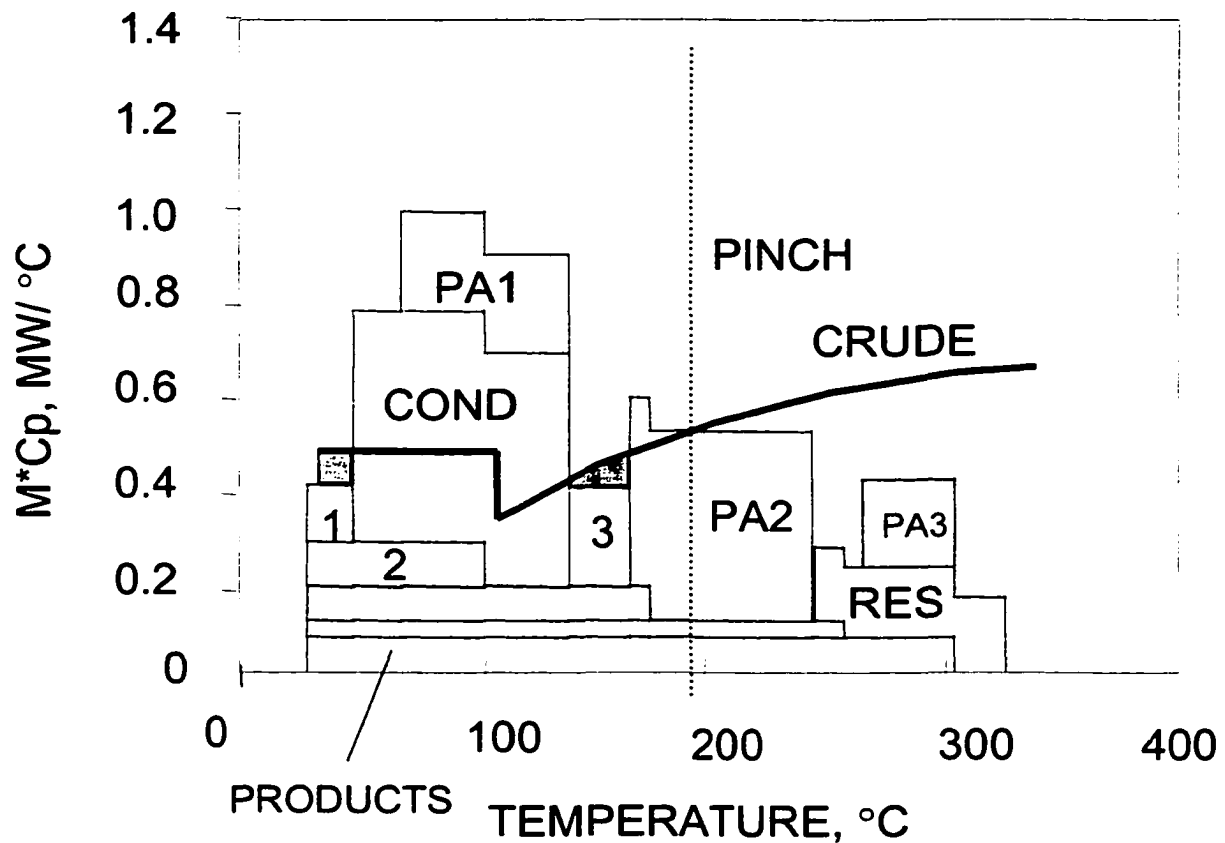


Figure 2.2 *Heat Demand-Supply Diagram of a Crude Distillation Unit.*

1. Naphtha and condensed water. 2. Sour water from the desalter. 3. Pump-around 1. COND: condenser. PA: pump-around. RES: residue. Products (from top to bottom): kerosene, diesel and gas oil.

The location of the pinch point can be easily obtained from this diagram. It is the lowest temperature at which the demand is larger than the supply after the shifting and area matching has been performed. Finally, the heating utility is given by the unmatched demand on the right, and the cooling utility is given by the extra supply on the left.

Three options to reduce energy consumption exist: decreasing demand, increasing supply and improving the match between the supply and the demand.

- *Decrease of demand*

- a) A decrease in heat demand can be realized by moving the demand line down, that is, decreasing the flowrate. One way of doing this is to flash the crude at lower temperatures and send the vapor to a tray above the flash zone. In practice, vaporization before the furnace inlet is pressure suppressed to avoid two-phase flow. This reduces energy saving opportunities. Such opportunity is analyzed in a separate work (Ji and Bagajewicz, 2000).
- b) Another way to decrease heat demand is to reduce the target temperature of the crude. This can be achieved by lowering the pressure drop from the outlet of the furnace to the overhead reflux drum of the column. In this sense, a vacuum operation is even better, but it is excluded for other reasons (mainly cost). Another way of decreasing the final temperature is using larger amount of steam, but the introduction of steam has complicating effects on energy consumption, which will be discussed in another paper.

- *Increase of the supply and/or the thermal quality*

Withdrawing certain products in the vapor phase instead of in a liquid phase has the advantage that condensation heat is released at a higher temperature. This option is not explored in this paper, mainly because it is a major departure from the conventional scheme.

- *Improvement of match between demand and supply*

Assume there is a large heat surplus in a moderate temperature range and a heat deficit in a higher temperature range. One way to improve this mismatch is to move a part of the heat surplus to a higher temperature by increasing the duties of the pump-around circuits. The design procedure proposed in this paper relies on the idea of distributing heat among the condenser and pump-around circuits. We focus on this procedure next.

2.4 Pump-around circuits and heat recovery

The original purpose of adding pump-around circuits was to reduce vapor and liquid traffic at the top section of the column (Watkins, 1979). Without pump-around circuits, all condensation heat has to be removed from the condenser, which results in a large vapor flowrate at the top trays. We explore now the limit of heat that could be removed from a pump-around circuit.

Maximum Heat Duty of Pump-Around Circuits

In Figure 2.3, envelope *III* contains *k* pump-around circuits. In order to calculate the maximum pump-around duty, we carry out a heat balance for this envelope.

$$\begin{aligned}
 & V_{FZ}^W \cdot h_{FZ}^W + V_{FZ}^O \cdot h_{FZ}^O + L_{j-1} \cdot h_{L_{j-1}} + \sum_{i \in III} F_{si} \cdot h_{si} + \sum_{k \in III} Q_k \\
 & = L_O \cdot h_{L_O} + \sum_{i \in III} F_{pi} \cdot h_{pi} + V_j^W \cdot h_{V_j}^W + V_j^O \cdot h_{V_j}^O
 \end{aligned} \tag{1.1}$$

In equation (1.1), V_{FZ}^W , V_{FZ}^O are the steam flowrate at the flash zone and the hydrocarbon vapor flowrate at the flash zone respectively, V_j^W , V_j^O are the steam flowrate at tray *j* and the hydrocarbon vapor flowrate at tray *j* respectively. In Figure 2.3,

we use $V_{FZ} = V_{FZ}^W + V_{FZ}^O$ and $V_j = V_j^W + V_j^O$. It is assumed that water is insoluble in liquid streams.

By applying material balance of hydrocarbons to envelope *I*, one obtains:

$$V_{FZ}^O = L_O + \sum_{i \in I} F_{pi} \quad (1.2)$$

Similarly, material balances for envelopes *II* and *III* are:

$$\begin{aligned} V_j^W &= V_{FZ}^W + \sum_{i \in III} F_{si} \\ V_j^O &= L_{j-1} + \sum_{i \in II} F_{pi} \end{aligned} \quad (1.3)$$

Replacing V_{FZ}^O , V_j^W and V_j^O in equation (1.1), one obtains:

$$\begin{aligned} \sum_{k \in III} Q_k &= L_O \cdot (h_{L_O} - h_{FZ}^O) + \sum_{i \in III} F_{pi} \cdot (h_{pi} - h_{FZ}^O) + \sum_{i \in II} F_{pi} \cdot (h_{V_j}^O - h_{FZ}^O) \\ &+ V_{FZ}^W \cdot (h_{V_j}^W - h_{FZ}^W) + \sum_{i \in III} F_{si} \cdot (h_{V_j}^W - h_{si}) + L_{j-1} \cdot (h_{V_j}^O - h_{L_{j-1}}) \end{aligned} \quad (1.4)$$

There are six terms on the right hand side of equation (1.4). From left to right, these terms represent condensation heat of the overflash stream L_O , condensation heat of the products leaving envelope III, apparent heat released by the hydrocarbon vapor V_j^O , and apparent heat released by the steam streams. The sixth term stands for the vaporization heat of internal reflux L_{j-1} . Apparently, when L_{j-1} goes to zero, the heat removal from envelope III reaches its maximum. By including more pump-arounds in envelope III and applying equation (1.4) accordingly, one can find the maximum heat duty for each pump-around circuit.

It can be shown through an overall heat balance that the total amount of heat to be removed from the column depends on the yields of the products. In addition, shifting heat

from envelope II to envelope III results in a decrease of L_{j-1} . Thus, the shifting can take place as long as L_{j-1} remains positive.

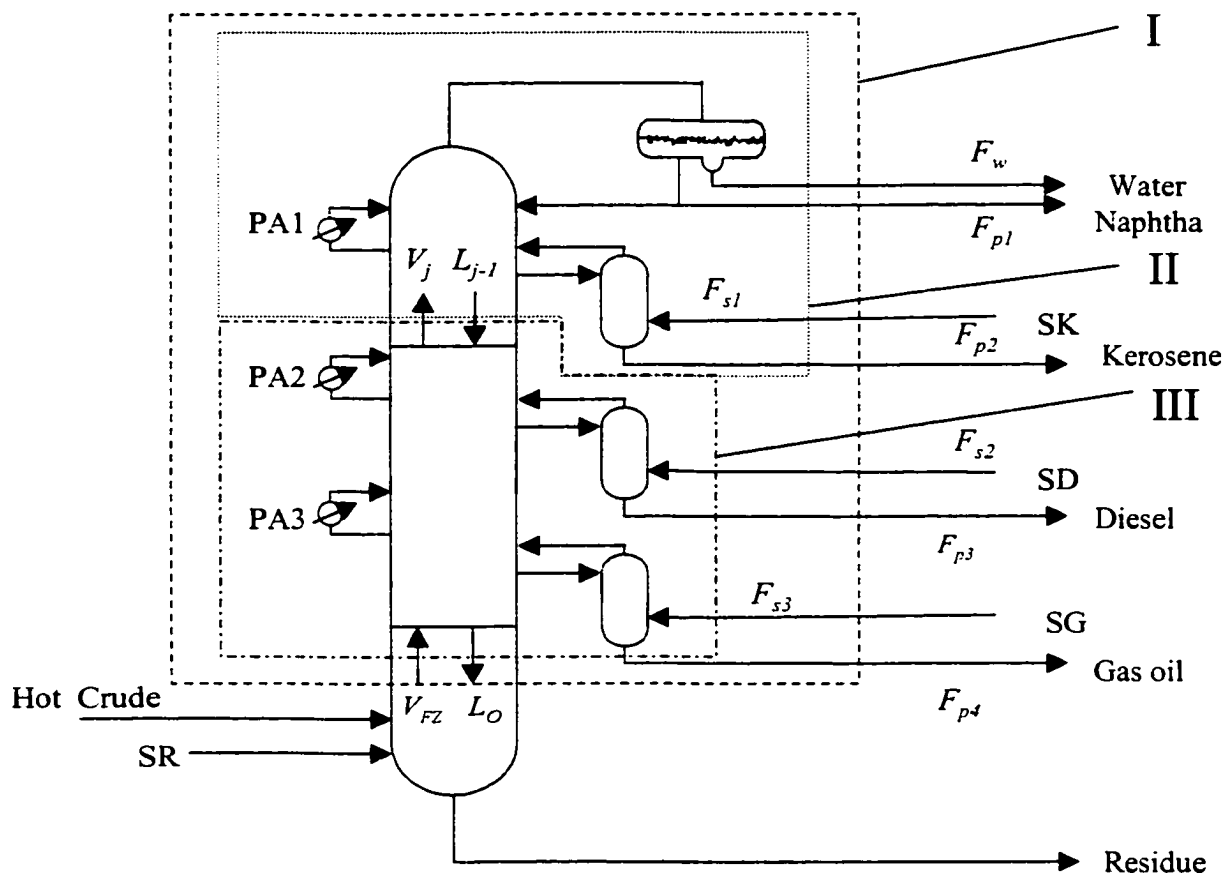


Figure 2.3 Heat Balance of the Distillation Column

Effect of Heat Shifting on Separation

It is well known that heat shifting reduces separation efficiency. The presence of the pump-around circuit decreases the number of effective ideal trays (Bagajewicz, 1998). The effect can be even more detrimental to separation if the flowrate of a pump-around circuit is increased. As we shall see later, these effects can be compensated to a

certain extent by increasing the steam rate in the side strippers. Another solution is to increase the number of trays. However, with the total number of trays kept constant, the aforementioned relationship between heat recovery and steam consumption can be incorporated into the design procedure.

2.5 Design procedure

We now summarize the technique for designing a multipurpose energy efficient atmospheric column. First, the Watkins design method is used to obtain an initial scheme without pump-around circuits. Then a heat demand-supply diagram is constructed, and the direction of heat shifting needed for maximum energy efficiency is determined. This procedure is repeated for at least the lightest crude and the heaviest crude that will be processed. Thus, the design procedure is divided into two parts, the targeting procedure and the multipurpose heat exchanger network design. This paper focuses on the targeting procedure, which is presented next. After this, the goals of the heat exchanger network design procedure are outlined. The heat exchanger network design procedure is presented in part II.

Step 1: Begin with the lightest crude to be processed. As the lightest crude has the highest yields of light distillates, the supply of heat is the largest. Next, the major design parameters (the number of trays in each section, the pressure drop, and the amount of stripping steam) are chosen using the guidelines offered by Watkins with one exception: No pump-around circuits are included at this point.

Step 2: The simulation is performed next. Usually the column is not difficult to converge, as the liquid reflux ratio is large.

Step 3: The heat demand-supply diagram is constructed.

Step 4: The maximum amount of heat is transferred to a pump-around circuit located in the region between the top tray and the first product withdrawal tray. The location of the pump-around circuit withdrawal and the return temperature are conveniently chosen so that the energy recovery is maximized. This is discussed further when presenting the example.

Step 5: If the product gap becomes smaller than required, the stripping steam flowrate is to be increased to fix the gap. As long as the steam added has a lower cost than the energy saved, one can continue shifting loads. Otherwise, it is advisable to stop when a trade-off has been reached.

Step 6: If there is heat surplus from the pump-around circuit just added, transfer the heat to the next pump-around circuit between draws in the same way as in step 4. If not, stop.

At this stage, once this procedure is repeated for different crudes, one is left with heat removal targets from the condenser, the products and several pump-around circuit streams. Typically, since the light crude is the one that needs a larger reflux, it exhibits a larger amount of pump-around circuit duties. After these targets are determined, it is shown that there is still some flexibility to move heat from one pump-around to another, a feature that may be helpful in the final design of the heat exchanger network, or for retrofit. The above procedure is illustrated first. The results of this targeting procedure are

used as motivating material to discuss the goals of the multipurpose heat exchanger network, which is presented in part II.

2.6 Illustration

The properties of the light crude, intermediate crude and heavy crude are shown in Tables 2.1, 2 and 3. Table 2.4 indicates the specifications of the products. The product withdraw locations are determined according to Watkins' guidelines and the results are shown in Table 2.5.

Table 1 Feedstock Used for the Design

Crude	Density (kg/m ³)	Throughput (m ³ /hr)
Light Crude	845 (36.0 API)	795
Intermediate Crude	889 (27.7 API)	795
Heavy Crude	934 (20.0 API)	795

Table 2.2 TBP Data

Vol. %	Light Crude (°C)	Intermediate Crude (°C)	Heavy Crude (°C)
5	45	94	133
10	82	131	237
30	186	265	344
50	281	380	482
70	382	506	640
90	552	670	N/A

Table 2.3 Light-ends Composition of Crude in volume per cent

Compound	Light Crude	Intermediate Crude	Heavy Crude
Ethane	0.13	0.1	0
Propane	0.78	0.3	0.04
Isobutane	0.49	0.2	0.04
n-Butane	1.36	0.7	0.11
Isopentane	1.05	0	0.14
n-Pentane	1.30	0	0.16
Total	5.11	1.3	0.48

Table 2.4 Product Specifications and Withdrawal Tray

Product	Specification	Withdrawal Tray
Naphtha	D86 (95% point) =182 °C	1
Kerosene	D86 (95% point) =271 °C	9
Diesel	D86 (95% point) =327 °C	16
Gas Oil	D86 (95% point) =377-410 °C	25
Overflash rate	0.03	
Kerosene –Naphtha	(5-95) Gap \geq 16.7 °C	
Diesel- Kerosene	(5-95) Gap \geq 0 °C	
Gas Oil- Diesel	(5-95) Gap = -5.6 °C to -11 °C	
Feed Tray		29
Total Trays		34

There are 34 trays in the main column and 4 trays in each stripper. The flowrates of stripping steam streams are estimated and adjusted to 10 lb per barrel of product, as

suggested by Watkins. The total energy consumption (E) is calculated using the following expression:

$$E = U + 0.7 * \sum H_i^s \quad (2.5)$$

where U is the minimum heating utility obtained using straight pinch analysis, and $\sum H_i^s$ is the summation of energy flow of all steam streams. Because low-pressure steam is cheaper than fuel gas on the same amount of heat content, a weight factor of 0.7 is used for the steam. The total energy consumption is used as an objective function.

Simulation results for the initial scheme with no pump-around circuits are shown in Table 2.6. Note the product gaps are well above the specifications.

Table 2.5 Tray Requirements in Watkins Design

Separation	Number of Trays
Light Naphtha to Heavy Naphtha	6 to 8
Heavy Naphtha to Light Distillate	6 to 8
Light Distillate to Heavy Distillate	4 to 6
Heavy Distillate to Gas Oil	4 to 6
Flash Zone to First Draw Tray	3 to 4
Steam Stripping Sections	4

The heat demand-supply diagram corresponding to the solution in Table 2.6 is shown in Figure 2.4. There is huge heat surplus in the condenser region, which results in a large cooling utility. Meanwhile, a large heat deficit exists above 155 °C. As the total heat supply is almost constant, the way toward energy savings is to change the heat supply profile. That is, instead of supplying all heat at a low temperature, some heat can

be supplied at a higher temperature where the heat demand is larger than the heat supply. In other words, transfer some heat from the condenser to a pump-around circuit as indicated by the arrow in Figure 2.4.

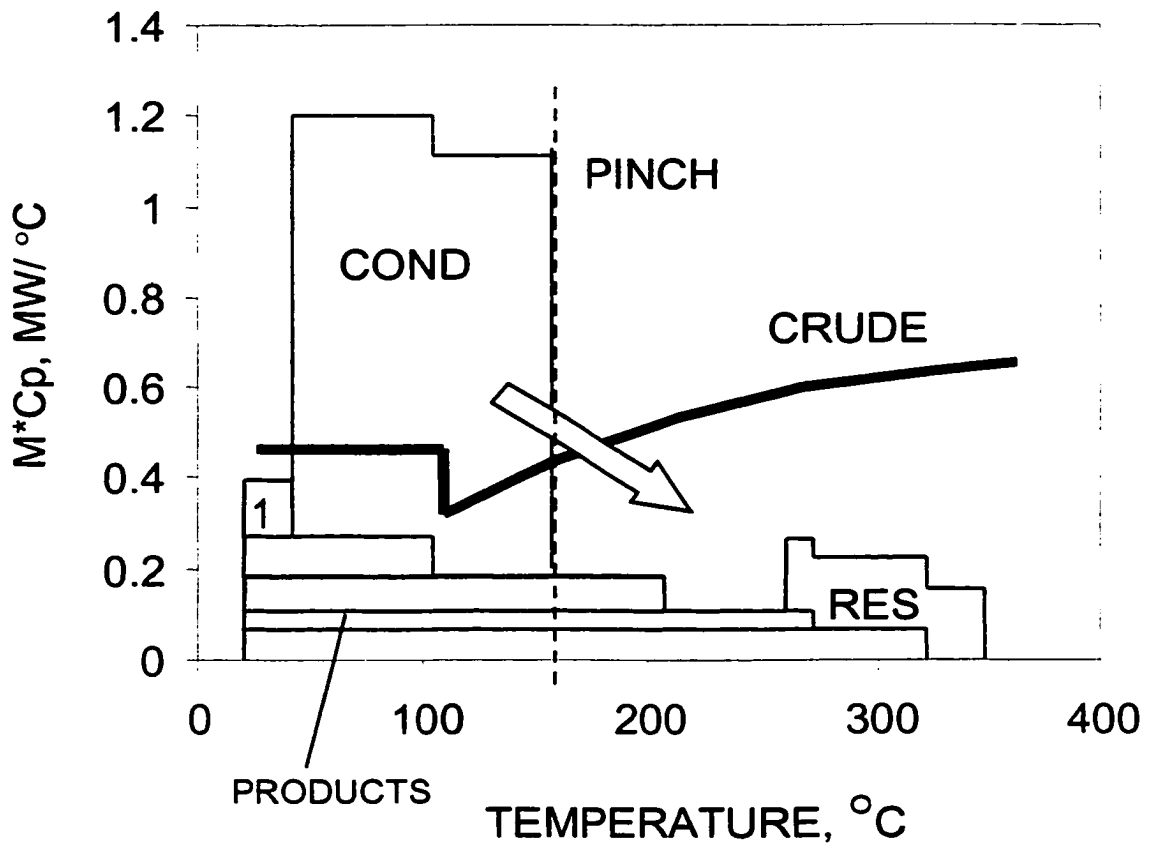


Figure 2.4 Heat Demand-Supply Diagram for Crude Distillation without Pump-Around Circuits

One Pump-Around Circuit

If a pump-around is above all side-withdrawal product lines, the heat that can be transferred from the condenser will be the maximum. Therefore, the first pump-around

has to be above the kerosene withdrawal tray. The question is how many trays one should put between the condenser and the top pump-around region. We recommend the top pump-around region be adjacent to the condenser. No tray is put in between. This is based on the observation that the trays below a product withdraw line and above an adjacent pump-around circuit receive little reflux and barely contribute to separation. The pump-around stream is withdrawn from tray 4, cooled in the heat exchangers and returned to tray 2. The return temperature is 104.4 °C, which is optimized after the duty is determined.

The duty of the top pump-around (PA1) is increased gradually and product gaps are examined in each simulation. The kerosene-naphtha gap decreases with the increase of PA1 duty, but remains well above that of specification, while the other gaps are almost unchanged. The heat shift continues without violating the gap specifications until the reflux ratio is around 0.1. Further heat shift would result in liquid drying up on the top tray. Thus, the limit of the heat shifting has been reached. The duty of 62 MW represents the total amount of heat one could obtain from all pump-around circuits. The following steps consist of distributing this amount of heat properly among several pump-around circuits. The main operation variables of the scheme with one pump-around are shown in Table 2.6.

The major conclusions are:

- The total energy consumption (E) decreases by 7 MW compared to the no pump-around scheme.
- The kerosene-naphtha gap is reduced from 25 °C to 23 °C, remaining well above the specification of 16.7 °C.

Table 2.6 Comparative Results of One Top Pump-Around and No Pump-Around

Product	No Pump-around	One Pump-around
Naphtha Flowrate	250 m ³ /hr	248 m ³ /hr
Kerosene Flowrate	144 m ³ /hr	146 m ³ /hr
Diesel Flowrate	70 m ³ /hr	70 m ³ /hr
Gas Oil Flowrate	121 m ³ /hr	121 m ³ /hr
Residue Flowrate	211 m ³ /hr	211 m ³ /hr
Kerosene Stripping Steam Ratio*	9.82	9.68
Diesel Stripping Steam Ratio	10.22	10.27
Gas Oil Stripping Steam Ratio	10.12	10.11
Residue Stripping Steam Ratio	10.19	10.19
Kerosene-Naphtha (5%-95%) Gap	25.12°C	23.0°C
(5-95) Diesel-Kerosene Gap	5.14°C	5.31°C
(5-95) Gas Oil- Diesel Gap	0.93°C	0.91°C
Kerosene Withdrawal Tray Temperature	238.8°C	237.1°C
Diesel Withdrawal Tray Temperature	298.7°C	298.7°C
Gas Oil Withdrawal Tray Temperature	338.7°C	338.7°C
Residue Withdrawal Temperature	347.8°C	347.8°C
Condenser Duty	103.86 MW	41.70 MW
Condenser Temperature Range	155-43.3 °C	146.4-43.3 °C
Pump-around 1 Duty	-	62.14 MW
Pump-around 1 Temperature Range	-	179.6-104.4 °C
Flash Zone Temperature	358.6 °C	358.6 °C
Energy Consumption (E)	103.78 MW	96.77 MW

*Steam amount in lb/hr over the amount of product in bbl/hr.

- The yield of naphtha decreases and the yield of kerosene increases. This is because some light components of the vapor are absorbed by the cold pump-around stream and carried to the kerosene withdrawal tray. Note that the total yield of the two products remains constant.
- Little change takes place below the kerosene withdrawal tray.

We now turn our attention to the resulting heat demand-supply diagram (Figure 2.5). The shaded area is the energy savings achieved by adding PA1. The heat surplus in the condenser region is greatly reduced, but it is still significant. However, it is impossible to shift more heat from the condenser to PA1.

The return temperature of PA1 is not important in terms of energy consumption, because the heat surplus is larger than the demand below the PA1 withdrawal temperature. To reduce the heat surplus in the region of PA1, a second pump-around is installed at a position as indicated in Figure 2.5.

The second pump-around (PA2) is positioned between tray 10 and tray 12, just below the kerosene withdrawal tray. The return temperature is chosen to be approximately equal to that of the withdrawal temperature of PA1. A lower temperature would result in heat surplus in the region of PA1, while a very high return temperature would not alter the energy savings but result in a heavier liquid traffic in the PA2 region. With the increase of the PA2 duty, the gap between kerosene and naphtha decreases quickly. Table 2.7 shows the change of gaps as a function of the duty of pump-around PA2.

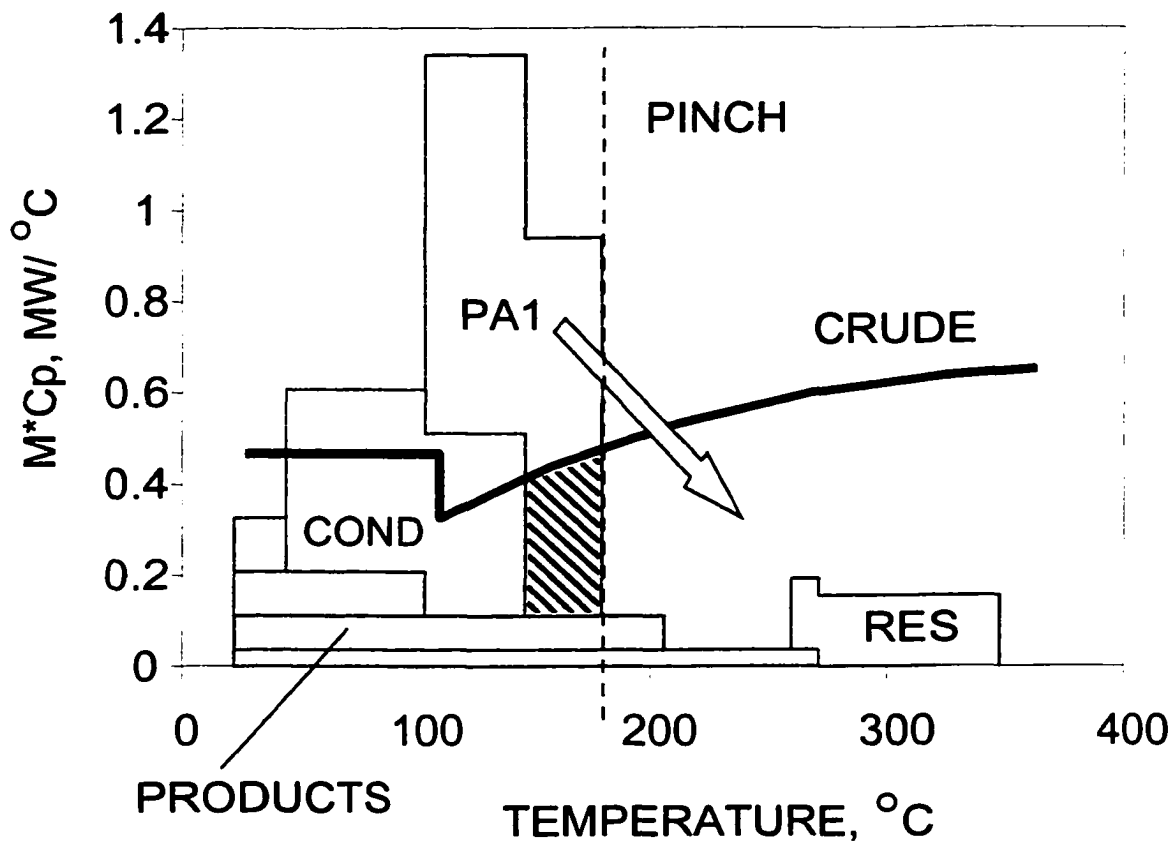


Figure 2.5 Heat Demand-Supply Diagram for Crude Distillation with a Top Pump-around Two Pump-Around Circuits

When the duty of PA2 is larger than 33.7 MW, the kerosene-naphtha gap does not satisfy the specification. To recover this gap, one could increase the stripping steam flowrate or increase the number of trays in the naphtha-kerosene section. The former option is used in this work, while the latter may not be sufficient or even practical on its own. The kerosene and diesel stripping steam flowrates are adjusted with a controller in which the gap specifications are defined.

Table 2.7 Effect of Increasing PA2 Duty without Changing Steam Flowrates

	1	2
Duty of PA2	29.31 MW	33.71 MW
Duty of PA1	32.83 MW	28.43 MW
Duty of Condenser	41.94 MW	42.03 MW
(5-95) Kerosene-Naphtha Gap	18.49 °C	16.60 °C
(5-95) Diesel-Kerosene Gap	1.63 °C	1.48 °C
(5-95) Gas Oil- Diesel Gap	1.22 °C	1.23 °C
Energy Consumption	70.59 MW	67.35 MW

With the help of the stripping steam, it is possible to move more heat from PA1 to PA2. The trade off between increasing energy recovery and spending more steam is evaluated using equation (2.5). Heat shifting continues until the liquid reflux at the kerosene withdrawal tray is small and /or the kerosene-naphtha gap cannot be recovered even with increased amounts of stripping steam. This is a limit imposed by the separation requirement. The limiting case is shown in Table 2.9 (first column) and should be compared with the second column of Table 2.6.

The major changes from one pump-around to two pump-around circuits are:

- The net energy consumption decreases sharply by 32 MW.
- The flowrate of the kerosene stripping steam is nearly doubled. The large extra steam is used to strip a significant amount of light components in the kerosene withdrawal stream. The top section of the column becomes less hot because of the increased stripping steam. The kerosene withdrawal temperature drops by 33 °C.
- The yield of diesel increases while the yield of naphtha decreases.

The heat demand-supply diagram (Figure 2.6) shows a good match, and the pinch temperature increases to the value of the PA2 withdrawal temperature. The heat surplus in the region of PA1 is still high, but further shifting would cost too much steam to be beneficial. Therefore, this remaining heat surplus is useless. Now the only heat surplus transferable is located in the PA2 circuit, shown as the shaded area in Figure 2.6. To make use of this heat surplus, it is necessary to add a third pump-around circuit.

Three Pump-Around Scheme

The third pump-around (PA3) is located between tray 17 and tray 19. The return temperature is 232 °C. Heat is shifted gradually from PA2 to PA3, with the gaps maintained by adjusting steam flowrates. The effect of the duty of PA3 on energy consumption is shown in Table 2.8. A summary of all variables is given in Table 2.9.

Table 2.8 Effect of the Duty of PA3 on Energy Consumption

PA3 Duty (MW)	Energy Consumption (MW)
6.45	61.96
8.79	61.64
13.19	61.67
23.45	63.76
26.67	64.56

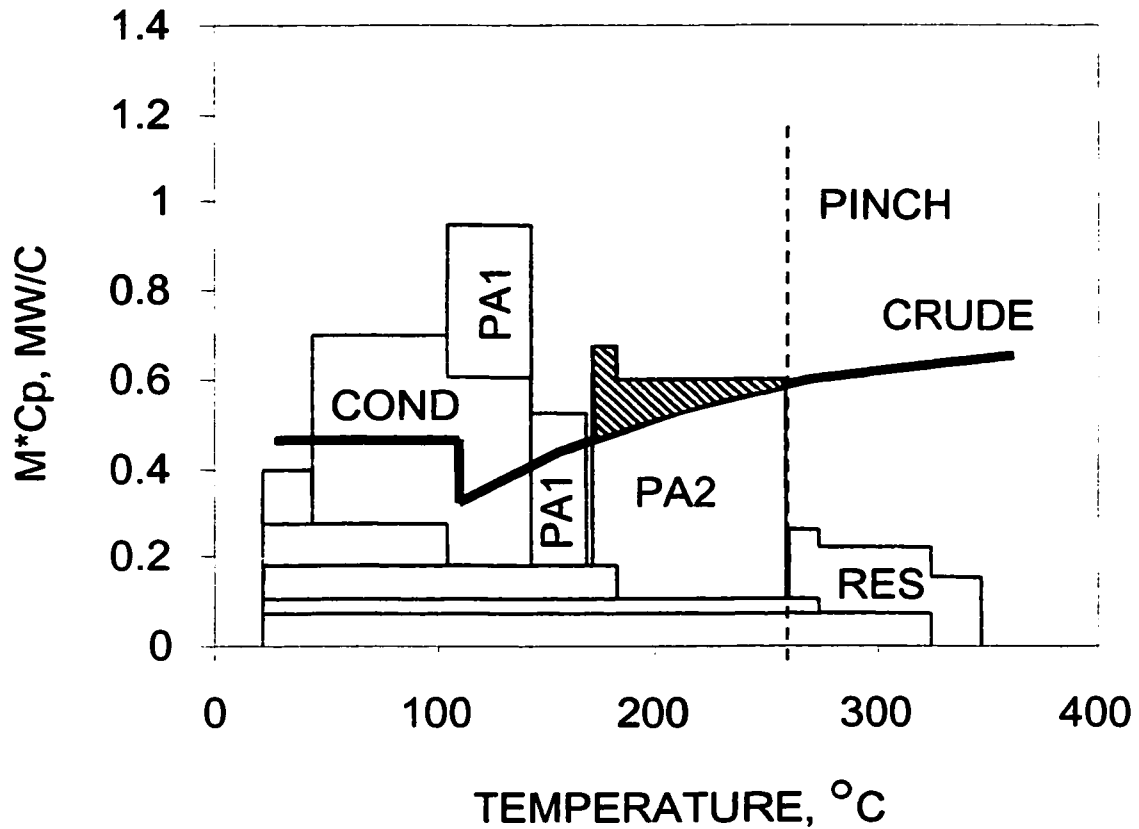


Figure 2.6 Heat Demand-Supply Diagram for Crude Distillation with Two Pump-Around Circuits.

At the beginning, the energy consumption decreases with the increase of the duty of PA3. However, when the PA3 duty exceeds 8.8 MW, the energy consumption stays constant in a rather wide range (Table 2.8). This is because little heat surplus exists in the region of PA2. Therefore, more heat shift makes no difference. Beyond this stable range, more heat shift to PA3 results in an increase in energy consumption due to increased use of steam, which means that the cost of additional steam consumption outweighs the gain in energy recovery. Clearly 8.8 MW is the right point to stop. This effect cannot be captured with other design procedures.

Table 2.9 Comparative Results for Two and Three Pump-Around Circuits

Product	2 Pump-around circuits	3 Pump-around circuits
Naphtha Flowrate	244 m ³ /hr	244 m ³ /hr
Kerosene Flowrate	145.6 m ³ /hr	145.5 m ³ /hr
Diesel Flowrate	73.6 m ³ /hr	72.5 m ³ /hr
Gas Oil Flowrate	121.6 m ³ /hr	123.85 m ³ /hr
Residue Flowrate	210.5 m ³ /hr	209.7 m ³ /hr
Kerosene Stripping Steam Ratio*	19.02	18.04
Diesel Stripping Steam Ratio	8.11	12.54
Gas Oil Stripping Steam Ratio	7.84	7.71
Residue Stripping Steam Ratio	10.20	10.24
(5-95) Kerosene-Naphtha Gap	16.7 °C	16.7 °C
(5-95) Diesel-Kerosene Gap	0 °C	0 °C
(5-95) Gas Oil- Diesel Gap	-2.0 °C	-2.9 °C
Kerosene Withdrawal Tray Temperature	202.2 °C	212.7 °C
Diesel Withdrawal Tray Temperature	291.2 °C	289.9 °C
Gas Oil Withdrawal Tray Temperature	336.1 °C	338.9 °C
Residue Withdrawal Temperature	347.9 °C	348.2 °C
Condenser Duty	42.4 MW	43.3 MW
Condenser Temperature Range	143.6-43.3 °C	143.5-43.3 °C
Pump-around 1 Duty	22.3 MW	22.3 MW
Pump-around 1 Temperature Range	169.2-104.4 °C	169.4-104.4 °C
Pump-around 2 Duty	42.5 MW	33.7 MW
Pump-around 2 Temperature Range	257.9-171.1 °C	255.3-171.1 °C
Pump-around 3 Duty	-	8.8 MW
Pump-around 3 Temperature Range	-	310.6-232.2 °C
Flash Zone Temperature	358.7°C	359 °C
Energy Consumption	64.73 MW	61.64 MW

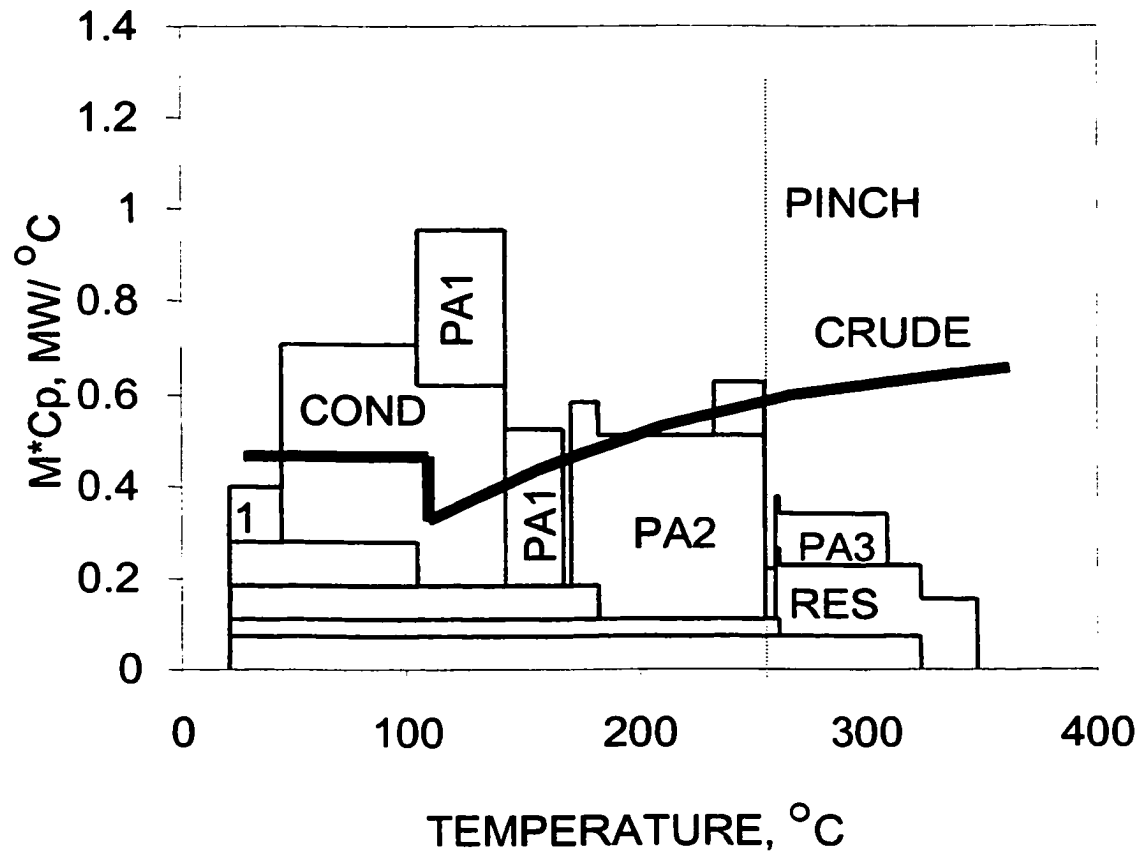


Figure 2.7 Heat Demand-Supply Diagram for Crude Distillation with Three Pump-Around Circuits

Figure 2.7 is the heat demand-supply diagram. The heat surplus previously in the region of PA2 (Figure 2.6) has been moved to the PA3, which accounts for the decrease in energy consumption.

It should be pointed out that the distribution of pump-around duty has a remarkable effect on the column temperature profile. Figure 2.8 shows stream temperature changes as a function of the duty of the third pump-around. With the

increase of these duties, the temperatures of the products and the pump-around circuits decrease.

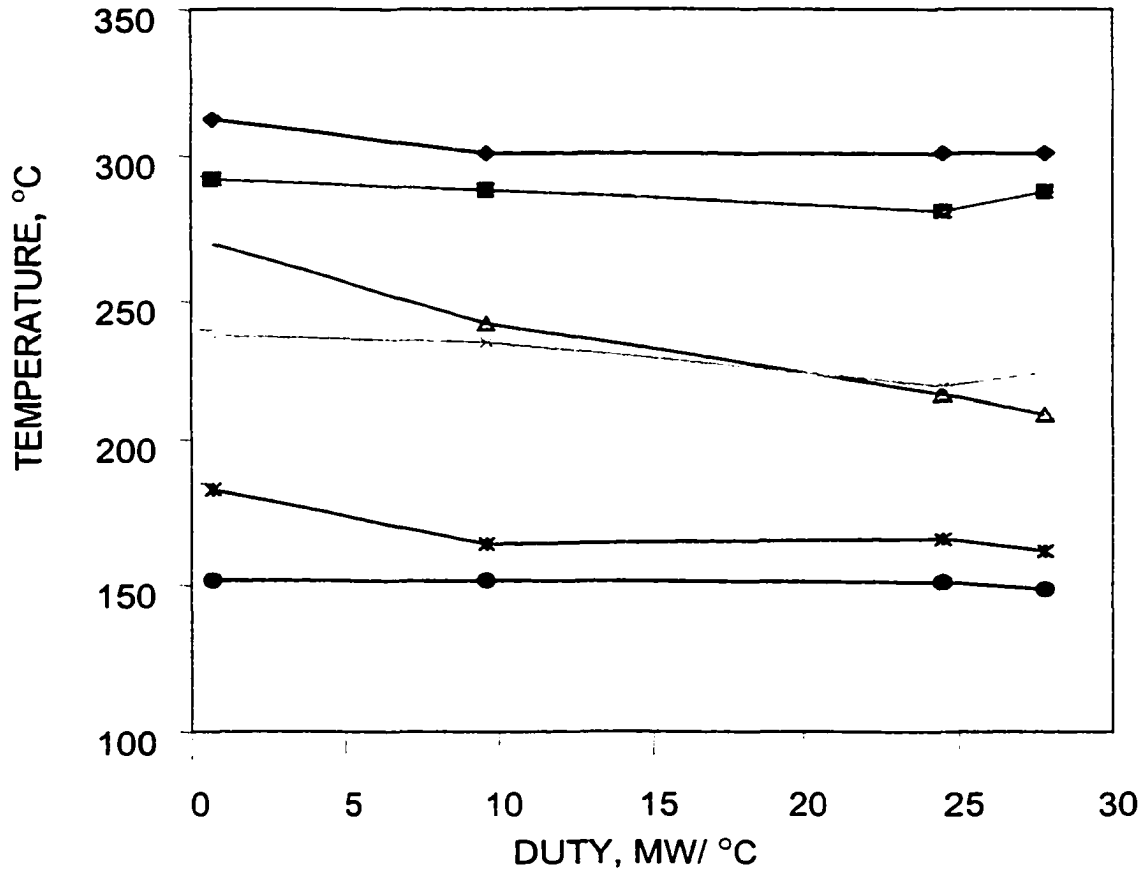


Figure 2.8 Pump-Around Withdrawal Temperatures and Product Temperatures as a Function of the Duty of the third Pump-Around (Light Crude)

Finally, the effect of the pump-around return temperatures is briefly explored. As the pinch temperature is located in the region of PA2, its return temperature affects the energy consumption. Figure 2.9 shows this effect.

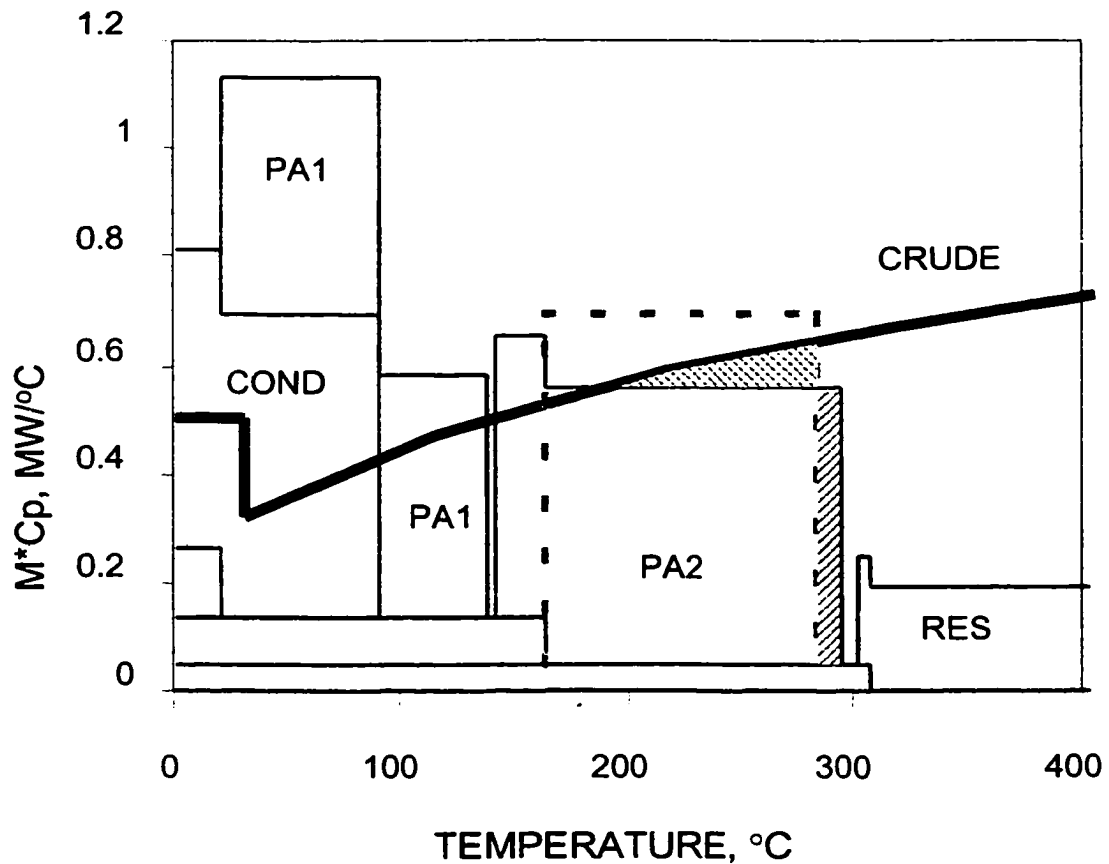


Figure 2.9 Effect of the Return Temperature of PA2 on Energy Consumption

In the figure, PA3 is not shown for simplicity. The dotted line is the new PA2 region with a higher return temperature and the shaded areas are the changes incurred. When the PA2 duty is constant, a higher return temperature results in a lower withdrawal temperature. The total effect depends on the trade off between these two effects, or the area difference between the shaded triangle and the shaded rectangle. The trade off is shown in Table 2.10. The optimal return temperature is found to be 177.8 °C.

Table 2.10 Effect of the Return Temperature of PA2 on Energy Consumption

PA2 Return Temperature (°C)	Withdrawal Temperature (°C)	Diesel Stripping Steam (MW)	Energy Consumption (MW)
171.1	255.3	2.15	61.64
177.8	254.4	2.17	60.91
193.3	251.9	2.25	61.96

At this point we have reached the best scheme for the light crude. Next we perform the same analysis for the heavy crude.

Heavy Crude

The total energy consumption and the pump-around duty distribution are shown in Table 2.11. The heat demand-supply diagram and the operation variables for a scheme with three pump-around circuits are shown in Figure 2.10 and Table 2.12. The following results are observed:

Table 2.11 Effect of Pump-Around Duties on Energy Consumption
(Heavy Crude, $\Delta T = 5.6$ °C)

PA1 Duty (MW)	PA2 Duty (MW)	PA3 Duty (MW)	Energy Consumption (MW)
0	0	0	24.27
6.10	0	0	23.88
2.32	4.34	0	23.88
2.32	2.20	2.14	23.79

- The energy consumption changes very little when shifting heat from the condenser to the pump-around circuits, especially when heat is shifted from PA1 to PA2 or PA3.
- This is because that there is no heat surplus in the condenser region (Figure 2.10). However, because the light crude and the medium crude require the PA2 and PA3 heat exchangers, shifting heat from PA1 to PA2 and PA3 in heavy crude design may be necessary.

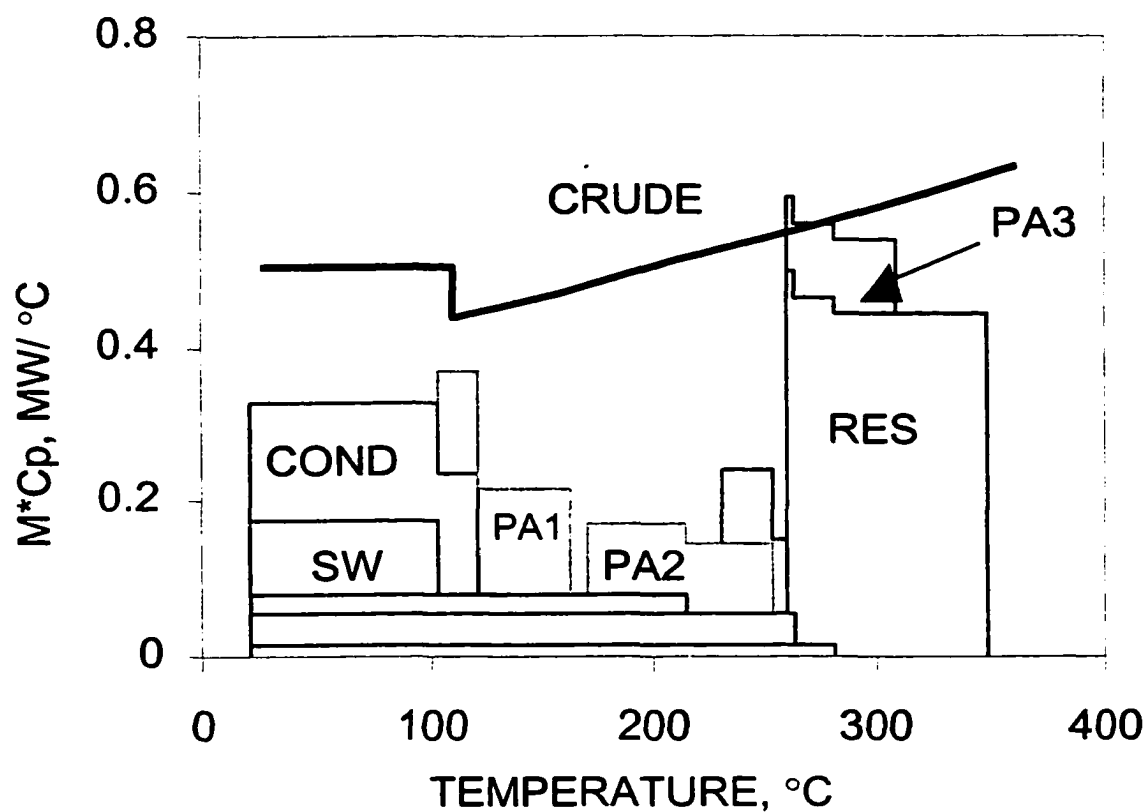


Figure 2.10 Heat Demand-Supply Diagram for Heavy Crude Distillation

Table 2.12 Results for Heavy Crude

Product	Heavy Crude
Naphtha Flowrate	55.37 m ³ /hr
Kerosene Flowrate	48.64 m ³ /hr
Diesel Flowrate	69.36 m ³ /hr
Gas Oil Flowrate	29.37 m ³ /hr
Residue Flowrate	592.51 m ³ /hr
Kerosene Stripping Steam Ratio*	1.63
Diesel Stripping Steam Ratio	2.98
Gas Oil Stripping Steam Ratio	37.9
Residue Stripping Steam Ratio	2.68
(5-95) Kerosene-Naphtha Gap	26.07 °C
(5-95) Diesel-Kerosene Gap	0.86 °C
(5-95) Gas Oil- Diesel Gap	-5.84°C
Kerosene Withdrawal Tray Temperature	259.7°C
Diesel Withdrawal Tray Temperature	317.4 °C
Gas Oil Withdrawal Tray Temperature	344.4 °C
Residue Withdrawal Temperature	366.7 °C
Condenser Duty	14.8 MW
Condenser Temperature Range	123.3-18.5 °C
PA1 Duty	20.8 MW
PA1 Temperature Range	175.7-104.4 °C
Flash Zone Temperature	353.2 °C
Energy Consumption	81.49 MW

When heat is shifted to PA2 and PA3, more steam is needed for the diesel stripper to regain the kerosene-diesel gap. The diesel stripping steam flowrates for the designs with one pump-around, two pump-around and three pump-around circuits are 32.5, 48.5 and

113.4 kg-mole/hr respectively. Although the steam consumption increases, the total energy consumption is barely affected because the heat from the extra steam is utilized to cover the heat deficit in the condenser region.

- The separation of kerosene and diesel in the column is much easier than that of the light crude. Before stripping, the gap between kerosene and naphtha is 17.2 °C, satisfying the separation requirement.

2.7 Effect of minimum temperature approach

The effect of HRAT on the optimal pump-around duty distribution is shown in Tables 13, 14 and 15.

Table 2.13 Effect of HRAT on Energy Consumption (Light Crude)

HRAT (°C)	PA1 Duty (MW)	PA2 Duty (MW)	PA3 Duty (MW)	Energy Consumption (MW)
5.6	22.3	34	8.8	61
22.2	22.3	29	8.8	69.8
44.4	22.3	23	13.2	81.2

Table 2.14 Effect of HRAT on Energy Consumption (Heavy Crude)

HRAT (°C)	PA1 Duty (MW)	PA2 Duty (MW)	PA3 Duty (MW)	Energy Consumption (MW)
5.6	7.9	7.5	7.3	81.2
22.2	22.6	0	0	86.4
44.4	22.6	0	0	93.1

Note that for the light crude, PA3 duty increases with the increase of HRAT. This can be explained using the heat demand-supply diagram (Figure 2.7). When the HRAT is 5.6°C, there is almost no heat surplus in the region of PA2. However, when HRAT is increased, the crude demand curve is moved to the right and heat surplus appears again. Thus, the heat surplus needs to be reduced to achieve the maximum energy savings. The heavy crude behaves differently. As there is no heat surplus in the region of the condenser and PA1, shifting heat from PA1 to PA2 or PA3 does not reduce the net heat demand while more stripping steam is needed to keep the product gaps. At low HRAT (e.g., 5.6 °C), most of the heat coming from the condenser can be used because of the heat deficit in the condenser region. However, when HRAT is raised, the overlapping between the crude curve and the condenser curve reduces, and part of the heat from the condenser is at a temperature that is too low to be usable. In such a case, the heat from the increased steam cannot be used. Therefore, heat shifting to the lower pump-around circuits is not beneficial.

Table 2.15 Effect of HRAT on Energy Consumption (Medium Crude)

HRAT (°C)	PA1 Duty (MW)	PA2 Duty (MW)	PA3 Duty (MW)	Energy Consumption (MW)
5.6	15.2	26.4	0	63.1
22.2	15.2	26.4	0	70.4
44.4	15.2	26.4	0	79.9

These calculations were also performed for the intermediate crude (Table 2.15). In this case, the heat distribution does not change with HRAT. This is because there is always a heat surplus in the region of PA1 and a heat deficit in the region of PA2. The

heat surplus in the region of PA1 prompts maximum heat shift to PA2, while the heat deficit in PA2 excludes the need for shifting heat to PA3. Thus, the optimal solution is to maximize the duty of PA2.

2.8 Flexibility

The basis of this design procedure is the transferring of heat duty from the condenser to the lower pump-around circuits. In doing so, limits to this transfer are encountered. In addition, heat surplus can be transferred back. For example, the heat surplus observed in the pump-around PA1 for the light crude (Figure 2.7) could in principle be transferred back to the condenser without affecting the utility consumption. Such flexibility is further discussed in part II.

2.9 Reboiler

Reboilers are rarely used in the conventional crude distillation because their installation is expensive and sometimes they are less efficient than steam stripping. However, Liebmann *et al.* (1998) suggested that the use of reboilers can lead to energy savings. This conclusion is made by analyzing a scenario where water to produce steam is considered as another cold stream. We now revisit this analysis.

If one assumes that steam is another heat sink, then the location of the pinch changes. Figure 2.11 shows the demand-supply diagram of the light crude. The heavy solid curve represents the heat demand for both the crude and the steam. The heat demand for the crude is shown as a broken curve for comparison. In this figure, a heat surplus can be observed in the PA2 region.

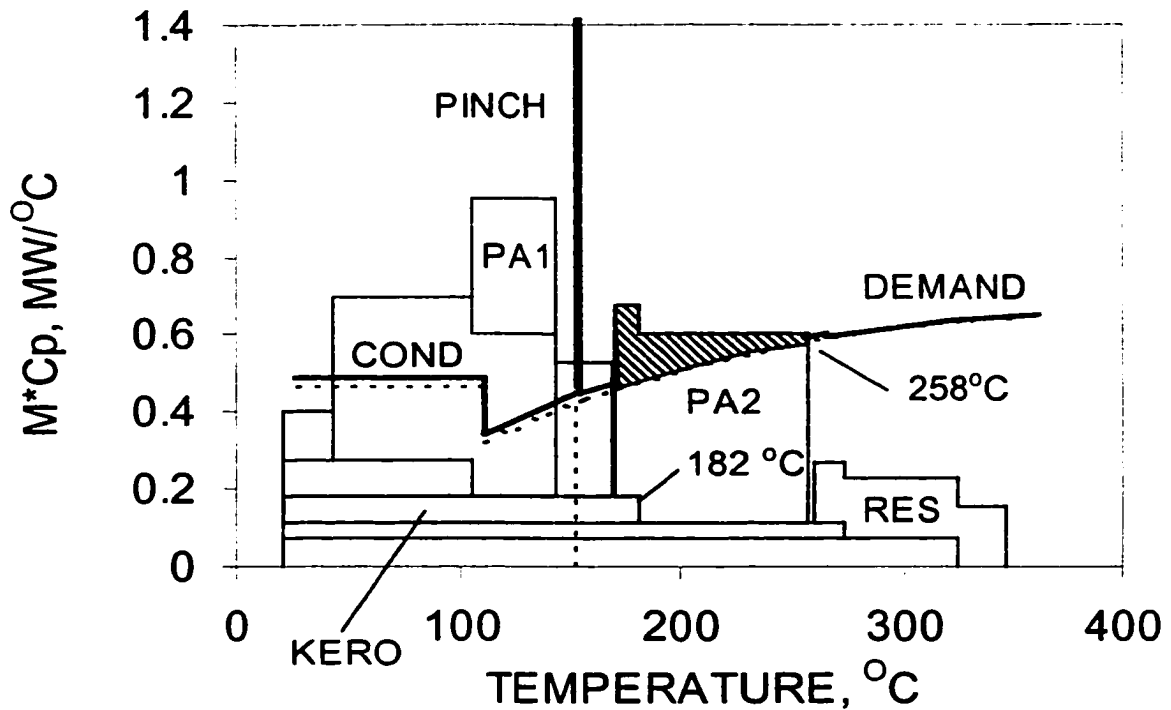


Figure 2.11 Heat Demand-Supply Diagram for Light Crude Including Steam as Cold Stream

To utilize the heat surplus, there are three options:

- Shift the heat to the third pump-around.
- Produce low-pressure steam.
- Install a reboiler for stripping kerosene.

Each option has its advantage. Shifting the heat surplus to the third pump-around can reduce the duty of the furnace. Heat provided by the furnace is relatively expensive, because the furnace is usually less efficient than a boiler. However, heat shifting from PA2 to PA3 deteriorates the separation and consequently, extra steam is needed for

stripping gas oil. Thus, the choice between the first two options is a matter of a cost-benefit analysis, and it can not be determined merely on energy savings considerations.

The choice between producing steam versus installing a reboiler depends on the amount of light components to be stripped. The use of steam is more efficient for stripping a low amount of light components, while a reboiler is better for removing a relatively large amount of components (Nelson, 1958, Liebmann *et al.*, 1998). It is also possible that a combination of these options offers an optimal solution. To find the best design, all options should be carefully evaluated.

When steam is considered free or is priced as it is proposed in this article, without allowing its production to participate in the design procedure, then the installation of reboilers should be analyzed using the demand-supply diagram offered in Figure 2.6 or 7. In this case, the shifting of heat to PA3 is energy savings related and the use of reboilers needs to be made by using some other external heat source because process heat is no longer available in this case. Thus, their installation can only influence the steam consumption but it is replaced by a similar duty. The choice is therefore not driven by energy savings, but by a cost-benefit analysis that depends on the cost of the reboilers to install and their efficiency relative to direct steam.

2.10 Applicability to other crudes

The light crude and the heavy crude represent two extremes in the raw material spectrum. Any other crude could be thought of as a mixture of the two crudes. Based on the above information, we may design an optimal HEN that allows several crudes being processed at optimal conditions. The conjecture is that building a network addressing the

extremes allows also processing a crude of intermediate density at maximum energy efficiency. This is explored in more detail in part II.

2.11 Conclusion

In this paper, a rigorous targeting design procedure has been proposed for the design of conventional crude distillation units. This procedure is an improvement over the existing procedures for several reasons. First, this procedure aims at finding the best scheme for a multipurpose crude distillation unit that processes a variety of crudes. Second, the procedure is more straightforward. Heat demand-supply diagrams, instead of grand composite curves are used as a guide directing the search for optimal schemes. An advantage of heat demand-supply diagrams is that the role of each stream, heater or cooler in the total energy consumption is clearly shown, so the search of the best scheme is straightforward. Third, the approach is rigorous. The trade off between different operating parameters is considered and the decision is based on quantitative calculations instead of simple assumptions. The second part paper concentrates on the design of heat exchange network.

2.12 Nomenclature

CR = (hot) crude oil

E = energy consumption defined by equation (5), MW

F = mass flowrate, kg/s

F_{pi} = mass flowrate of product i , kg/s

F_{si} = mass flowrate of steam i , kg/s

H_i^s = enthalpy of stripping steam i , MW

h_{FZ}^w = enthalpy of water (steam) at the flash zone, kJ/kg

h_{FZ}^o = enthalpy of hydrocarbon vapor at the flash zone, kJ/kg

$h_{L_{j-1}}$ = enthalpy of liquid falling from tray $j-1$, kJ/kg

h_{L_o} = enthalpy of liquid falling into the flash zone, kJ/kg

h_{pi} = enthalpy of product i , kJ/kg

h_{si} = enthalpy of steam i , kJ/kg

$h_{V_j}^w$ = enthalpy of water (steam) rising from tray j , kJ/kg

$h_{V_j}^o$ = enthalpy of hydrocarbon vapor rising from tray j , kJ/kg

L_o = overflow rate, kg/s

Q_k = duty of pump-around circuit k

R = reflux ratio

R_{min} = minimum reflux ratio

RES = Residue

S = steam

SD = diesel stripping steam

SG = gas oil stripping steam

SK = kerosene stripping steam

SR = residue stripping steam

V_j^w = water (steam) flowrate at tray j

V_{FZ} = vapor flowrate at flash zone

V_{FZ}^W = water (steam) flowrate at flash zone

V_{FZ}^O = hydrocarbon vapor flowrate at flash zone

V_j = vapor flowrate at tray j

V_j^O = hydrocarbon vapor flowrate at tray j

U = minimum heating utility excluding steam, MW

2.13 References

1. Agrawal, R., *Synthesis of Distillation Column Configurations for a Multicomponent Separation*. Ind. Eng. Chem. Res. 35, 1059-1071, (1996).
2. Andrecovich, M., and Westerberg, A., *A Simple Synthesis Method Based on Utility Bounding for Heat-integrated Distillation Sequences*, AIChE Journal, 31(3), 363-375, (1985).
3. Bagajewicz, M., *On the Design Flexibility of Crude Atmospheric Plants*. Chemical Engineering Communications, 166, 111-136, (1998).
4. Bagajewicz, M., S. Ji and J. Soto. *A Step-By-Step Targeting Procedure for The Design of Conventional Crude Distillation*. Enpromer 99, Florianopolis, Brazil, September. Submitted to Latin American Applied Research (1999).
5. Brugma, A. J., *The Brugma Process*. Refiner and Natural Gasoline Manufacturer, 20(9), 86, (1941).
6. Dhole, V. R. and Linnhoff, B., *Distillation Column targets*. Computers and Chemical engineering, 17(5/6), 549-560, (1993)

7. Glinos, K., and Malone, M. F., *Optimality Regions for Complex Column Alternatives in Distillation Systems*. Chem. Eng. Res. Des., 66, 229-240, (1988).
8. Hohmann, E. C., *Optimum Networks for Heat Exchangers*. Ph.D. Thesis, University of Southern California, (1971).
9. Huang, F., and Elshout, R., *Optimizing the Heat Recovery of Crude Units*. Chemical Engineering Progress, 72(7), 68-74, (1976).
10. Ji S. and M. Bagajewicz. *Rigorous Targeting Procedure For The Design Of Crude Fractionation Units With Pre-Flashing*. Escape 10. Florence, Italy (2000).
11. Liebmann, K., and Dhole, V. R., *Integrated Crude Distillation Design*. Computers & Chemical Engineering, 19, Supplement ,S119,(1995)
12. Liebmann, K.; Dhole, V. R. and Jobson, M., *Integration Design Of A Conventional Crude Oil Distillation Tower Using Pinch Analysis*. Institution of Chemical Engineers, 76(3), part A, 335-347, (1998).
13. Linnhoff, B., Dunford, H., and Smith R., *Heat Integration of Distillation Columns into Overall Process*. Chemical Engineering Science, 38(8), 1175-1188, (1983).
14. Miller, W. and Osborne, H. G. *History and Development of Some Important Phases of Petroleum Refining in the United States*. The Science of Petroleum (Oxford University Press, London), Volume 2, 1465-1477, (1938).
15. Nelson, W. L., *Petroleum Refinery Engineering*, 4th ed., New York, (1958).
16. Packie, J.W., *Distillation Equipment in the Oil Refining Industry*. AIChE Transactions 37, 51-58. (1941).

17. Naka, Y., Terashita, M., Hayashiguchi S., and Takamatsu T., *An Intermediate Heating and Cooling Method for a Distillation Column*. Journal of Chemical Engineering of Japan, 13(2), 123-129, (1980).
18. Sharma, R., Jindal, A., Mandawala, D., and Jana, S. K., *Design/Retrofit targets of Pump-around Refluxes for Better Energy Integration of a Crude Distillation Column*, Ind. Eng. Chem. Res. 38, 2411-2417, (1999)
19. Terranova, B., and Westerberg, A., *Temperature-Heat Diagrams for Complex Columns. 1. Intercooled/Interheated Distillation Columns*. Ind. Eng. Chem. Res. 28, 1374-1379, (1989)
20. Tedder, D.W., *The Heuristic Synthesis and Topology of Optimal Distillation Networks*. Ph.D. Thesis, University of Wisconsin, Madison, (1975).
21. Watkins, R. N., *Petroleum Refinery Distillation*. Gulf Publishing Company, (1979).

Chapter 3 Rigorous Targeting Procedure for the Design of Crude Fractionation with Pre-flashing

3.1 Overview

This paper presents a systematic procedure to obtain design targets for heat integration in conventional crude fractionation units that use pre-fractionation columns or pre-flash drums. It is shown that under the same high product yield conditions, pre-fractionation or pre-flashing are not advantageous from the energy point of view. This is in great part due to the loss of the carrier effect that light components have in separating heavy gas-oil fractions in the flash zone. However, if one accepts the yield of atmospheric gas oil to be smaller, then these pre-fractionation/pre-flash options consume less energy.

3.2 Introduction

In previous work (Bagajewicz and Ji, 2001), a systematic procedure for the design of conventional crude fractionation units was presented. This procedure is based on a step-by-step combination of rigorous simulation and heat integration. The procedure starts with a column without pump around circuits and as heat is transferred from the condenser to pump around circuits with higher temperature, a trade off between steam usage and furnace savings is established. This transfer of heat is possible due to the well-known operating and design flexibility that crude fractionation installations exhibit, knowledge that was formalized in detail by Bagajewicz (1998). The procedure presented by Bagajewicz and Ji (2001) makes use of rigorous simulations and heat supply-demand

diagrams similar to those introduced by Andrecovich and Westerberg (1985) and Terranova and Westerberg (1989). Based on these targets, a heat exchanger network design procedure to handle crudes of different density at maximum efficiency was developed (Bagajewicz and Ji, 2001; Bagajewicz and Soto, 2001). These design procedures did not use any pre-flashing or pre-fractionation schemes.

In this paper, a rigorous procedure to obtain targets of energy consumption and column reflux arrangements for pre-fractionation/pre-flashing units is presented. Figures 3.1 and 3.2 depict both schemes.

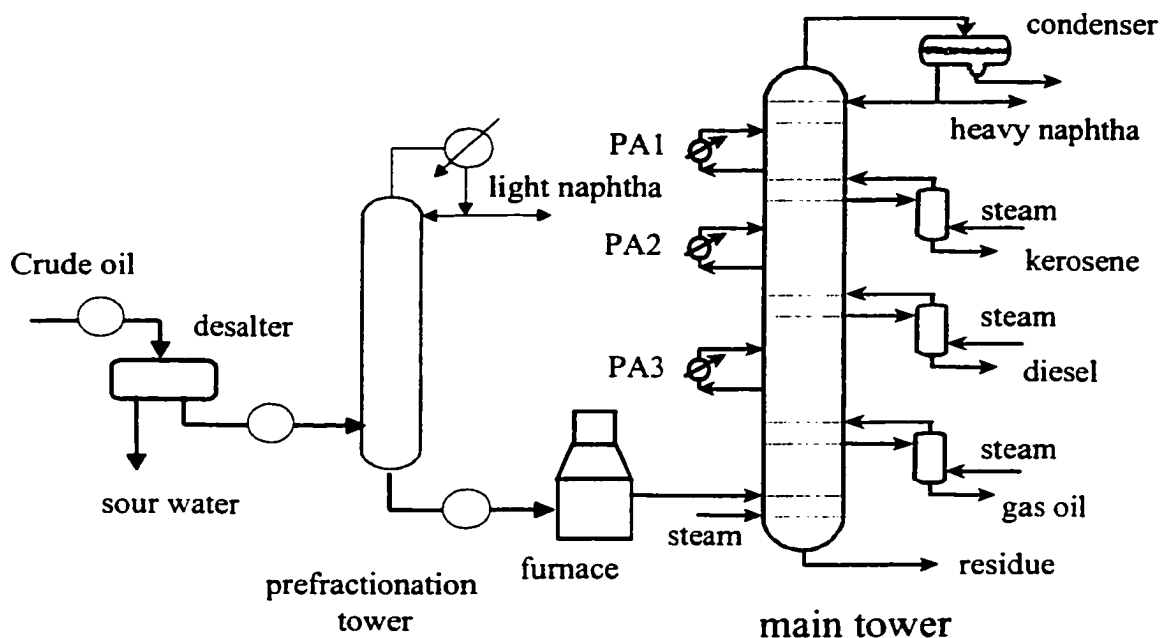


Figure 3.1 Basic Pre-fractionation Design (Heat exchanger network is omitted).

In the pre-flash scheme (Figure 3.2) the intended effect is to avoid unnecessary heating of light components in the furnace, short-circuiting them to be injected at an appropriate tray in the column for further fractionation. In the pre-fractionation scheme

(Figure 3.1), light products obtained in the pre-fractionation column are not sent to the main column.

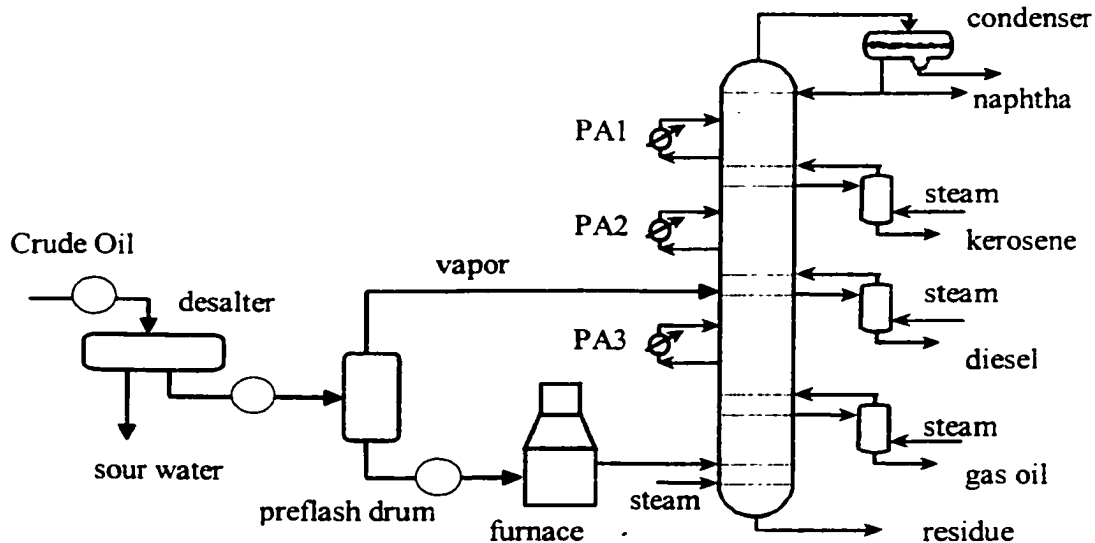


Figure 3.2 Basic Pre-flash Design (Heat exchanger network is omitted).

There are several unresolved questions regarding these designs. Among others:

1. In the case of pre-flashing, what is the optimum temperature of the flash drum?
2. In the case of pre-fractionation, what is the optimum temperature of the pre-fractionation column feed?
3. In the case of pre-flashing, what is the feed tray that one needs to use to feed the vapor from the drum into the column?
4. What are the loads of the pump-around circuits and what are the steam flowrates for stripping that produce the most energy efficient combination?

In addition, both schemes avoid introducing lights in the feed tray (flash zone) with the aforementioned expectation that one would avoid heating these lights unnecessarily. However, the so-called carrier effect of lights is known to increase the

separation of atmospheric gas-oil from the residue (Golden, 1997). Since steam can act as a carrier too, the question is whether it can actually substitute for the light hydrocarbons. Finally, if yield is to be sacrificed, what is the extent of yield reduction compared to energy savings? In other words, would it be worth reducing the yield to achieve energy efficiency?

All these questions have to be answered taking into account the fact that a specific quality of products (given by TBP or ASTM D86 points) needs to be guaranteed equally for all options that are compared.

3.3 Effect of pre-flashing on products

In this section the step-by-step procedure proposed by Bagajewicz and Ji (2001) is applied to both pre-fractionation and pre-flash schemes. In the case of pre-fractionation, the method can be applied directly. In the case of pre-flashing, the introduction of the vapor feed from the flash drum changes the heat load distribution in the column affecting the heat duty distribution of the pump around circuits. Thus, to better study the effect of the drum temperature and the feed tray, a column without pump around circuits is first used. Pump-around circuits are systematically added later.

The main column has 34 trays and side products are withdrawn at trays 9, 16 and 25 respectively. The outlet temperature of the furnace is set at 360 °C and the condenser temperature is fixed at 32 °C. Two crude oils, one light and one heavy are used in the study. Details of the assay data and product 95% distillation temperatures were given in by Bagajewicz and Ji (2000). The over flash rate chosen is 3%, the flowrates of side withdrawals and the condenser duty are adjusted to achieve the specifications of the over

flash rate and product 95% distillation temperatures and the flowrates of stripping steams are maintained constant. Finally the minimum approach temperature for energy targeting (HRAT) is 22.2 °C (40 °F), as suggested by Bagajewicz and Soto (2001)

Consider first a pre-flash drum operated at 163 °C and the feed tray to be tray 15. Tray 15 is chosen because the vapor concentration best matches the composition of the vapor from the drum. The effect of changing these two values will be studied later. The simulation results corresponding to a light crude with no pump-around circuits are shown in Table 3.1 and Figure 3.3. As shown by Bagajewicz (1998), pump-around circuits have an effect on energy recovery, but a very slight effect on product yield. Thus, as we shall see later, the energy consumption shown in Table 3.1 should further decrease as pump-around circuits are added.

Table 3.1 Comparison between Conventional and Pre-flash Design (Light crude)

	Conventional	Preflashing
Naphtha, M ³ /hr	249.6	249.3
Kerosene, M ³ /hr	144.1	143.9
Diesel, M ³ /hr	70.5	69.7
Gas oil, M ³ /hr	118.6	101.9
Residue, M ³ /hr	212.5	230.6
Product gaps, C		
Naphtha-Kerosene	25.1	24.5
Kerosene-Diesel	5	3.2
Diesel-GO	0.6	-0.9
Heating utility, MW	103.6	97.3
Energy consumption, MW	113	106.8

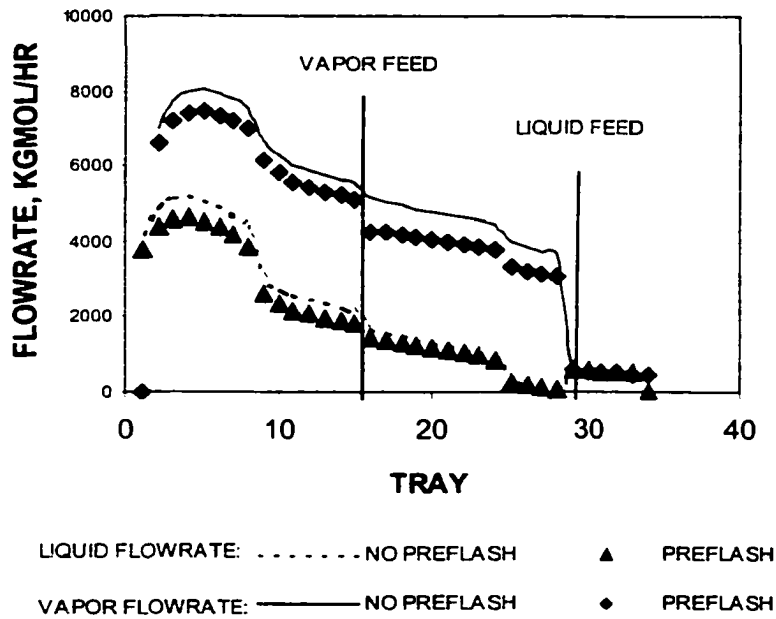


Figure 3.3 Comparison of Vapor and Liquid Distribution

The major differences are:

1. The vapor and liquid traffic decrease as a result of decreased heat input in the feed. That is, a lower reflux is needed.
2. The yield of gas oil decreases and the yield of residue increases as a result of less stripping ends existing at the flash zone of the column, and
3. The gaps between the different products decrease.

As we shall see later, the difference in yield for the gas-oil and the residues cannot be reconciled. Essentially, the presence of lights in the flash zone for the conventional case, which provide the so-called carrier effect, cannot be substituted by other stripping means in the case of the pre-flash or pre-fractionation designs. The comparison with a

pre-fractionation design is omitted as the same effect is expected for the reasons just outlined.

The same comparison was performed for the case of a heavy crude (Table 3.2). In this case no pump around circuits were used either.

Table 3.2 Comparison between Conventional and Pre-flashing Design (heavy crude)

	Conventional	Preflashing
Naphtha, M ³ /hr	54.5	54.2
Kerosene, M ³ /hr	47.9	48.4
Diesel, M ³ /hr	71.1	70.8
Gas oil, M ³ /hr	28.8	26.4
Residue, M ³ /hr	593.0	595.4
Product gaps, C		
Naphtha-Kerosene	19.8	18.6
Kerosene-Diesel	1.3	1.0
Diesel-GO	-5.6	-5.1
Heating utility, MW	101.3	100.5
Energy consumption, MW	106.5	105.8

Specifically, the yield of gas oil decreases. As the heavy crude contains less light distillates, vaporization in the heat exchanger network train is not severe and can be suppressed under moderate pressure. On the other hand, the heavy crude flashing at a low temperature (e.g., 163 °C) does not produce much vapor. From the viewpoint of energy savings, a small amount of vapor bypassing the furnace cannot significantly reduce the duty of the furnace. We can see from Table 3.2 that the energy consumption for the pre-flash design is only slightly lower. Therefore, the pre-flash design is not justified for heavy crude. The same can be said for the pre-fractionation design.

We now proceed to determine the optimal pump-around circuit loads. The heat is shifted from the condenser to the pump around circuits step-by-step, as proposed by Bagajewicz and Ji (2001). Briefly, the method consists of transferring as much heat as possible from the condenser to the pump around circuits until the overall minimum utility consumption reaches a minimum. The procedure is summarized next.

Step 1: Start with a column configuration suggested by Watkins with one exception: No pump-around circuits.

Step 2: Perform a simulation.

Step 3: Construct the supply-demand diagram.

Step 4: Transfer the optimum amount of heat to a pump-around circuit located in the region between the top tray and the first draw.

Step 5: If needed, increase the steam in the first side-stripper until the desired gap is restored.

Step 6: If there is heat surplus from the pump-around circuit just added, transfer the heat to the next region between draws in the same way as in step 4, if not, stop.

The fact that pre-flashing reduces gas oil yield reveals that the light components in the crude help the vaporization of heavy components. However, the yield of gas oil can also be increased by using more stripping steam. In other words, both light components in the crude oil and stripping steam have a stripping effect. We now discuss both cases:

- The stripping agent is steam.
- The stripping agent is a hydrocarbon, which exists in the mixture to be stripped.

Table 3.3 Comparison between Conventional and Pre-flash Designs with pump around circuits (light crude)

	Conventional	Preflashing
Naphtha, M ³ /hr	246.6	245.4
Kerosene, M ³ /hr	143.1	142.6
Diesel, M ³ /hr	73.9	74.4
Gas oil, M ³ /hr	119.4	102.4
Residue, M ³ /hr	212.5	230.6
Product gaps, C		
Naphtha-Kerosene	20.5	18.8
Kerosene-Diesel	-1.9	-6.6
Diesel-GO	-0.3	-1.7
Heating utility, MW	84.2	78.4
Energy consumption, MW	93.7	87.9

In the rest of the article, we will first explore the carrier effect and its intricacies in the case of crude fractionation, and then present a comparison between the pre-flash design and the conventional design for processing the light crude oil on the basis that both designs produce the same amount of residue.

3.4 Carrier effects

For the purpose of our analysis, the stripping effect of a component is defined as the differential change in the amount of residual liquid over the differential change of the amount of this component in the feed, provided that the system temperature, pressure and the quantities of other components are constant. Thus, when the addition of a component to the feed decreases the liquid rate, the assumption is that it happens at the expense of

vaporizing more of the heavy or intermediate components. Translated into the crude fractionation field, the presence of light ends, decreases the residue yield and therefore, increases the gas oil yield at its expense. We now analyze both stripping agents separately.

Case 1: Steam stripping

Stichlmair and Fair (1998) present a few charts obtained numerically, showing that the liquid yield in a flash is lowered when light components are added to a mixture. We attempt to explain this theoretically. We start using the well-known flash equations:

$$\left. \begin{aligned} x_i &= \frac{z_i}{\frac{L}{F} + (1 - \frac{L}{F}) \cdot K_i} \\ \sum_i x_i &= 1 \\ K_i &= \frac{P_i^s}{P} \end{aligned} \right\} \quad (3.1)$$

where x_i and z_i are the molar fraction of component i in the liquid and in the feed, P_i^s is the saturated pressure of component i , P is the total pressure of the system and L and F are the liquid flowrate and the feed respectively. The set of equations (1) is referred to as the no-steam equation. The vapor-liquid phase behavior is assumed to follow Raoult law, which is appropriate for hydrocarbons.

Let z_i^*, y_i^* be the dry compositions and F^*, V^* the dry flowrates. The temperature is assumed to be high enough so that any water in the liquid is neglected. A simple balance tells that:

$$y_i = y_i^* \left(1 - \frac{P_{st}}{P^*} \right) \quad (3.2)$$

where P_{st} is the partial pressure of steam, and P^* is the system pressure. For atmospheric distillation, P^* is somewhere between 0.24 and 0.37 MPa. Since $P^* \cdot y_i = P_i^s \cdot x_i$, we obtain:

$$\frac{y_i^*}{x_i^*} = \frac{P_i^s}{P^* - P_{st}} \quad (3.3)$$

For convenience, we define $K_i^* = \frac{y_i^*}{x_i^*}$. K_i^* is called the modified vapor-liquid equilibrium constant of component i . Finally, combining a dry component balance $F_i^* \cdot z_i^* = L \cdot x_i^* + V^* \cdot y_i^*$:

$$\left. \begin{aligned} x_i^* &= \frac{z_i^*}{\frac{L}{F^*} + \left(1 - \frac{L}{F^*}\right) \cdot K_i^*} \\ \sum_i x_i^* &= 1 \\ K_i^* &= \frac{P_i^s}{P^* - P_{st}} \end{aligned} \right\} \quad (3.4)$$

We now compare (1) and (4). For a given hydrocarbon mixture flashing at a fixed temperature, we have $z_i^* = z_i$ and $F^* = F$. Suppose the flash without steam and the flash with steam take place at the same temperature, then the saturated pressure of component i does not change. When $P = P^* - P_{st}$, we have $K_i^* = K_i$ and $x_i^* = x_i$. *This means that injecting steam is equivalent to reducing the system pressure.* Note that equation (3) still holds if steam is replaced by a gas that is insoluble in the hydrocarbon mixture. The use of steam, however, has some operational limits that will be explored later.

Case 2: Hydrocarbon stripping

We now consider the stripping effect of light components that distribute in both phases. Thus, using the following flash equations

$$l_i = \frac{f_i}{1 + \frac{F-L}{L} \cdot K_i} \quad (3.5)$$

$$L = \sum_j l_j \quad (3.6)$$

where l_i is the flowrate of component i in the liquid phase.

Differentiate (5) and consider that $\partial F / \partial f_i = 1$, to get:

$$\left(\frac{\partial L}{\partial f_i} \right)_{T,P,f_{j \neq i}} = \frac{l_i / f_i - \sum_j y_j \cdot l_j / f_j}{1 - (F/L) \cdot \sum_j y_j \cdot l_j / f_j} \quad (3.7)$$

Because the liquid-phase partition ratio l_i/f_i is less than 1, the summation in equation (7) is less than 1. Accordingly, the denominator is positive. Therefore, whether the derivative is negative or not depends on the nominator. The nominator consists of two terms. The first term represents the liquid-phase partition ratio of component i in the liquid phase, the second term is the average partition ratio of the mixture. If the partition ratio of component i is smaller than the average partition ratio, the derivative is negative, and the component has stripping effect. Thus, equation (7) can be used to determine if at a given pressure and temperature, a component is a stripping agent, that is, increasing its composition in the feed leads to a decrease of the liquid flowrate in the flash.

The stripping effect of each component in a mixture of aliphatic hydrocarbons is studied next. The composition of a mixture and the K-values of each component are shown in Table 3.4. The mixture is allowed to flash at 0.1 MPa and 393 °C. Figure 3.4

shows the residue/ feed ratio as a function of K-values of the added components. The molar ratios of the pure component added to the feed are 1/100, 5/100, 10/100, 20/100 and 30/100, respectively.

Table 3.4 Mixture Composition and K-values

	Molar Composition	K-Value
Water	0	267
Ethane	0	138
Propane	0	115
n-Butane	0	85.6
n-Hexane	0	45.2
n-Octane	0	27.4
n-Decane	0	17.8
n-Dodecane	0.04	12.2
n-Tetradecane	0.053	8.68
n-Hexadecane	0.064	5.84
n-Octadecane	0.077	3.79
n-C20	0.089	2.56
n-C22	0.098	1.75
n-C24	0.108	1.14
n-C26	0.117	0.79
n-C28	0.121	0.54
n-C30	0.107	0.38
n-C32	0.081	0.26
n-C36	0.045	0.13

Originally, the residue/feed ratio is 0.43. The residue/feed ratio decreases with an increasing K-value of the added component. Note that all curves intersect at $K=1.35$, at

which $\left(\frac{\partial L}{\partial f_i}\right)_{T,P,f_{j \neq i}}$ equals zero. When the K-value of the added component is greater than 1.35, the residue/feed ratio is lower than 0.43. This means these components act as stripping components. With the increase of the K-value, the residue/feed ratio decreases. When the K-value is greater than 30, the residue/feed ratio is almost constant. In this sense, water, ethane, propane and butane have the same stripping effect on a molar basis.

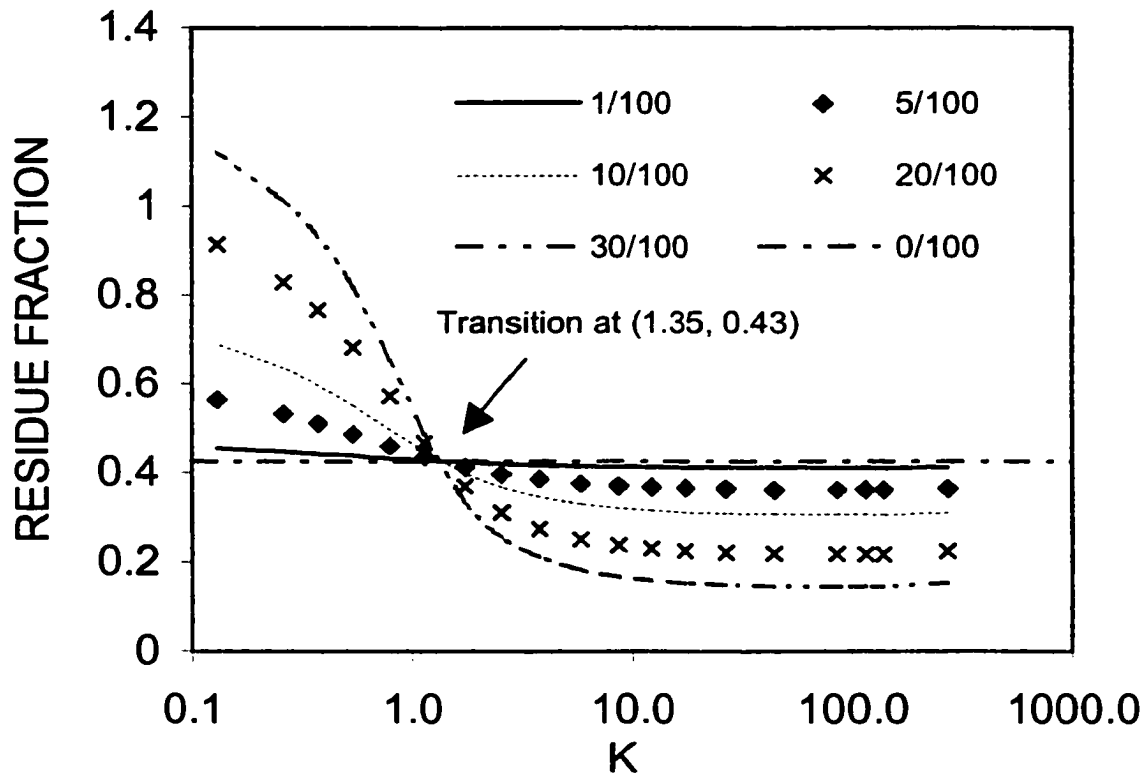


Figure 3.4 Stripping effect as a function of K-values

(C₁₀ through C₃₆ mixture, 0.1 MPa, 393 °C)

At the same time, it can be seen that for a given component with K value greater than 1.35, the residue/feed ratio decreases with an increasing amount of the added component. When K-value is less than 1.35, the residue/feed ratio is higher than that without stripping

component. This means that the component added is not a stripping agent. Instead, it prevents vaporization.

The phenomena can be explained as follows. An added component helps the vaporization by increasing its partial pressure, but it also hurts vaporization of other components by reducing their liquid molar compositions. Furthermore, the part of the component distributed in the liquid phase will contribute to a larger residue/feed ratio. When the K value of a component is large, it generates a large partial pressure, and most of it stays in the vapor phase, so the net effect is stripping. On the other hand, when the K value is small or in other words, the component is heavy, a large portion of the component stays in the liquid phase, resulting in a larger residue/feed ratio.

To determine if this effect manifests quantitatively in the same approximate way for crudes, the light crude was mixed with stripping agents and flashed at 360 °C. The heavy crude was mixed with stripping agents and flashed at 343 °C. The results are shown in Figure 3.5 and 6, which depict similar trends to that seen in Figure 3.4. The residue/feed ratio in light crude stripping, however, does not go down as much because of the existence of a large amount of light components in the mixture. The effect is shown parametric as percentages, which are the amount of stripping agent divided by the amount of the crude on molar basis.

In practice, the crude experiences flashing at the flash zone of the main tower, and the resultant liquid is further stripped with steam at the bottom part of the main tower. To show how light components affect the flowrate of the residue leaving the main tower, we split the vapor from the pre-flash drum (163 °C) into two parts as shown in Figure 3.7.

One part goes to the main tower and the other mixes with the remaining crude again and resultant mixture enters the furnace. Now concentrate on the furnace and examine the effect of the light components entering into it. The outlet temperature of the furnace is fixed at 360 °C. By changing the remixing ratio, one can control the amount of light components entering the furnace. The result is shown in Figure 3.8.

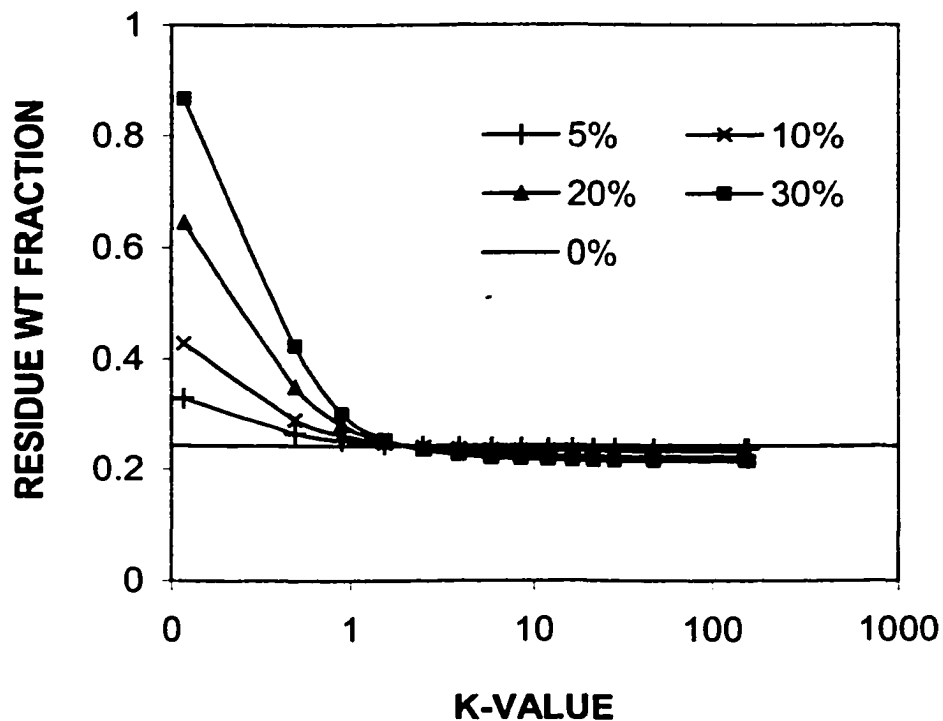


Figure 3.5 Stripping effect for light crude

The amount of residue increases constantly with an increasing vapor separation ratio. The vapor remixing ratio of one corresponds to the conventional design, and the ratio of zero corresponds to the common pre-flash design. It is seen that the yield of the residue decreases constantly with the increasing vapor remixing ratio. The trend is consistent with what we saw in Figure 3.4 through 6.

Following, we first discuss the effect of steam temperature and the location of its injection. We then investigate the energy requirement associated with the use of stripping agents, and lastly we study the effect of process pressure.

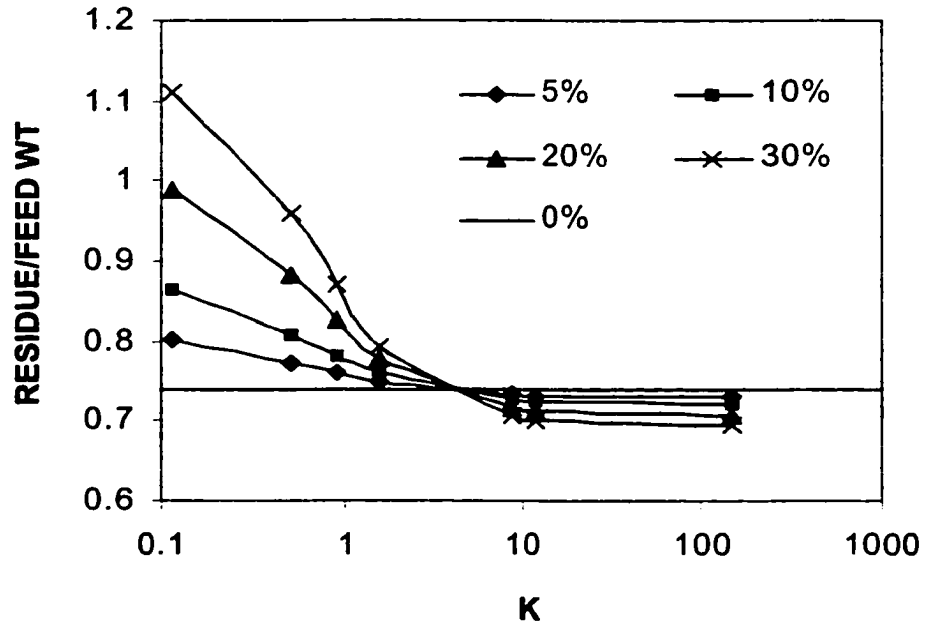


Figure 3.6 Stripping effect for heavy crude.

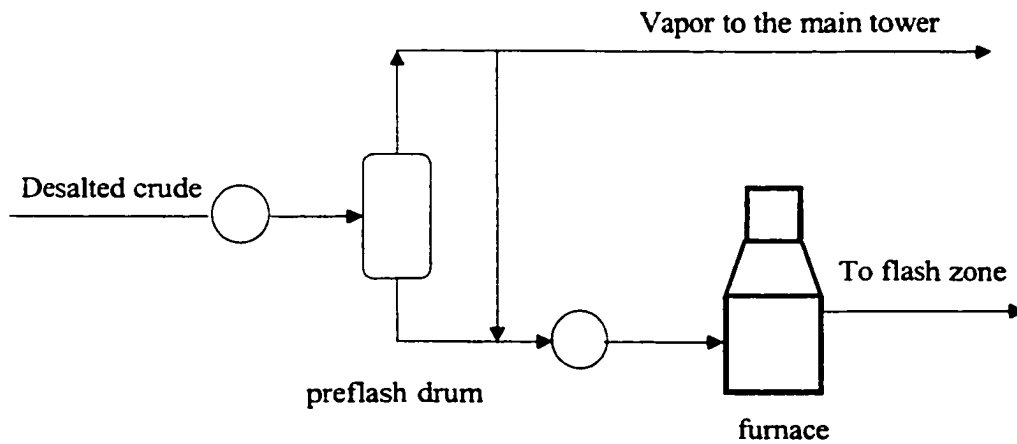


Figure 3.7 A schematic diagram for pre-flash vapor splitting

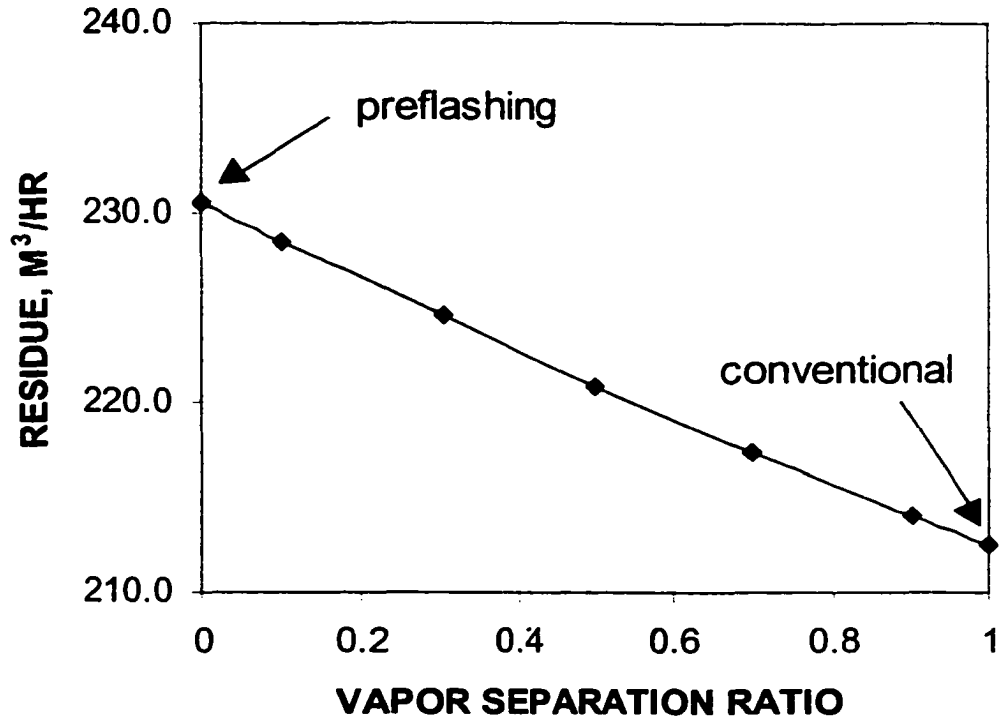


Figure 3.8 Residue yield as a function of vapor separation ratio in pre-flash design

3.5 Steam Stripping: Effect of the temperature

Typically, there is a temperature drop of about 17 °C between the flash zone and the bottom tray of the atmospheric column (Watkins, 1979). The temperature drop is related to the vaporization of relatively light components being directly stripped by the steam. The question is whether a higher steam temperature reduces the residue yield. As the atmospheric column does not allow large flowrate of steam, which would result in the formation of free water on top trays, we use the flowchart of Figure 3.9 to perform this study.

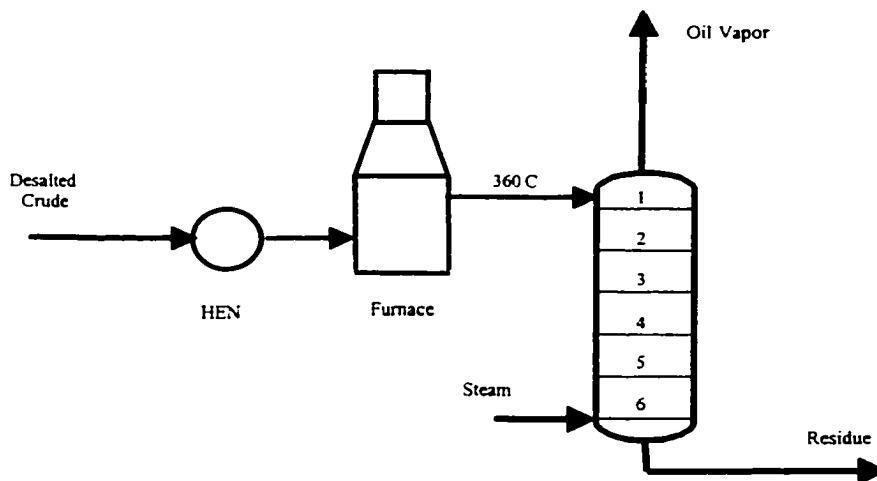
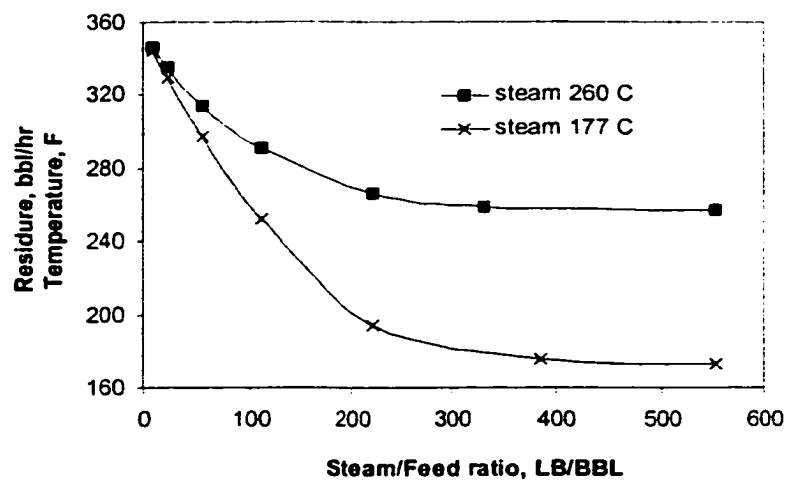


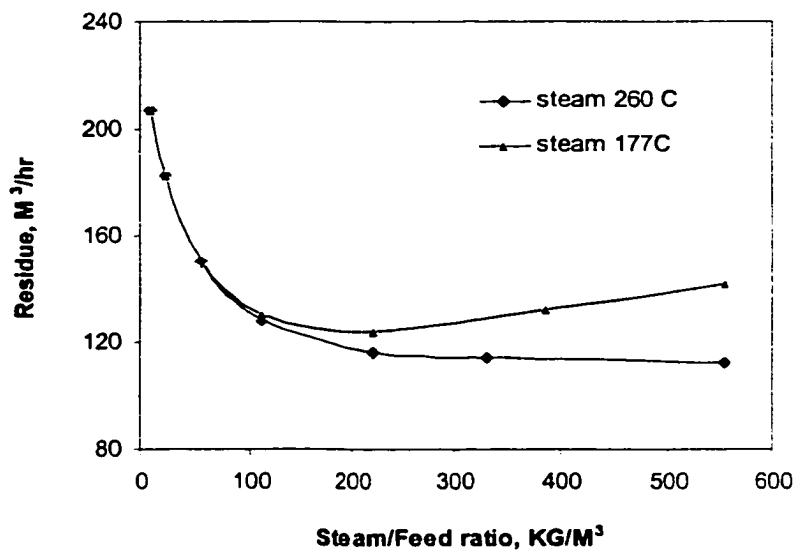
Figure 3.9 Flowsheet for Studying the Effect of Light Components

The stripping power of steam as a function of flowrate at different temperatures is depicted in Figure 3.10.

To show the limit of the stripping power, the value of the steam/feed ratio is allowed to reach high values. Some of these values are unrealistic, but they help illustrate the point. When the steam/feed ratio is small, the temperature of the steam does not affect the yield of residue because the heat steam extracted from the oil is very small. When the steam/feed ratio is raised to about 40, the amount of heat taken by the steam becomes significant, and the 177 °C steam is worse than the 260 °C steam due to a lower temperature profile at the stripping section of the column. On the 177 °C steam curve, a minimum point is observed at a steam/feed ratio of 75. This means that above this ratio, the cooling effect of the steam dominates and the yield of residue goes up with an increasing amount of stripping steam.



(a)



(b)

Figure 3.10 Residue yield and temperature as functions of the flowrate of stripping steam

(a) Residue flowrate

(b) residue temperature

3.6 Steam Injection

In this section, we discuss two cases: injecting steam into the crude before the furnace and after the furnace. Figure 3.11 is used for the simulation. The flash zone pressure is assumed to be the same as that of the outlet of the furnace. The results are shown in Table 3.5.

Table 3.5 Effect of steam injection location

Steam/feed, KG/M ³	Residue for SBF*, M ³ /hr	Residue for SAF*, M ³ /hr	Flash zone temp. for SAF*, C
0.0	207.3	207.3	360.0
3.3	202.7	204.1	359.4
5.5	199.8	202.0	359.1
11.0	193.0	197.2	358.3
22.1	181.6	188.6	357.0

*SBF= steam injected at the inlet of the furnace. SAF = steam injected at the outlet of the furnace.

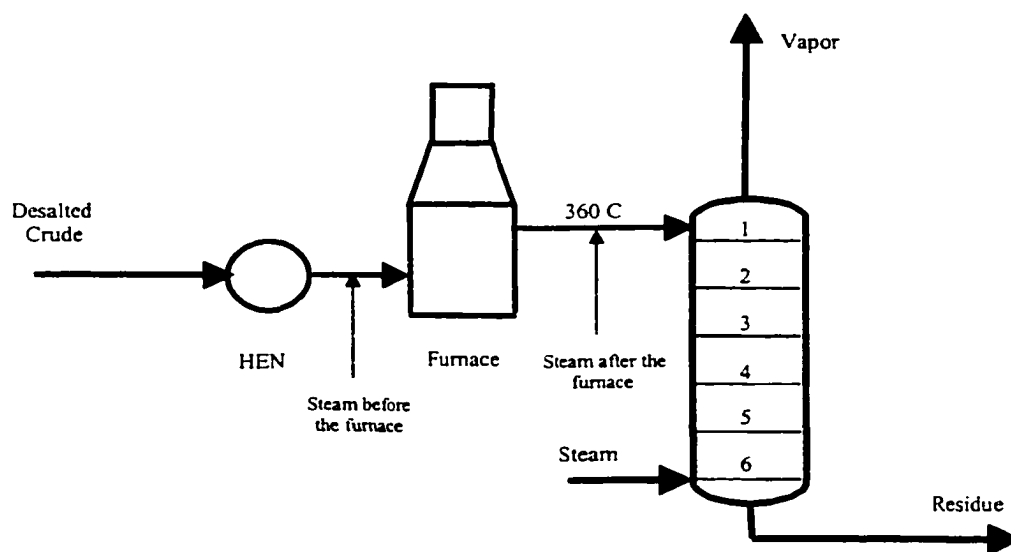


Figure 3.11 Flowsheet for Studying the Effect of Steam Injection

In both cases, the yield of residue decreases with the increased steam/feed ratio. For the same steam/feed ratio, however, injecting before the furnace produces less residue. This is because in this scheme, the steam-crude mixture leaving the furnace has achieved a vapor-liquid equilibrium and no temperature change takes place between the outlet of the furnace and the flash zone. In the other case, the hot crude, which is vapor-liquid mixture at 360 °C, meets with the injected steam (also 360 °C). Because of the stripping effect, more hydrocarbons vaporize. As the vaporization process is adiabatic, the temperature of the system goes down. The last column in Table 3.5 shows the temperatures in the flash zone. *Therefore, injecting steam before the furnace is more advantageous.*

3.7 Energy requirements for stripping agents

We showed that substances with large K-values have the same stripping effect on molar basis. However, the energy requirement for heating a gas to an elevated temperature varies. From the viewpoint of energy efficiency, gases requiring the lowest energy are the best. Figure 3.12 shows heating curves for water, N₂, H₂ and light hydrocarbons. Water has the largest heating requirement due to the heat of vaporization. Nitrogen and hydrogen have the smallest energy demands, and light hydrocarbons lie in between, with the energy demand increasing with their molecular weight. Therefore, nitrogen and hydrogen are the best stripping agents. The replacement of steam by N₂ or H₂ has the advantage that corrosion related to water formation in the distillation system is reduced or even eliminated. The drawback is that they need to be separated from the overhead product and recycled back. The flowsheet containing N₂ or H₂ stripping is

therefore slightly more complex, and an economic analysis is needed to determine whether they are economically more beneficial than the conventional steam stripping.

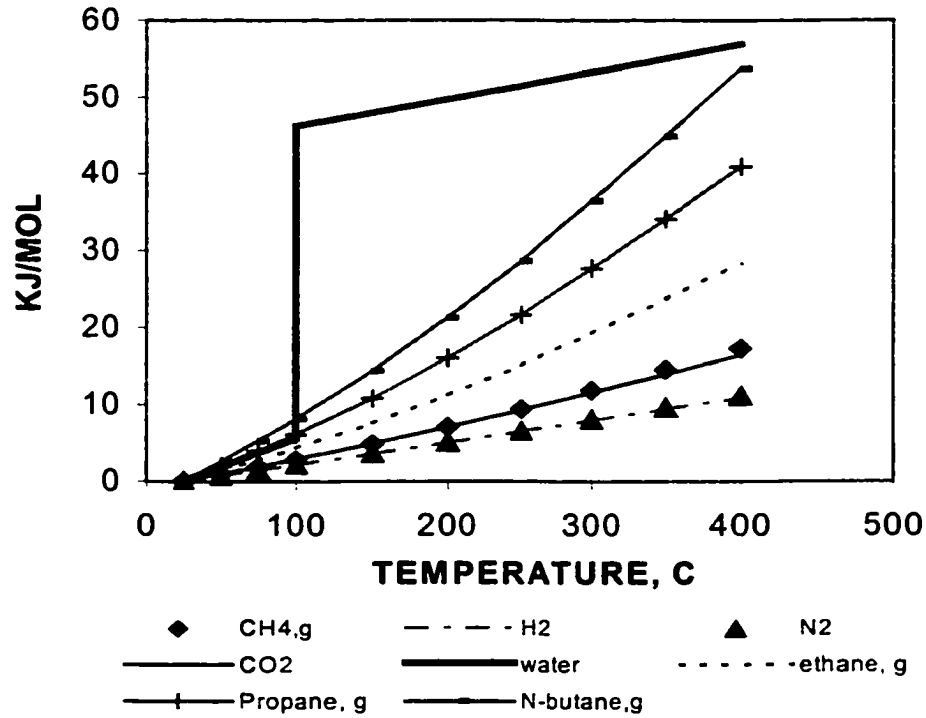


Figure 3.12 Enthalpy increase as a function of the final temperatures
(base: 25 °C, 1 atm)

3.8 Effect of pressure

The atmospheric tower operates at a pressure in the range of 0.2-0.3 MPa. Figure 3.13 shows the heating curves for n-butane and N412, which is a pseudo component with a molecular weight of 167.1, at 0.1 MPa and 0.26 MPa, respectively. The figure shows that pressure only shifts the temperature at which vaporization takes place. It is also seen that on a weight basis, the heat requirements for components with large difference in molecular weight are very close.

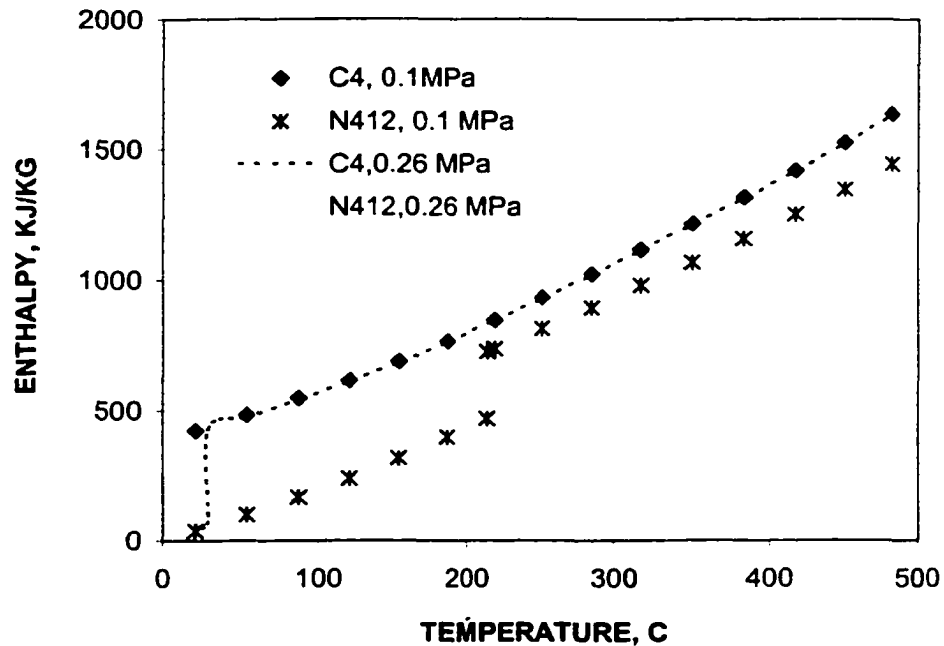


Figure 3.13 Effect of pressure on heating curves

From the above study, we reach the following conclusions:

- Steam stripping enhances vaporization by lowering the partial pressure of the hydrocarbon vapor.
- The stripping effect of a hydrocarbon not only depends on its property, but also depends on the property of the mixture to be stripped.
- The temperature of the bottom stripping steam does not affect the yield of the residue when the steam/feed ratio is less than 40.
- Injecting steam before the furnace produces less residue than injecting after the furnace.

- N_2 and H_2 and light hydrocarbons have the same stripping ability as water but require less heat to be heated up. From the standpoint of energy savings, they are better than water.
- Pressure does not affect the heating curve except postponing the vaporization.

Finally, we can naturally envision two ways to increase the vaporization ratio at a fixed temperature. One is to put more light components into the crude, which can be achieved by adding stripping gases or recycling light distillates such as naphtha or kerosene. The other way is to remove heavy components from the crude. We leave the investigation of these points for the future.

3.9 Comparison for lower AGO yield

We now compare the pre-flash and pre-fractionation options with the conventional option at *lower AGO yields*. Table 3.6 summarizes the result. In this comparison, the stripping steams were adjusted so that both designs have the same amount of residue and the same product gaps.

The heat demand-supply diagrams corresponding to the optimal solution are shown in Figure 3.14. Not all the heat possible to transfer from the second pump-around (PA2) to the third (PA3) was transferred because the trade off between this load and the increased steam consumption created a trade-off.

Table 3.6 Comparison between Conventional, Pre-flash and Pre-fractionation Designs
(light crude)

	Conventional	Preflashing	Prefractionation
Naphtha, M ³ /hr	246.1	245.5	222.5
Kerosene, M ³ /hr	144.5	144.8	148.8
Diesel, M ³ /hr	70.7	71.6	71.5
Gas oil, M ³ /hr	103.6	102.9	105.7
Residue, M ³ /hr	230.5	230.6	227.5
Product gaps, C			
Naphtha-Kerosene	19.9	19.1	18.2
Kerosene-Diesel	0.4	0.0	-0.4
Diesel-GO	-2.5	-1.9	-1.7
Heating utility, MW	82.2	76.0	80.4
Energy consumption, MW	92.5	87.7	90.4

* Pre-flash temperature: 163 °C. Vapor feed at tray 15. $\Delta T=22.2$ °C.

It is shown that energy consumption of the pre-flash design is 4.8 MW lower than that of conventional design. Thus, the energy consumption of the pre-fractionation design lies between the two designs. To understand the results, two aspects have to be taken into consideration: one is the temperature level of the heat to be recovered and another is the amount of components bypassing the furnace. As the pre-fractionation column operates at a low-temperature where the heat supply is in surplus, distributing heat between the pre-fractionation condenser and the main column condenser does not affect the heating utility requirement. Therefore, the only aspect affecting the energy consumption would be the amount of components bypassing the furnace. When the temperature of the feed entering the pre-fractionation column is the same as that entering the pre-flash drum, the amount

of components bypassing the furnace in the former would be lower because a part of the vapor entering the column is condensed as the reflux and then mixes with the crude at the bottom of the pre-fractionation column. In terms of energy consumption, such a pre-fractionation design would be equivalent to a pre-flash design operating at a lower flashing temperature.

Note that product distributions vary considerably from one design to another, although the product gaps are exactly the same. For example, the pre-flash design gives more diesel and less gas oil compared to the conventional design. This might be preferable in some cases.

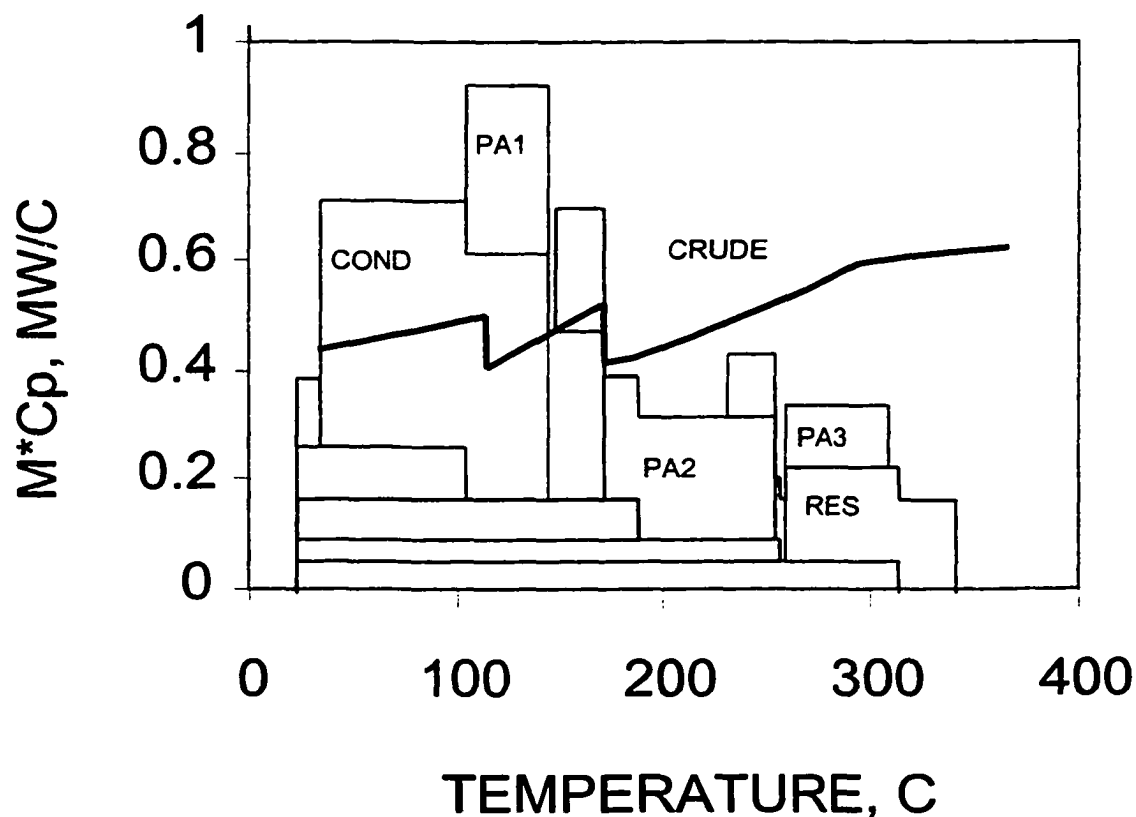


Figure 3.14 Final Heat Supply-demand Diagram for a Pre-flash Design ($\Delta T = 22.2\text{ }^{\circ}\text{C}$)

C: condenser. PA1, PA2 and PA3: pump-around circuits. RES: residue.

3.10 Effect of pre-flash temperature

The necessity of a pre-flash drum depends on the property of the crude, the temperature of the crude entering the furnace and the operating pressure. The bubble temperatures of the lighter crude are higher than that of the heavier crude (Figure 3.15). The higher the operating pressure, the higher is the bubble temperature. If the temperature of a crude oil exceeds its bubble temperature considerably before entering the furnace, a pre-flash drum would be necessary.

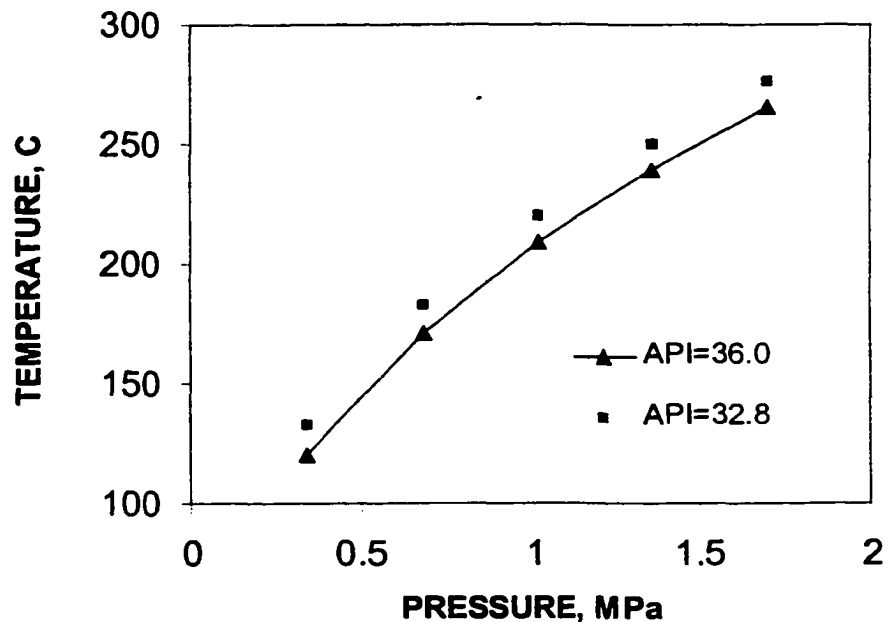


Figure 3.15 Crude Oil Bubble Temperature as a Function of Pressure

The effect of the pre-flash drum temperature on the low AGO yield arrangement is shown in Figure 3.16. With the increase of the pre-flash temperature, the heating utility decreases continuously because of more light components bypassing the furnace.

On the other hand, the steam consumption increases rapidly as more steams are needed for both keeping the gas oil yield and fixing the product gaps. Although the total energy consumption reaches a minimum at 177 °C, the differences in the curve are relatively small. However, if steam is in surplus in the refinery, heating utility only counts and lower temperatures should be used.

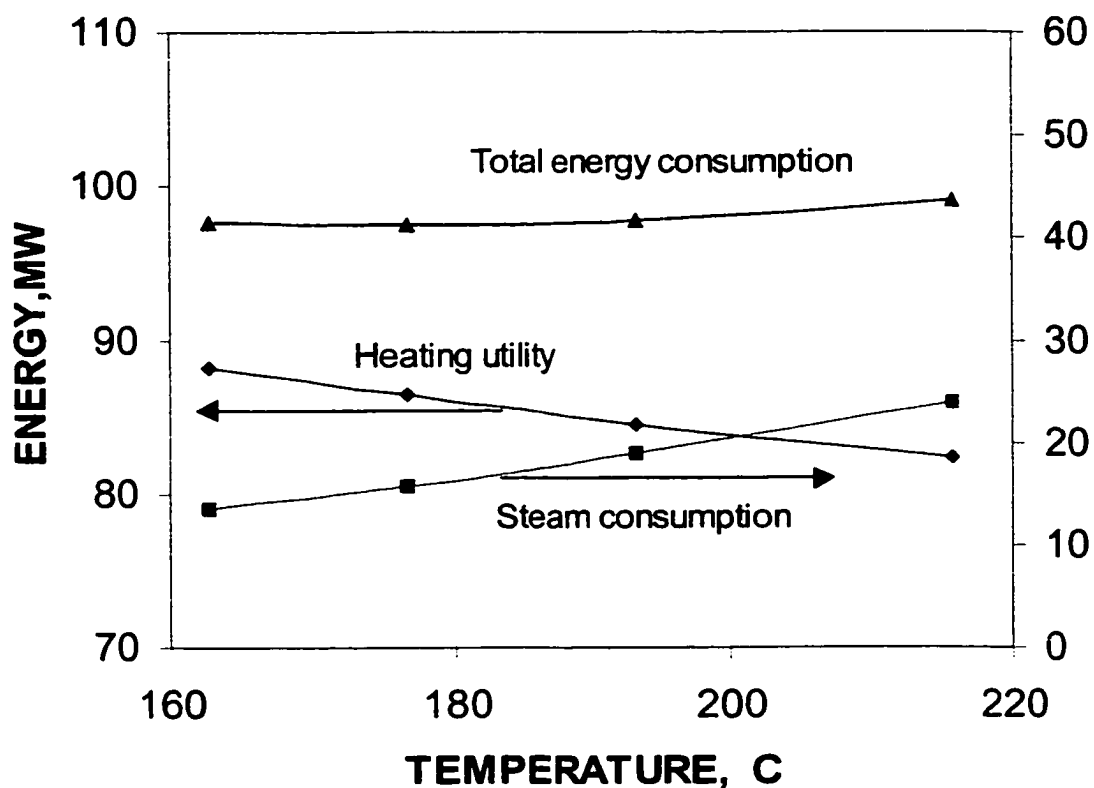


Figure 3.16 Effect of the pre-flashing temperature on total energy consumption

3.11 Feed location of pre-flash drum vapors

The vapor produced in the pre-flash drum at 163 °C has properties very similar to naphtha. It contains 53% light ends (C₂-C₅). Its 98% boiling point is 169 °C, lower than

the 95% temperature of naphtha (182 °C). We compared the effect of locating this feed in different trays in the column. During the comparison steam flowrates have been kept constant, allowing the gaps to change. The results are given in Table 3.7.

Table 3.7 Effect of Vapor Feeding Locations

	Tray 8	Tray 15	Tray 18	Tray 27	Tray 29
Naphtha, M ³ /hr	249.5	249.3	249.3	249.3	249.5
Kerosene, M ³ /hr	143.8	143.9	143.5	143.4	143.9
Diesel, M ³ /hr	69.6	69.7	70.3	68.6	68.7
Gas oil, M ³ /hr	101.9	101.9	101.8	103.5	102.3
Residue, M ³ /hr	230.6	230.6	230.6	230.6	231.0
Product gaps (°C)					
Naphtha-kerosene	24.9	24.5	24.5	24.5	24.9
Kerosene-Diesel	3.8	3.2	2.1	2.5	4.0
Diesel-gas oil	-0.9	-0.9	-0.8	-4.7	-0.9

We have the following observations:

1. The naphtha yield and the gap between naphtha and kerosene are constant. This is because the vapor feed is basically naphtha components and the naphtha-kerosene separation section (tray 1 to tray 9) is almost not affected in the above feeding locations.
2. When the vapor feed location is lower than that of the gas oil withdrawal (tray 25), the yield of diesel is significantly lower and the yield of gas oil is higher. This is

because that the temperature of vapor feed is much lower than that of the vapor rising from the flash zone and a portion of the hot vapor is condensed with the effect of some diesel components going to the gas oil draw stream. In Table 3.7, we can see when the vapor feed tray is 27, not only the yield of diesel decreases but also the diesel-gas oil gap moves in the negative direction. Therefore, vapor feed between flash zone and gas oil withdrawal tray is not appropriate.

- When the vapor feed is sent to a tray above the flash zone, the residue yield is constant. This is because that the residue yield depends on four factors: the composition and temperature of the crude at the outlet of the furnace, the flowrate of stripping steam entering from the bottom of the main column, and the over flash rate. In the above situations, all the four factors are the same.

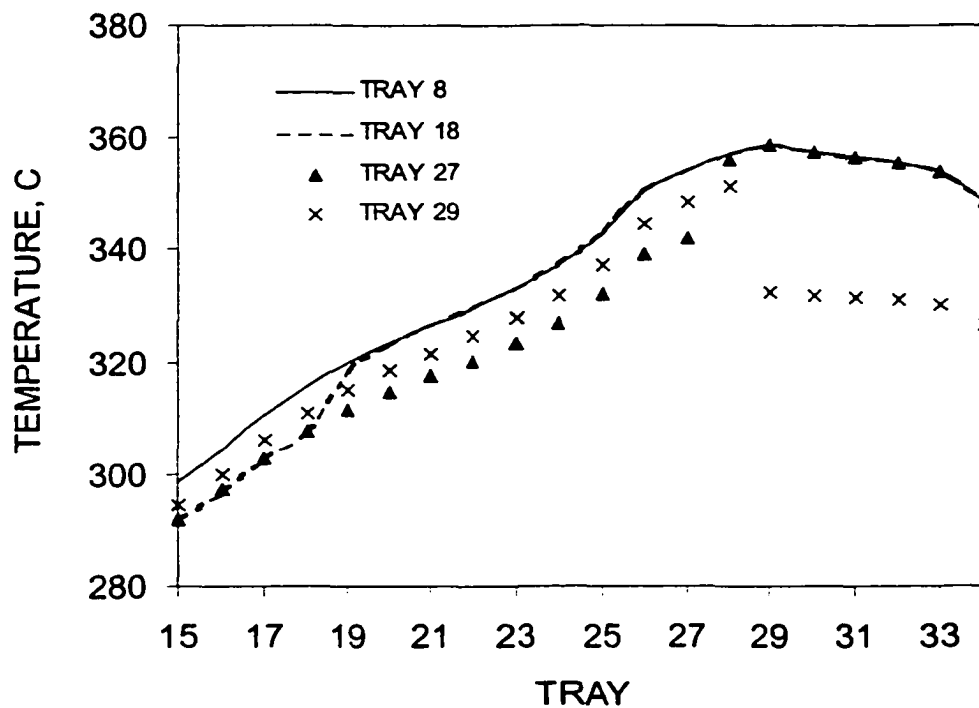


Figure 3.17 Temperature Profiles for Various Vapor Feeding Locations

The temperature profiles are shown in Figure 3.17. The tray temperatures are highest when the vapor is fed at tray 8, the highest location. When the vapor is fed at tray 18, the tray temperatures above the vapor-feeding tray are lower, which is due to the cooling effect of the low temperature-feeding vapor. The tray temperatures below the vapor feed tray are exactly the same as that when the vapor is fed at tray 8. When the vapor feed location continues to move down, the same tendency appears as expected.

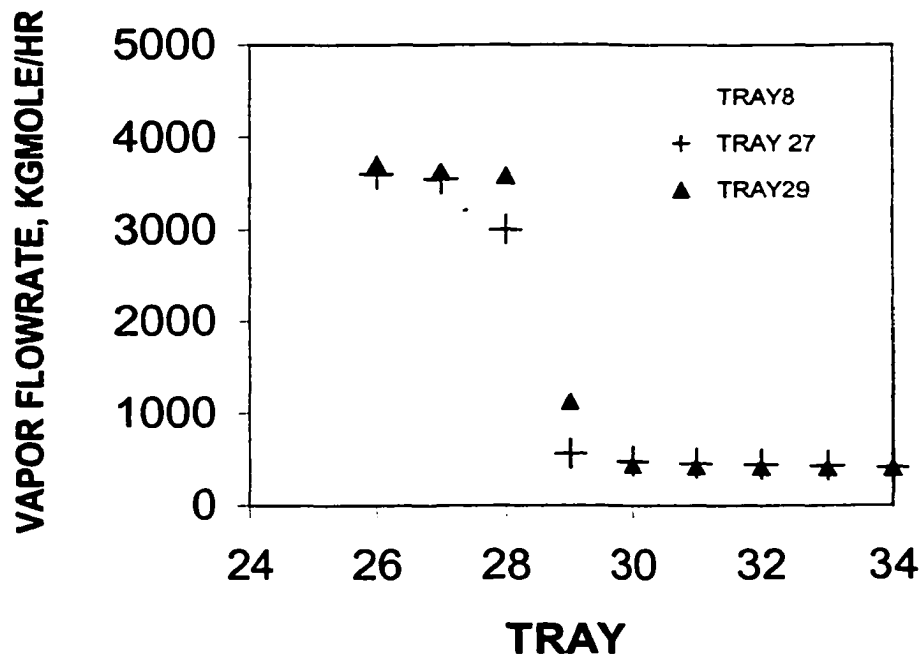


Figure 3.18 Vapor Profiles as a Function of Vapor Feeding Tray

Finally, when the vapor location reaches its lowest location --- the flash zone (tray 29), the temperatures of tray 29 through tray 34 are much lower than all the others with other vapor feed location. At the flash zone, the hot crude flashes and splits into rising hot vapor and descending hot unstripped residue. The hot vapor meets with the cold pre-

flashed vapor immediately and condensation occurs. The condensed liquid, basically gas oil and diesel components, mixes with the unstripped residue on the tray 29. However, the condensed liquid does not stay with the unstripped residue and is stripped out when the mixture of the unstripped residue and the condensate meets the steam coming from tray 30.

In Figure 3.18, we can see that the vapor flowrate of tray 29 is about twice as large as that when the pre-flashed vapor is fed at other locations. The overall effect is equivalent to that of conventional design with lower outlet temperature of furnace. It can be predicted that heating of the pre-flashed vapor to higher temperature would reduce the temperature drop at tray 29 and help increase the output of distillates.

From the above comparison, we can conclude that product yields and gaps are not sensitive to vapor feed location. Specifically, the residue yield keeps constant. As a higher temperature profile is favorable in heat recovery through pump-around circuits, higher vapor feed is preferred. However, as pointed by Golden (1997), a higher vapor feed would have the risk of contaminating the products withdrawn below the feed tray when liquid oil entrains.

3.12 Conclusion

A rigorous targeting for the design of a crude distillation unit with pre-flash drums and pre-fractionation is presented. The major conclusion of this study is that pre-flashing and pre-fractionation designs can only be advantageous from the point of view of energy consumption if one accepts the yield of gas oil to be reduced. Other findings of

the study show that in practice, the equivalent of the carrier effect of lights cannot always be obtained using steam.

In addition, the introduction of a flash drum into an already complicated heat exchanger network needs to be considered carefully. For example, it might be advantageous to pay the penalty of higher energy consumption just to see the number of units in the preheating train reduced. Finally, heat efficiency and network simplicity is desired for a variety of crudes simultaneously. This, together with measures to improve the performance of these units will be analyzed in future work.

3.13 Nomenclature

f_i = flowrate of component i in the feed

F = feed flowrate, kgmol/hr

F^* = dry flowrate of the feed, kgmol/hr

K_i = vapor-liquid equilibrium constant for component i

K_i^* = modified vapor-liquid equilibrium constant for component i

L = liquid flowrate, kgmol/hr

l_i = flowrate of component i in the liquid phase

P_{st} = partial pressure of steam in the vapor phase

P = total pressure of the system without steam

P^* = total pressure of the system with steam

P_i^s = saturated pressure of component i at the system temperature

V = vapor flowrate, kgmol/hr

V^* = vapor dry flowrate, kgmol/hr

x_i = molar fraction of component i in the liquid phase

x_i^* = dry molar composition of component i in the liquid phase

y_i = molar fraction of component i in the vapor phase

y_i^* = dry molar composition of component i in the vapor phase

z_i = molar fraction of component i in the feed

z_i^* = dry molar composition of component i in the feed

3.14 References

1. Andrecovich, M., and Westerberg, A., A Simple Synthesis Method Based on Utility Bounding for Heat-integrated Distillation Sequences. *AIChE Journal*, 31(3), 363-375, (1985).
2. Bagajewicz, M., On the Design Flexibility of Crude Atmospheric Plants. *Chemical Engineering Communications*, 166, 111-136, (1998).
3. Bagajewicz M. and S. Ji. Rigorous Procedure for the Design of Conventional Atmospheric Crude Fractionation Units Part I: Targeting. *Industrial and Engineering Chemistry Research*. Vol. 40, No 2, pp. 617-626 (2001).
4. Bagajewicz M. and J. Soto. Rigorous Procedure for the Design of Conventional Atmospheric Crude Fractionation Units Part II: Heat Exchanger Networks. *Industrial and Engineering Chemistry Research*. Vol. 40, No 2, pp. 627-634 (2001).
5. Golden, S., Prevent Pre-flash Drum Foaming, *Hydrocarbon Processing*, May 1997, pp141-153.
6. Stichlmair, J.G, and Fair J. R, *Distillation Principles and Practices*, Wiley-VCH, New York, 1998.p76.

7. Terranova, B., and Westerberg, A., Temperature-Heat Diagrams for Complex Columns. 1. Intercooled/Interheated Distillation Columns. *Ind. Eng. Chem. Res.* 28, 1374-1379, (1989).

Chapter 4 On the Energy Efficiency of Stripping-Type Crude Distillation

4.1 Overview

In this chapter, the energy efficiency of crude fractionation using stripping-type columns is analyzed. Rigorous simulations prove that in the case of processing a light crude of reference, previous reports indicating that this option is advantageous over the conventional design cannot be generalized.

4.2 Introduction

In conventional crude atmospheric distillation, the crude is fed at the bottom part of the column, and the main part of the column functions as a rectifying section. Watkins (1979) suggested the possibility of using direct and indirect rectifying sequences. The conventional design that he chose to describe in detail is shown in Figure 4.1. Its connection to an indirect sequence of distillation columns is shown in Figure 4.2. In recent years, the alternative indirect sequence (Figure 4.3) was proposed by Liebmann (1995).

In previous work (Bagajewicz and Ji, 2001, Bagajewicz and Soto, 2001), a systematic procedure for the design of conventional crude fractionation units was presented. This procedure is based on a step-by-step combination of rigorous simulation and heat integration. The procedure starts with a column without pump-around circuits. When heat is transferred from the condenser to pump-around circuits, a trade-off between the steam usage and the fuel gas savings is established. This transfer of heat is possible due to the operating and design flexibility that crude fractionation installations exhibit.

Such design flexibility was studied in detail by Bagajewicz (1998). The procedure makes use of rigorous simulations and heat supply-demand diagrams similar to those introduced by Andrecovich and Westerberg (1985), and Terranova and Westerberg (1989). Based on these targets, a universal heat exchanger network which allows several crudes to be processed with the minimal energy consumption can be found (Bagajewicz and Soto, 2001).

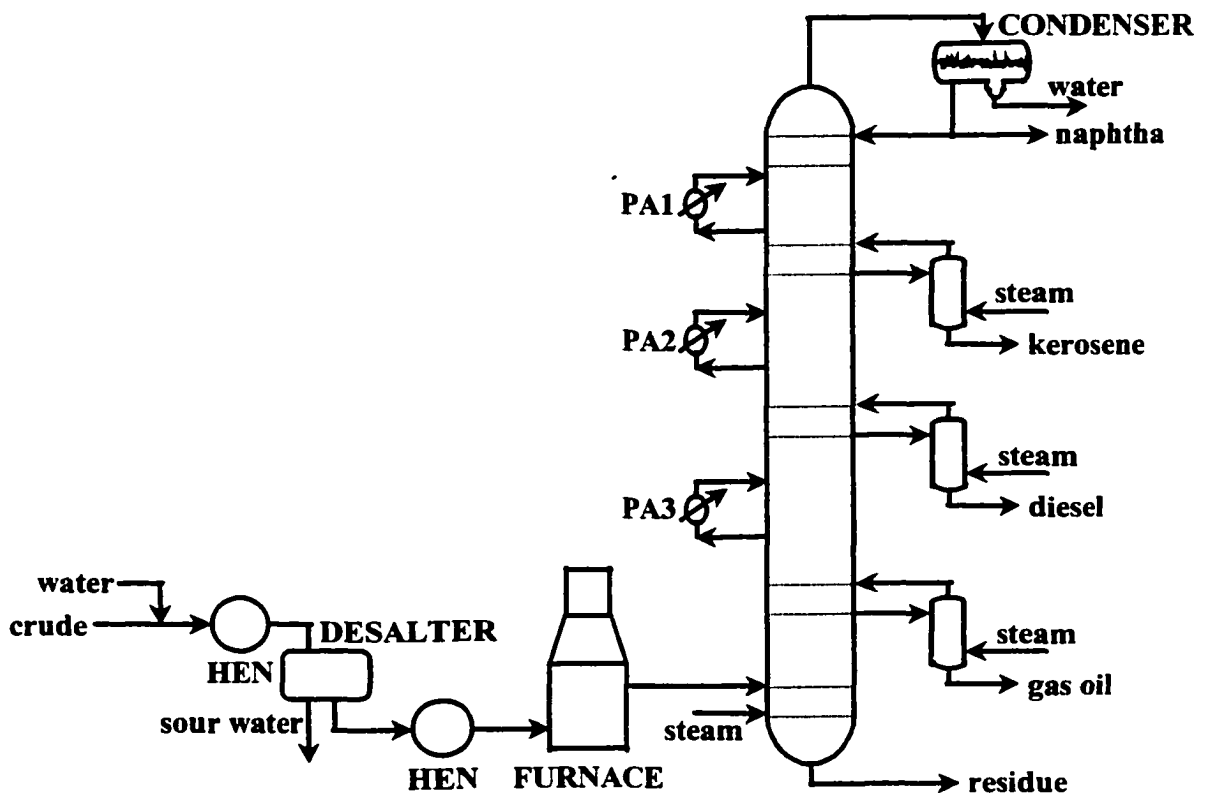


Figure 4.1 Conventional Crude Distillation

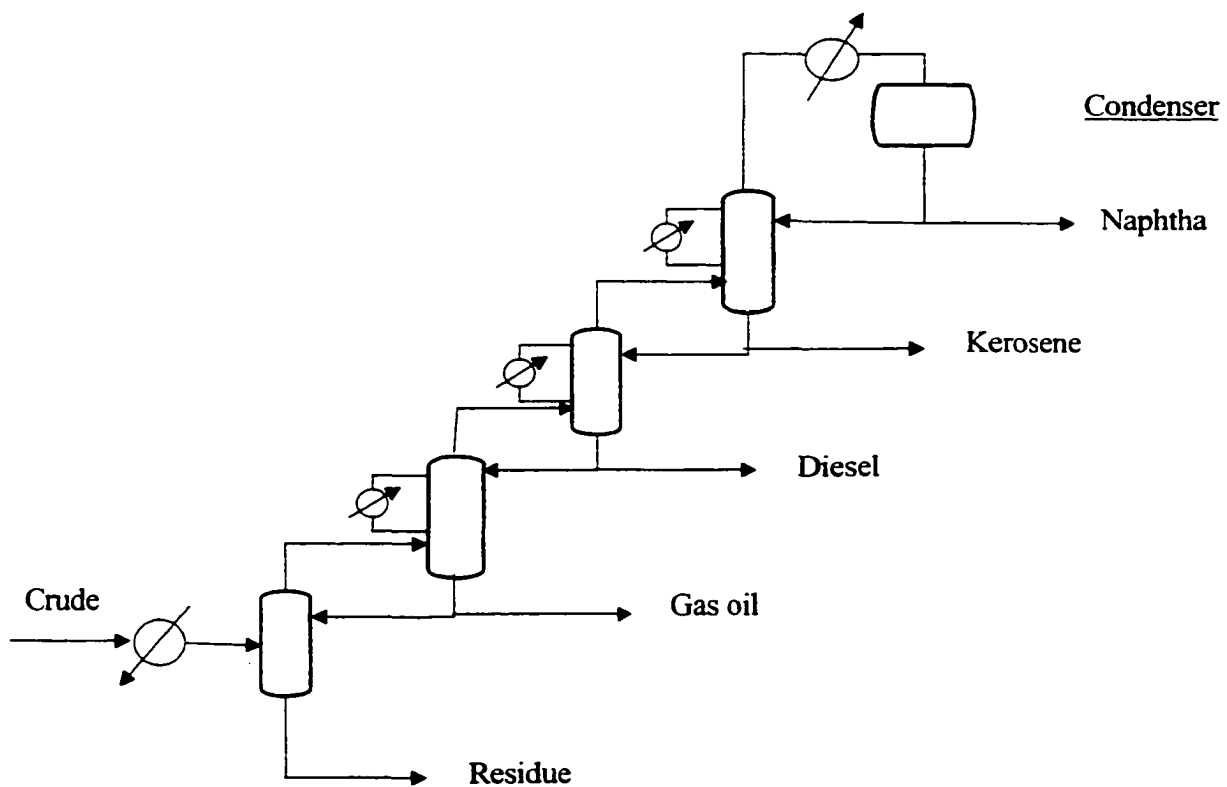


Figure 4.2 Indirect sequence (Watkins, 1979)

In the stripping-type design, the crude is heated to a relative low temperature (about 150°C) and fed at the top of the column. Because the crude temperature is low, the vapor ratio of the feed is small. The crude goes down the column and is heated consecutively in three heaters (the upper heater, middle heater and lower heater). Side products are withdrawn from the vapor phases, and rectified in the side rectifiers.

Liebmann and Dohle (1995) reported that this design could feature 5% less utility cost than the optimized conventional design. However, the comparison was not on the same allowable temperature basis. The maximum allowable temperature is limited by the thermal stability property of the crude being processed and is found by lab testing. For

the Venezuela crude oil used in Liebmann's paper, the allowable temperature is 343 °C (Watkins, 1979). However, in their stripping-type design, the crude was heated to 370 °C in both the middle heater and the lower heater. It can be expected that at this temperature, severe thermal cracking takes place. Such operation is not allowed in practice. Because of the above limitation of their study, a re-evaluation of the stripping-type design is necessary. This chapter performs the evaluation using the method proposed by Bagajewicz and Ji (2001), taking into account the temperature limit of thermal cracking.

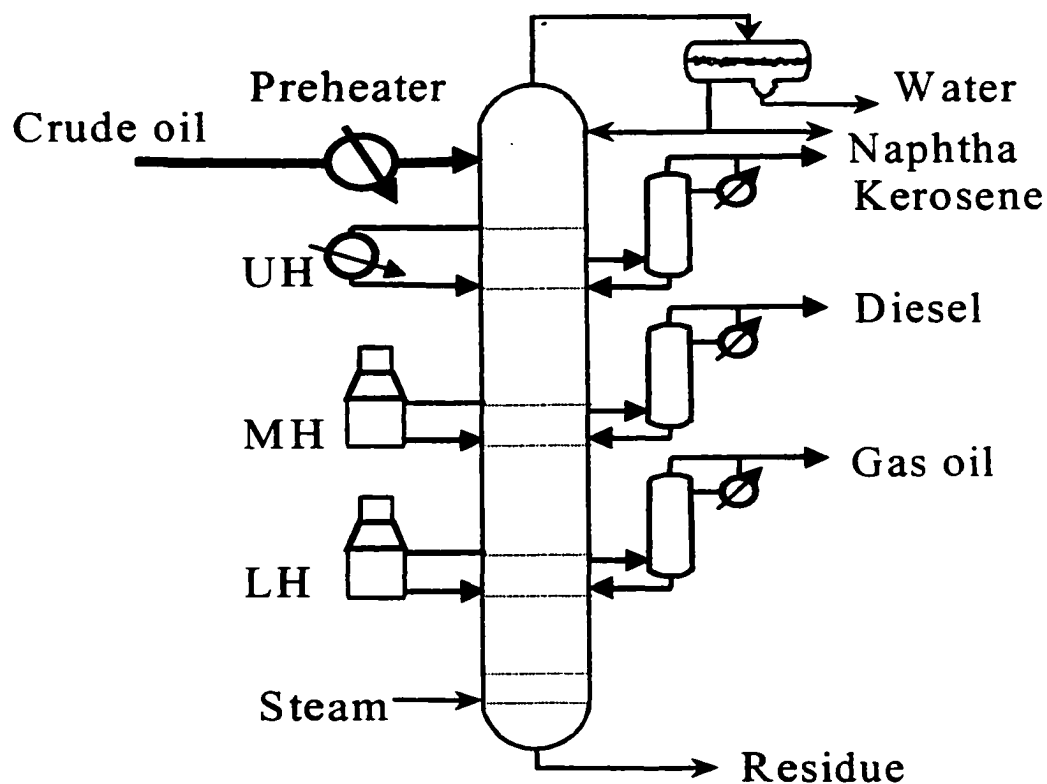


Figure 4.3 Stripping Type Crude Distillation Column

4.3 Crude vaporization patterns and heat demand

A major difference between the conventional design and the stripping-type design is the heating pattern of the crude oil. Because in the stripping-type design crude oil is heated step-by-step and the vapor is separated immediately after it is generated, the amount of crude to be heated in the stripping section is smaller than in the conventional design. On the contrary, the amount of crude being heated in the conventional design is constant, that is, no vapor is separated until the heating is completed at the outlet of the furnace.

To better understand the difference between the two heating patterns, one should analyze the distillation curves. It is well known that distillation curves can be used to approximate the distillation behavior in terms of product distribution and vaporization ratio. The two relevant distillation curves, ASTM D86 and EFV, are useful tools.

ASTM D86 distillation is carried out in a glass flask equipped with an electric heater and a water cooler. The oil sample is heated in the flask and the resultant vapor is condensed and collected in a receiver at laboratory pressure. The temperature versus amount collected is recorded. Virtually no fractionation occurs in this distillation.

Equilibrium flash vaporization (EFV) is a test used to determine the vaporization ratios of crude oils as a function of temperature. In this test, the crude oil is continuously heated without separating the vapor from the remaining liquid (Nelson, 1958). The temperature versus liquid amount is recorded. To obtain the EFV curve, a series of runs at different temperatures are carried out, and each run constitutes one point (of temperature and percentage vaporized) on the flash curve.

The equilibrium flash vaporization (EFV) distillation provides a relation between system temperature and the percentage of vapor generated. EFV distillation is a batch process during which no vapor is separated. In principle, the heating process in EFV is similar to that in the conventional distillation. In practice, the EFV curve is used to estimate the vaporization ratio for the conventional design (Nelson, 1958).

Similarly, a close relation between ASTM D86 distillation and the stripping-type distillation is apparent. Suppose a stripping-type tower has infinite number of heaters with a vapor withdraw line between adjacent heaters as well as zero pressure drop in the tower, one would obtain exactly the same temperature vs. vaporization curve as ASTM D86 distillation.

Now the ASTM D86 and EFV curves are used to answer two questions:

- For the same temperature limit, which distillation option produces more vapor, this is, more distillates yield?
- To achieve the same vaporization ratio, which distillation option demands more heat?

The first question can also be rephrased as follows: to achieve the same vaporization ratio, which distillation requires a higher temperature? This question is important because we want to achieve the maximal vaporization at the allowable maximal temperature. Although the answer to this is well-known, a review will highlight the differences. Figure 4.4 shows a comparison of the two curves.

The ASTM curve is located above the EFV curve. This means that at the same temperature limit, ASTM distillation always produces less vapor than EFV distillation. In this sense, the stripping-type design will likely produce less amount of distillates and

more residue under the same temperature limit. Whether other operating variables, such as steam, could correct this problem remains to be answered.

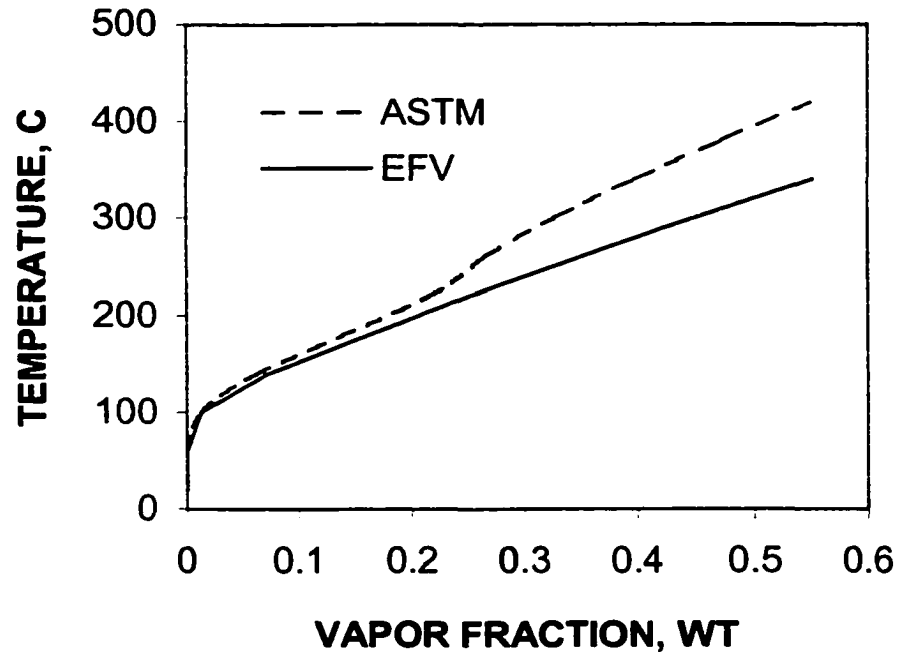


Figure 4.4 ASTM curve and EFV curve of the Venezuela crude (see Appendix A)

The second question refers to which heating pattern is more energy-efficient. From the viewpoint of energy efficiency, the stripping-type design reduces the heat demand from the light components (naphtha and kerosene components), which are only heated to low temperatures. Conversely, in the conventional design, light components are heated to the temperature limit. The heating pattern for the stripping-type design (ASTM) is, however, not advantageous for the heavy components (gas oil components). As mentioned before, the distillation temperature for the ASTM to achieve the same vaporization ratio is higher. This means that the heavy components vaporize at a higher

temperature than they would in the EFV distillation. Therefore, the heat demand for heavy components is higher.

Whether ASTM requires less energy to achieve the same vaporization ratio, ignoring the temperature limit of thermal cracking, will depend on the trade-off between the heat saving for light components and the larger energy consumption for heavy components. To obtain the ASTM heating curve, 9 heaters and 9 separators were used to simulate the ASTM distillation. Figure 4.5 shows part of the flow sheet used for this simulation. The crude was heated at 760 mmHg step-by-step and vapors were withdrawn in each step. The resulting curves for heat demand are shown in Figure 4.6.

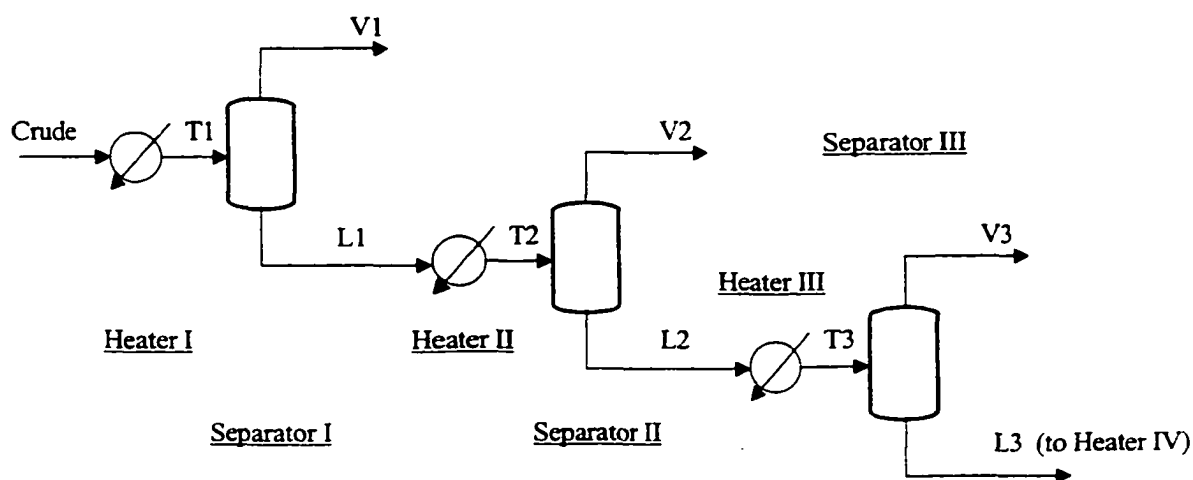


Figure 4.5. Simulation of ASTM D86 distillation

Heaters 4 through 9 and separators 4 through 9 are not shown in this figure.

Figure 4.6 shows that for small vaporization ratios (less than 0.25), the two curves coincide. For larger vaporization ratios, however, the heat demand for ASTM is always

higher than that for EFV distillation. To explain this, a comparison of temperatures and heat demands needed for achieving 0.473 vaporization are listed in Table 4.1.

Because the vapor generated is not separated in EFV distillation, on average 24% of the crude in the form of vapor is overheated from 100 °C to 307 °C. In ASTM distillation, the overheating of vapor is entirely avoided, as the vapor is withdrawn from the system after it is generated. However, ASTM distillation has to further heat the liquid (59% of the crude) from 307 °C to 380 °C. The above analysis means that the effort to reduce the heat demand by avoiding overheating of light components in the stripping-type distillation may not be successful.

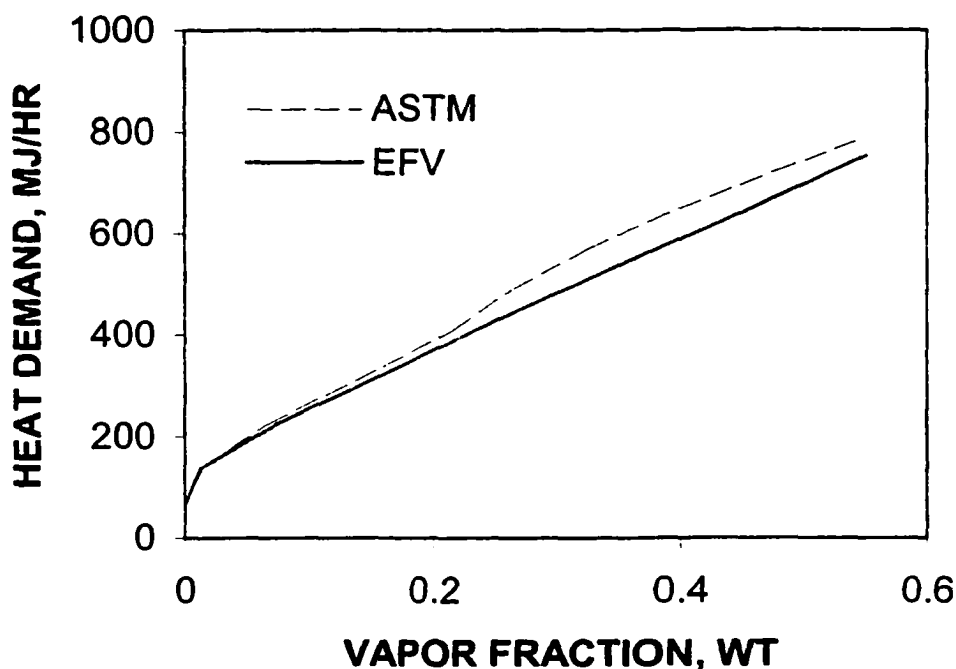


Figure 4.6 Heat requirements for ASTM distillation and EFV distillation at 760 mmHg (1M3/hr, Venezuela crude, see Appendix A)

Table 4.1. Comparison of temperature and heat demand

	Temperature °C	Crude vaporized Wt. fraction	Liquid remained wt.	Heat demand MJ/hr
EFV	100	0.014	0.986	138.8
	307	0.473	0.527	670
ASTM	307	0.345	0.655	582
	380	0.473	0.527	720.3

4.4 Features of a stripping type design

As discussed in the previous section, the stripping-type design has to heat the crude to a higher temperature in order to achieve the same amount of vaporization as in the conventional design. In addition, light components help vaporize heavy components at lower temperatures. This is called the carrier effect and it was discussed in detail by Ji and Bagajewicz (2001). Such light components are not present in the stripping-type design.

The second feature is the different pattern of product composition. In the conventional design, all light components come from the bottom section of the tower and go through the trays where side products are withdrawn. As a result, light components appear in each side product withdraw line and have to be stripped off in the side strippers. In industry, this is called controlling the flash point. In contrast, the light components in the stripping-type design come from the top section and are withdrawn as soon as they are vaporized, not reaching therefore the trays where diesel and gas oil are withdrawn. Thus, the problem of the presence of light components does not exist. However, heavy

components have a large chance of being present in these side products and raise their end points.

The last feature is that the products are withdrawn in vapor phase instead of liquid phase. For the same composition of mixture, the dew point is higher than the boiling point. So, by withdrawing a vapor one may obtain the heat at a higher temperature level. This is advantageous from the point of view of energy efficiency. However, the vapor phase withdrawals also bring the corrosion problem to the side condensers if water is present.

4.5 Energy Targeting

The main column in Figure 4.1 contains 34 trays. A crude of API 36 is used in the simulation. The flowrate used is 5000 BBL/hr. The crude data were taken from a previous chapter (Bagajewicz and Ji, 2001). The properties of the crude are listed in Appendix B. Table 4.2 shows the product specifications.

Table 4.2 Stripping-type Column Specification

	Specification
Naphtha D86 95% point, °C	182.2
Kerosene D86 95% point, °C	271.1
Diesel D86 95% point, °C	326.7
Tray 29 temperature, °F	360
(5-95) Gaps, °C	
Kerosene –Naphtha	16.7
Diesel- Kerosene	0
Gas Oil- Diesel	-13.9

In simulating the stripping-type distillation, the feed temperature, the duties of upper, middle and low heaters, the duties of condensers are allowed to change in order to meet the specifications. Comparisons are made with a conventional column operating at maximum efficiency with the same specifications.

Effect of feed temperature

Figure 4.7 is a heat demand-supply diagram for the stripping-type design. The solid bold line stands for the crude heat demand curve, which is composed of the preheating section and the upper, middle and lower side heaters. The heat supply includes heat from the main condenser, side condensers, products and the residue. The demand curve is not continuous due to temperature gaps between adjacent heat sinks.

The discontinuity of the heat demand curve is an important feature. It affects the match between the heat demand and the heat supply. Consider the region between the preheating curve and the upper heater. In this region, heat supply is available from side condensers and the residue. However, there is no heat demand in this region. The only way to make use of this heat supply is to cascade the heat to regions at lower temperatures. In the preheating region, a heat deficit is present (shaded region), but it is much smaller than the heat supply aforementioned. Therefore, a large part of the heat supply can not be utilized. Finally a small match between supply and demand exists at the level of UH.

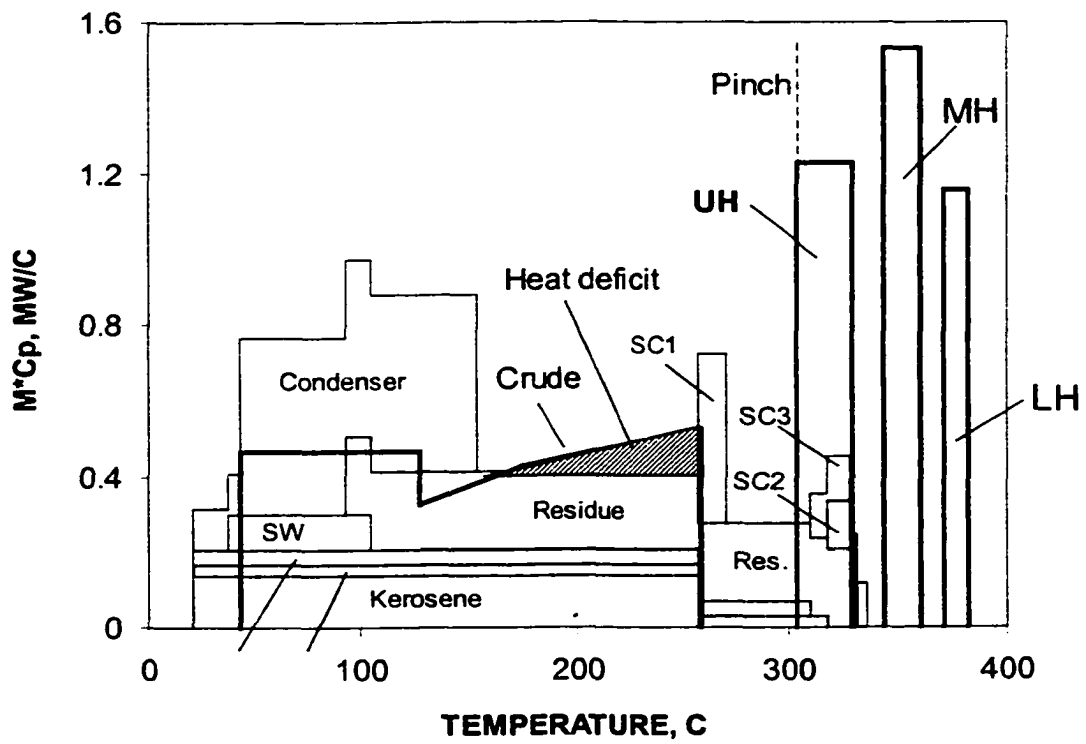


Figure 4.7 Effect of increasing the feed temperature

The location of the pinch point can be easily obtained from this diagram. It is the lowest temperature at which the demand is larger than the supply after the shifting and area matching has been performed (Figure 4.7). The heating utility is given by the unmatched demand on the right, and the cooling utility is given by the extra supply on the left.

The heating utility can be reduced by raising the temperature of the feed. That is, by shifting part of the upper heater duty into the crude preheater. The solid curve in Figure 4.8 represents the new heat demand curve for a higher feed temperature and the dashed line corresponds to the basis case. Figure 4.9 shows the complete diagram for the higher feed temperature.

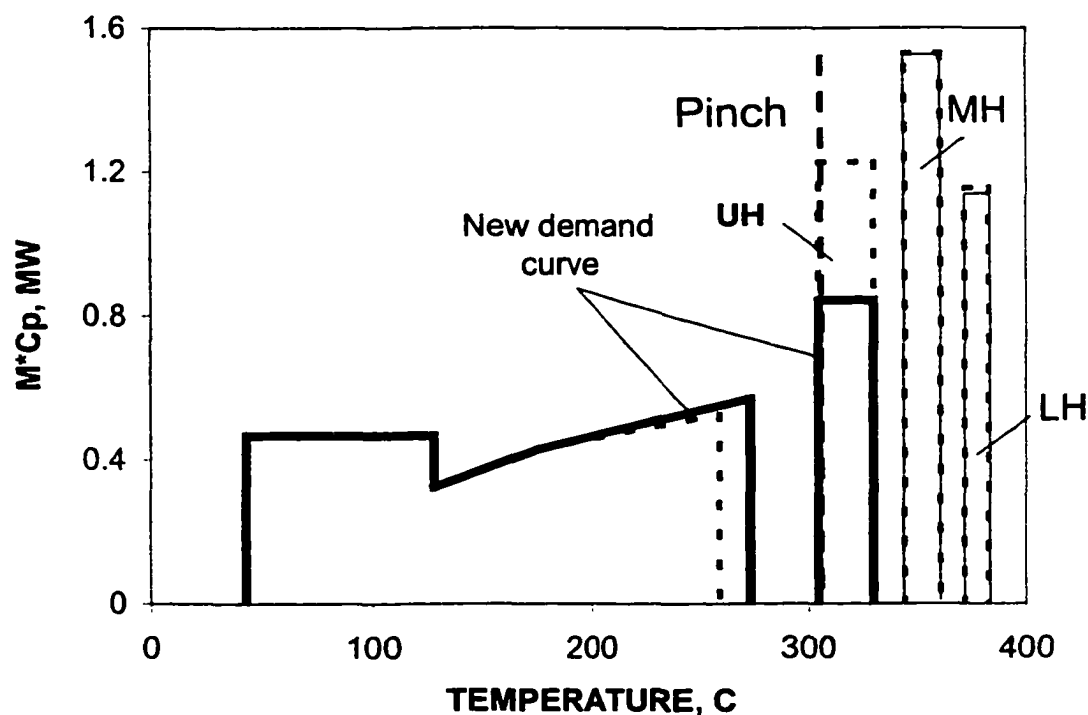


Figure 4.8 Effect of increasing the feed temperature on heat demand

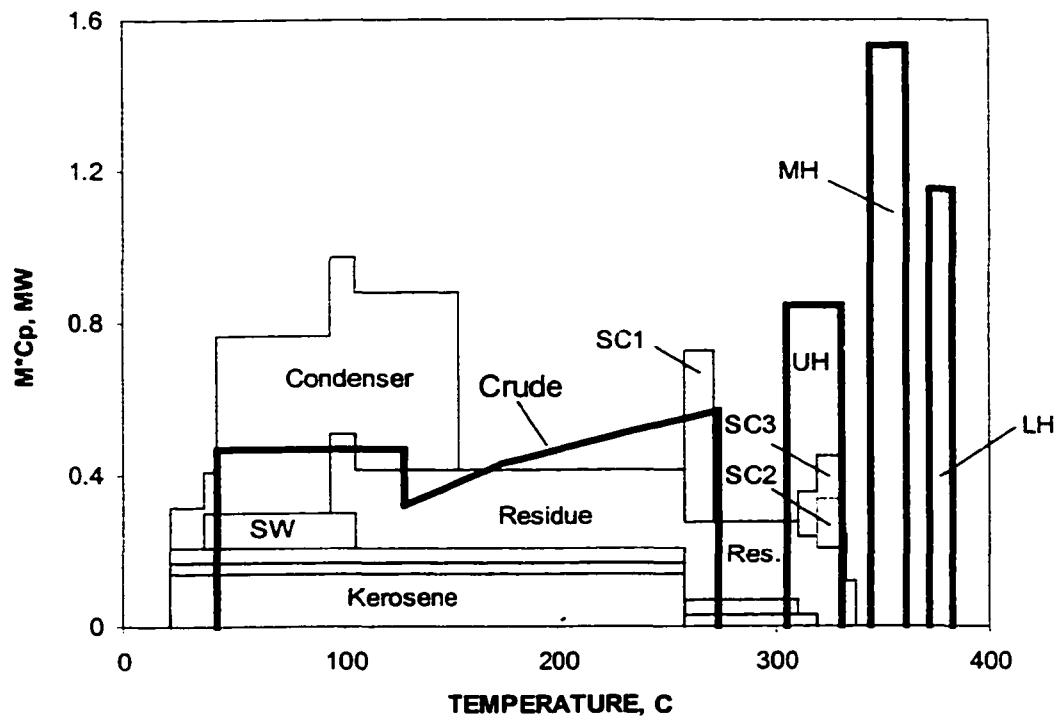


Figure 4.9 The complete heat demand-supply diagram for the higher feed temperature

Note that the location of the pinch does not change at all, however the heat deficit in the upper heater region decreases significantly. The demand of the middle and lower heaters remains the same.

A comparison of the strategy used above with that for the conventional design reveals a few important issues. With a fixed heat demand curve (the crude curve) in the conventional design, the strategy is to move the extra heat supply to higher temperature regions, which was realized by redistributing the pump-around duties (Bagajewicz and Ji, 2001). In the heat demand curve in the stripping-type design can be modified by redistributing heat among the preheater and the side heaters. Here the strategy is to move some heat demand from the high temperature region (the upper heater region) to the low temperature region (the preheater region).

However, there is a limit on the heat shift from the upper heater to the preheater. Table 4.3 shows that the naphtha-kerosene gap decreases with the increase of the feed temperature. This is because the vapor arising from the upper heater decreases in amount as a result of a lower upper heater duty. In the section of the column between the feed tray and the upper heater, the vapor strips off light components from the descending crude.

When the vapor flowrate is too low, the vapor cannot efficiently remove the light components from the crude, and the crude entering the upper heater will carry a significant amount of light components. In the upper heater, these components vaporize along with kerosene and enter the kerosene rectifier. As the rectifier has no way to remove light components, all the light components are present in the kerosene product, contributing to a lower 5% D86 boiling temperature.

Table 4.3 Effect of Feed Temperature in Stripping-type Design

	237.8 °C	260 °C
Preheater duty, MW	60.0	72.4
Upper heater duty, MW	42.3	31.9
Naphtha yield, M ³ /hr	244.8	235.2
Kerosene yield, M ³ /hr	141.0	155.1
Naphtha-kerosene gap, °C	18.8	5.3

4.6 Comparison with the conventional design

The residue yield of the stripping-type design is about 70% larger than that of the conventional design for the same temperature limit of 360 °C. This yield cannot be further reduced either by increasing steam injection or by adjusting the feeding temperature and/or the duties of the heaters. Because the residue yield has significant effect in energy consumption, to make comparisons meaningful, the conventional design was run at this large yield. *As a result, the maximum temperature in the conventional column drops to 324 °C.* While the yields of naphtha are almost the same, however, the yield of kerosene is significantly higher, and the yield of diesel is lower in the stripping-type design (Table 4.4). This is because in the conventional design, the light components, which constitute the kerosene, ascend through the trays where the gas oil and the diesel are withdrawn.

Some of these light components are carried out with the diesel and the gas oil. In the stripping-type design, the crude oil enters the column at the top. Therefore, the carrying of kerosene in the heavy products is ruled out. As expected, in the stripping-type design the gap between kerosene and diesel is much higher than that in the conventional design. Finally, the energy consumption is calculated: adding the minimum heating utility

of the heat exchanger network and 70% of the steam consumption, to account for cost differences. The minimum utility is calculated using pinch analysis.

Table 4.4 Comparison of Product Gaps, Yields and Energy Consumption

	Conventional	Stripping-type
Naphtha-Kerosene Gap (°C)	16.7	16.7
Kerosene-Diesel Gap (°C)	0.0	13.6
Diesel-Gas oil Gap (°C)	-13.2	-13.9
Naphtha yield, M ³ /hr	244.7	242.1
Kerosene yield, M ³ /hr	137.8	157.4
Diesel yield, M ³ /hr	52.8	35.9
Gas oil yield, M ³ /hr	43.9	35.0
Residue yield, M ³ /hr	316.4	324.5
Heating utility (furnaces, MW)	45.6	49.5
Steam consumption (MW)	19.1	16.4
Energy consumption (MW)	59.0	61.0

Simulations were performed for the stripping-type design using a higher temperature limit (399 °C) to obtain the same yield of residue as in the conventional column (360 °C). It is at such higher temperatures, which are not recommended in practice, when the stripping type design achieves around 6% less of total energy consumption.

Investment cost

The above comparison shows the stripping-type design can not achieve the same distillates yields as the conventional design for the same allowable heating temperature.

Since the crude is heated to a lower temperature, a less complex preheat train may be needed. Thus the trade-off between operating and investment costs needs to be analyzed.

The relative costs of both designs are shown in Table 4.5. The main tower for the stripping-type design is considered to be higher because the dirty crude goes through most of the trays. The dirty material reduces the tray efficiency and causes fouling problems. Therefore, additional trays are needed to offset the lower efficiency and especial designs are required to reduce fouling. Both requirements contribute to a higher manufacturing and maintenance cost.

Table 4.5 Relative costs for both designs

	Conventional	Stripping-type	Reason for higher cost
Main tower	lower	higher	Fouling
Furnace	lower	higher	Heating more cold streams
Heat exchangers	similar	similar	
Side columns	same	same	
Desalter	same	same	
Main condenser	same	same	
PA exchangers/side condensers	lower	higher	Corrosion
Total cost	lower	higher	

The side condensers used in the stripping-type design are considered more expensive than pump-around heat exchangers in the conventional design because the side

condensers have to deal with corrosion problem caused by the steam condensation. The corrosion problem becomes more severe when processing high sulfur crudes.

The investment cost for the furnace in the stripping-type design is considered higher because it handles four cold streams. The internal structure will be more complex than that of the conventional design where only one cold stream exists. Besides the energy consumption is higher.

The relative cost for all the other heat exchangers is not easy to estimate without designing the heat exchanger network. However, a comparison can be made on the bases of total number of exchangers because it is the dominating factor in the total cost. The total number of exchangers is estimated using the heat demand-supply diagrams.

For the case of the conventional column in the region above the desalter (Figure 4.10), there is one cold stream and 7 hot streams: PA1, PA2, PA3, residue, gas oil, diesel and kerosene.

By using the (N-1) rule (Biegler et al, 1997), seven heat exchangers and a heater are needed. The condenser is not included because the heat is in surplus and is cascaded into the region below the desalter. In the region below the desalter, there is a large heat surplus. Since the heat from the condenser is large enough, only one exchanger is needed. In addition, the four distillates and the condenser have to be cooled to the final temperatures, needing 5 coolers. Therefore the total number of exchangers is 13.

For the stripping type design above 260 °C, 3 exchangers are needed for the crude to extract heat from SC2, SC3 and the residue (Figure 4.11).

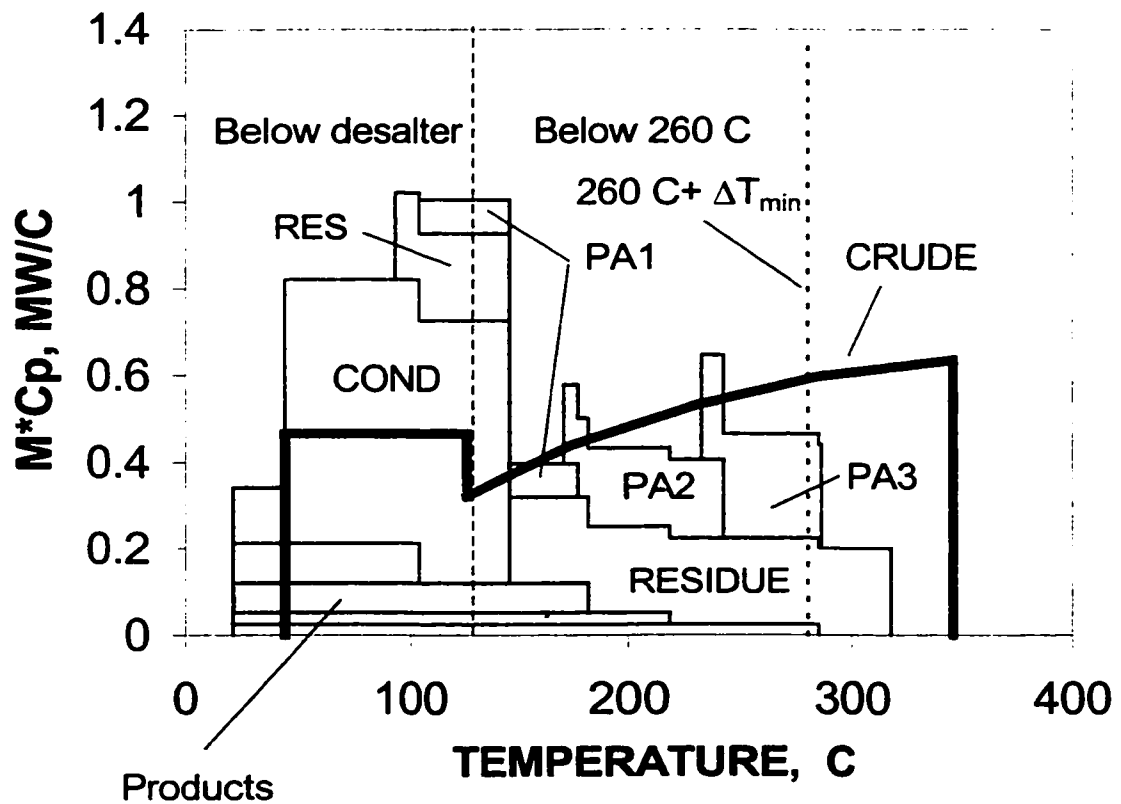


Figure 4.10 Heat Demand-supply Diagram for Conventional Design
 Products from the bottom up are: gas oil, diesel, kerosene and naphtha.

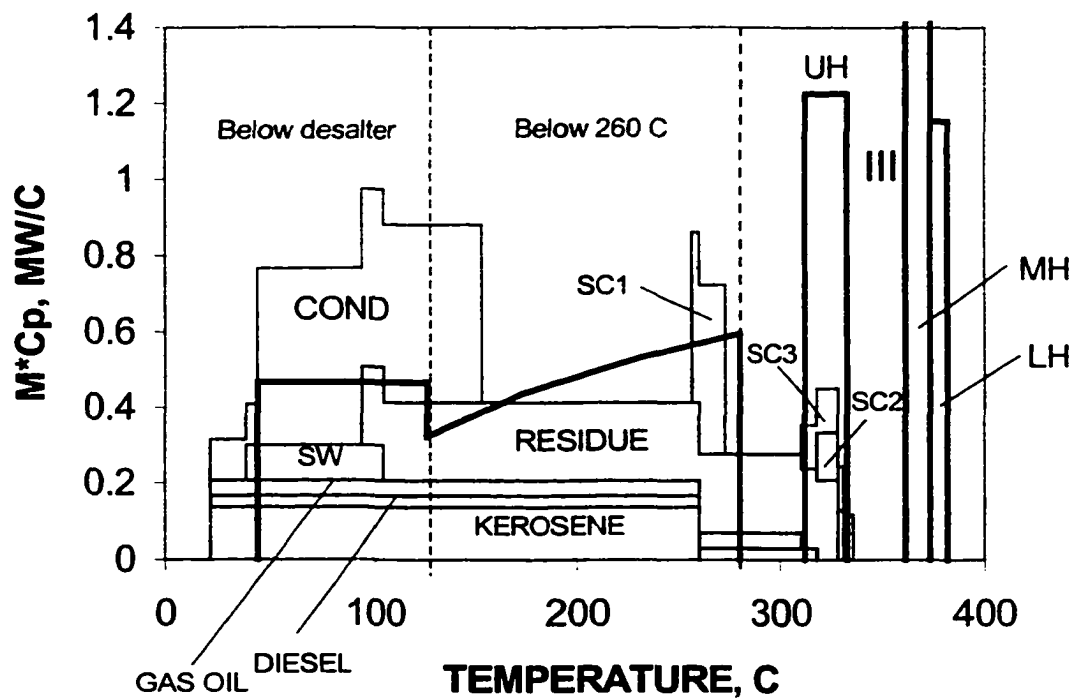


Figure 4.11 Heat Demand-supply Diagram for the Stripping-type Crude Distillation

SW: saline water. SC1: side condenser 1. SC2: side condenser 2. SC3: side condenser 3.

The heat supply to the left of UH has to be cascaded to lower temperatures for utilization. Above the desalter and below 260 °C, there are 5 hot streams: the residue, SC1, kerosene, diesel and gas oil. Similar to the conventional design, the condenser is not used. The number of exchangers is 5 in addition to the heater. Below the desalter, one exchanger is counted for heat exchange between the condenser and the crude. Four coolers are required for cooling the products. The total number of the exchangers besides the heater is 13.

Both designs take the same number of heat exchangers. Assume the number of exchangers is the dominating factor in pricing, we expect the costs for the exchangers to be close to each other. It is then concluded that the stripping-type design requires higher investment cost than the conventional design.

4.7 Conclusions

From this study one can conclude that the stripping-type design for crude fractionation cannot achieve low yields of residue, and under the same yield of products, it is not as efficient as previously reported. The difference may rely on different crudes used as well as design procedures that utilize temperatures that are too high.

4.8 References

1. Bagajewicz M. and S. Ji. Rigorous Procedure for the Design of Conventional Atmospheric Crude Fractionation Units Part I: Targeting. *Industrial and Engineering Chemistry Research*. 40 (2), pp. 617-626 (2001).
2. Biegler , L., Grossmann, I. And Westerberg, A., Systematic methods of chemical process design, Prentice Hall, 1997.
3. Ji Shuncheng and Bagajewicz, M., Rigorous targeting procedure for the design of crude fractionation units with pre-flashing or pre-fractionation, *Industrial and Engineering Chemistry Research*. Submitted.
4. Liebmann, K., Integrated crude oil distillation design, Ph.D. dissertation, University of Manchester Institute of Science & Technology, 1996.
5. Liebmann, K., and Dhole, V. R., Integrated Crude Distillation Design. *Computers & Chemical Engineering*, 19, Supplement, S119, (1995)
6. Liebmann, K.; Dhole, V. R. and Jobson, M., *Integration Design Of A Conventional Crude Oil Distillation Tower Using Pinch Analysis*. Inst. of Chem. Engineers, 76(3), part A, 335-347, (1998).
7. Glinos, K. and Malone, M. F., 1985, Minimum vapor flows in a distillation column with a side-stream stripper. *Ind. Eng. Chem. Proc. Des. Dev.* 24(4): 1087-1090.
8. Nelson, W. L., *Petroleum Refinery Engineering*, 4th ed., McGraw-Hill, New York, 1958.
9. Sharma, R.; Jindal, A.; Mandawala, D.; Jana, S. K. Design/Retrofit targets of Pump-around Refluxes for Better Energy Integration of a Crude Distillation Column. *Ind. Eng. Chem. Res.*, 38, 2411, (1999).

10. Watkins, R.N., *Petroleum Refinery Distillation*, 2nd edition, Gulf Publishers, 1979.

4.9 Appendix

Appendix A

The properties of the light crude are presented. There are taken from Watkins (1979). The crude is TIA JUANA light (Venezuela) having an API gravity of 31.6.

Table 4A.1 TBP data for TIA JUANA light

Percent distilled	Temperature, C
0	-3.0
5	63.5
10	101.7
30	221.8
50	336.9
70	462.9
90	680.4
95	787.2
100	894.0

Table 4A.2 Light ends for TIA JUANA light

Component	Percent of assay
C2	0.04876
C3	0.3762
I-C4	0.2774
N-C4	0.8908
Total	1.5932

Appendix B

The properties of the crude (API 36) used in Table 4.3 and 4.4 are shown here.

There are taken from Bagajewicz and Ji (2001).

Table 4A.3 TBP Data

Percent distilled	Temperature, °C
5	45
10	82
30	186
50	281
70	382
90	552

Table 4A.4 Light-ends Composition of Crude

Component	Percent of assay
Ethane	0.13
Propane	0.78
Isobutane	0.49
n-Butane	1.36
Isopentane	1.05
n-Pentane	1.30
Total	5.11

Appendix C

Table C1 lists the operating conditions of the designs reported by Liebmann (1996). The designs were carried out using ASPEN plus release 8.5-6. Column 1 is the

stripping-type design. Column 2 is the conventional design. The conventional design was simulated in this study using PRO II 5.11 and the results are listed in the last column.

Table 4A.5 Comparison of Operating conditions in two types of designs

	Liebmann-D-2	Base-Liebmann***	Base-this study
Flash zone in, C		343	343
FZT,C		340	341.5
FZP,kpa		261	261
Heaters:			
Heater-12 (UH)	195.2-248.5 C		
Heater-23 (MH)	202.5-370 C		
Heater-34 (LH)	340.6-370 C		
Flowrate, KG/S			
LN	16.92	18.60	18.91
HN	13.5	12.22	12.21
LD	28.93	28.56	27.02
HD	12.81	13.93	22.10
RES	87.14	85.99	80.13
Steam, KG/S			
HN-ST	0	0.21	0.49
LD-ST	6.5042	0.99	0.92
HD-ST	0	5.6MW*	0.72
RES-ST	5.1386	8.65	1.89
D86 5-95,C			
HN-LN		14	16.1
LD-HN		19.5	16.0
HD-LD		5.5	7.7

*Reboiler ** Crude 100,000 BBL/day

Chapter 5 Design of Crude Distillation plants with vacuum units. I. Energy Targeting

5.1 Overview

In previous work, the targeting procedures for atmospheric distillation plants were presented. These procedures were developed assuming that the atmospheric residue leaves the plant as a product. In many cases, however, this residue is distilled in vacuum towers to further extract more gas-oil. The addition of a vacuum tower has many implications on energy consumption. The energy targeting of three atmospheric distillation-vacuum distillation combinations is performed in this article, revealing that the addition of a vacuum column favors the pre-flashing distillation arrangement, which in turn is not as energy efficient as the conventional straight distillation arrangement when the vacuum column is not utilized.

5.2 Introduction

A complete crude distillation process consists of atmospheric distillation and vacuum distillation. Despite of the importance of crude distillation, studies on its optimal design are scarce. One of the important early publications is “Petroleum Refinery Engineering” by Nelson (1936). This book discusses the crude distillation in detail. It contains many charts and experimental data. The 4th edition was published in 1958. In the design procedure presented in this book, the amount of products is estimated from the crude distillation curve, then the number of trays between side withdraws are picked. Next, the temperature and pressure in each tray is calculated using empirical charts. Heat

balance is then carried out and the reflux is determined. The design procedure ends with the design of the preheat train.

Much later, another book on crude distillation was published by Watkins (1979). This procedure provided in this book is similar to the one proposed by Nelson (1958). In this design procedure, the distillation tower is designed first and followed by the design of heat exchanger network. With this procedure, it is difficult to take into account the interaction between the crude tower design and the heat exchanger network. Liebmann (1998) proposed an integrated design procedure for the design of the atmospheric tower. The design procedure starts with a sequence of simple columns that are generated by decomposing the crude main tower. Next, reboilers and thermal coupling are introduced in order to reduce utility consumption. The grand composite curve (a tool used in Pinch Technology) is used to assess the proposed modifications. After all the possible design modifications have been explored, these columns are merged into a single complex column.

Sharma et al (1999) proposed a method for calculating the maximum pump-around heat removal. First, a practical minimum reflux ratio for each column section is determined using Packie's empirical diagram (Packie, 1941). Then, the heat removal in the upper part of the column is calculated using a heat balance. The upper part may start from an arbitrary tray and end with the condenser. Following, the upper part is extended tray by tray and heat surplus is calculated for each tray. The resultant heat surplus data are used to construct a column grand composite curve. Finally, the maximum heat removal for each section is determined using the column grand composite curve. A major advantage of this method is that the maximum heat removal can be estimated quickly

without the need of simulation. However, as Packie's diagram is empirical and the effect of the stripping steam is not included, the heat removal calculated is not accurate. This suggests a procedure based on rigorous simulations that can capture the relationships between the column variables and the heat integration opportunities accurately.

Bagajewicz (1998) studied the flexibility aspects for the design of atmospheric columns using rigorous simulators. Bagajewicz and Ji (2001) proposed such a rigorous targeting design procedure has been proposed for the design of conventional crude distillation units. This procedure aims at finding the best scheme for a multipurpose crude distillation unit that processes a variety of crudes, which is an issue that had been overlooked by previous design procedures. Heat demand-supply diagrams, instead of grand composite curves are used as a guide directing the search for optimal schemes. An advantage of heat demand-supply diagrams is that the role of each stream, heater or cooler in the total energy consumption is clearly shown, so the search of the best scheme is straightforward. The trade off between different operating parameters is considered and the decision is based on quantitative calculations instead of simple assumptions (Bagajewicz and Soto, 2001).

Following the above procedure, the energy targets for a light crude and a heavy crude were obtained. The targets were later used for the design of a multipurpose heat exchanger network (Bagajewicz and Soto, 2001). The model for the multi-purpose heat exchanger network takes advantage of the flexibility identified and is able to predict the desalter temperature that needs to be used. A conjecture that a design for extreme crudes would be able to accommodate the processing of intermediate crude was posed and partially confirmed.

An important variant of atmospheric distillation is pre-flashing or pre-fractionation design. The pre-flashing and pre-fractionation designs are put in the same category because both feature vapor separation before the furnace. Ji and Bagajewicz (2001) presented a systematic procedure to obtain design targets for heat integration in conventional crude fractionation units that use pre-fractionation columns or pre-flash drums. It is shown that under the same high product yield conditions, pre-fractionation or pre-flashing are not advantageous from the energy point of view. This is in great part due to the loss of the carrier effect that light components have in separating heavy gas-oil fractions in the flash zone. The study also showed that the equivalent of the carrier effect of lights could not be obtained by increasing steam injection.

Soto and Bagajewicz (2001) noted that extensive splitting of crude streams has several drawbacks. For example, not much energy efficiency is lost if the branching is reduced and therefore the trade-off between heat utility and capital cost breaks even. The model proposed Soto and Bagajewicz (2001) by uses binary variables to account for the processing of different crudes and count heat exchangers. The second part of this paper improves the model by allowing a match between a given pair to take place in different intervals in different periods. Finally, none of recent papers addressed the heat exchanger network design for crude distillation with either the vacuum tower or with preflashing.

In this first part, the energy targeting of three atmospheric distillation-vacuum distillation combinations is performed. Alternatives for combined atmospheric distillation and vacuum distillation are first studied. Next, targeting procedures for all alternatives design are proposed. These procedures are used to find targets for the light crude. Finally, the conventional-vacuum design is performed for a heavy crude.

5.3 Alternatives for combined atmospheric-vacuum distillation

Figure 5.1 shows the conventional design of an atmospheric unit. Crude is mixed with water and heated in a heat exchanger network before entering a desalter where most of the water containing the salt is removed. The desalted crude enters another heat exchanger network and receives heat from hot streams. Both heat exchanger networks make use of the vapors of the main column condenser, the pump-around circuit streams, and the products that need to be cooled. The preheated crude then enters the furnace, where it is heated to about 340-370 °C. The partially vaporized crude is fed into the flash zone of the atmospheric column, where the vapor and liquid separate. The vapor includes all the components that comprise the products, while the liquid is the residue with a small amount of components in the range of gas oil. These components are removed from the residue by steam stripping at the bottom of the column.

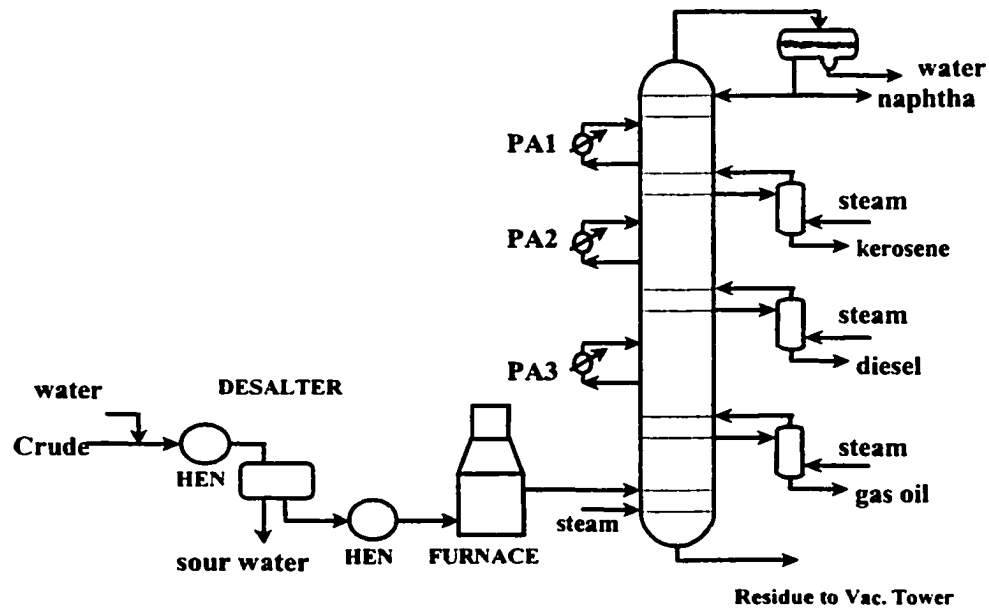


Figure 5.1 The conventional design

In addition to the overhead condenser, there are several pump-around circuits along the column, where liquid streams are withdrawn, cooled, and sent back to upper trays. Such arrangement distributes the reflux throughout the column. It also has beneficial effects for heat integration because the temperature of these liquid draws is higher than that of the condenser. Products are withdrawn in liquid state from different trays and then stripped by steam in side strippers to remove light components. The residue from the main tower is heated further in the vacuum furnace and sent to the vacuum tower to extract vacuum gas oils.

The preflash design (Figure 5.2) is a variation of the conventional design. It is used for processing some light crudes.

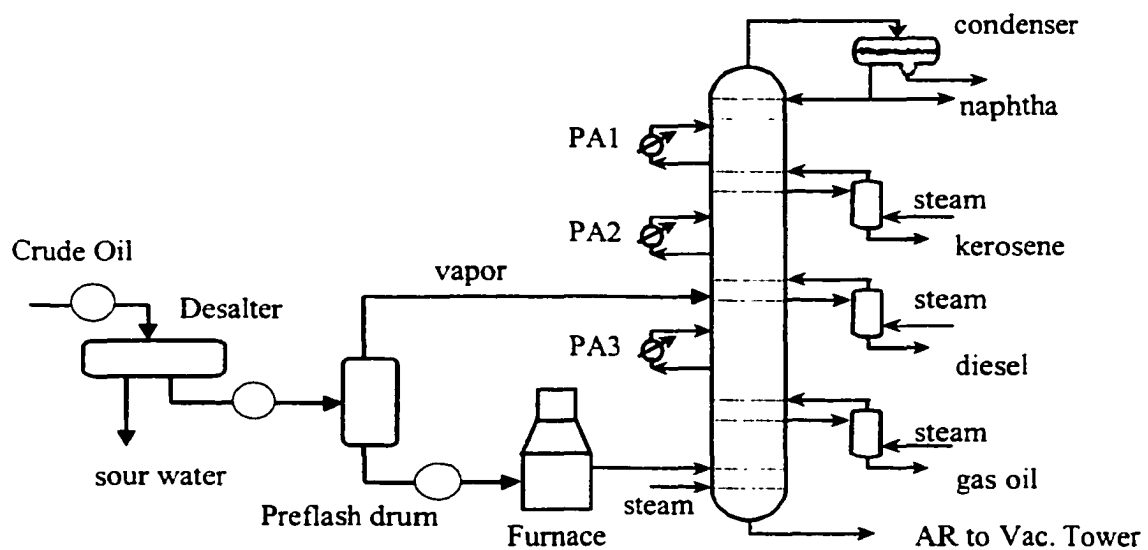


Figure 5.2 The preflashing design

In the preheat train, the crude is under pressure in order to suppress vaporization. In some cases, however, the crude is so light that above certain temperature, the pressure required to suppress vaporization is too high. The solution is to separate some light components before heating the crude further in the preheat train. The light components are sent to the main column directly.

A systematic procedure was presented (Ji and Bagajewicz, 2001) to obtain design targets for heat integration in conventional crude fractionation units that use pre-fractionation columns or pre-flash drums. It is shown that under the usual temperature limits to prevent thermal cracking, the pre-flash design generates more atmospheric residue and less gas oil. In a complete plant, the atmospheric gas oil loss can be picked up by the vacuum tower. The price is that the vacuum tower has to handle a larger amount of feed stock and the vacuum jet steam consumption increases. Whether the trade-off is beneficial is the question to be answered.

In the stripping-type design (Figure 5.3), the crude is heated to a relative low temperature (about 150°C) and fed at the top of the column. Because the crude temperature is low, the vapor ratio of the feed is small. The crude goes down the column and is heated consecutively in three heaters (the upper heater, middle heater and lower heater). Side products are withdrawn from the vapor phases, and rectified in side rectifiers.

Liebmann and Dohle (1995) reported that for atmospheric distillation, the stripping-type design could feature 5% less utility cost than the optimized conventional design (Figure 5.1). However, the comparison is not appropriate because in the stripping-type design, the crude oil was heated to a much higher temperature than in the

conventional design. The maximum allowable temperature is limited by the thermal stability property of the crude being processed and is found by lab testing. For the Venezuela crude oil used in Liebmann's paper, the allowable temperature is 343 °C (Watkins, 1979). However, in the stripping-type design presented by Liebmann (1996), the crude was heated to 370 °C in both the middle heater and the lower heater (see Appendix B). It can be expected that at this temperature, severe thermal cracking will take place. Such operation is not allowed in practice. Because of the above limitation of their study, a re-evaluation of the stripping-type design is necessary. Ji and Bagajewicz (2001) took into account the temperature limit of thermal cracking and made such evaluation.

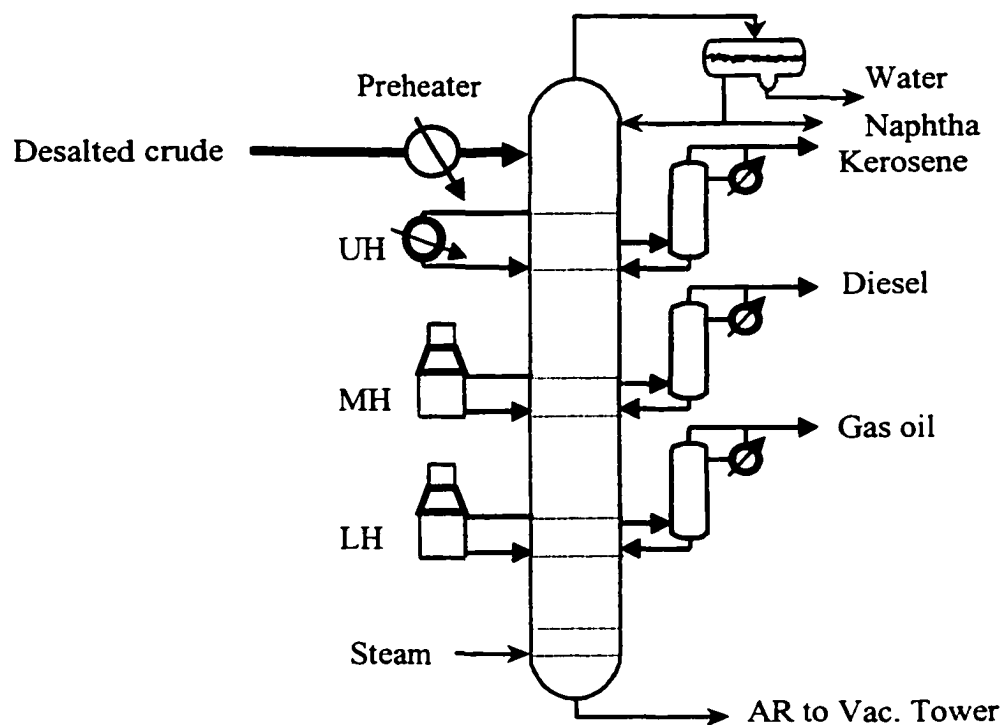


Figure 5.3 The stripping-type design

Similar to the preflash design, the loss of atmospheric gas oil is picked up in the vacuum column at the expense of extra vacuum jet steam consumption. In this paper, the question of whether the total energy consumption is lower than in the conventional design is evaluated.

5.4 Vacuum oil distillation

In this section features regarding vacuum distillation that are relevant for the energy targeting procedure are highlighted.

The topped crude leaving the atmospheric tower still contains significant amount of valuable oils. As discussed above, these oils cannot be distilled at atmospheric pressure because the temperature required would be so high that severe thermal cracking takes place. Vacuum distillation is based on the principle that the boiling point of a material decreases as the system pressure is reduced. In atmospheric distillation, the whole crude cut points between distillates and the atmospheric residual are somewhere from 370 to 430 °C. The cut point can be raised to 580 to 610 °C in vacuum distillation. Thus, the general function of the vacuum tower is to remove the maximum possible amount of distillate from the charge stock while meeting product specifications (Watkins, 1979).

Figure 5.4 is a schematic diagram for production of light vacuum gas oil (LVGO) and heavy vacuum gas oil (HVGO), but sometimes, depending on its properties, LVGO is blended with other products like diesel. Both are typically used as feed to fluid catalytic cracking units. The vacuum distillation consists of the vacuum furnace, vacuum tower and the vacuum producing system. The topped crude is heated up in the vacuum

furnace to about 400 °C. The temperature is controlled to be just below the temperature of thermal decomposition. The heated oil partially vaporizes in the furnace and the vapor-liquid mixture enters the flash zone of the vacuum tower. The vapor ascends in the column and condenses in the HVGO pump-around section and the LVGO pump-around section. Note that no strippers are used for the products because the initial boiling points of LVGO and HVGO are not specified (Gary, 1994).

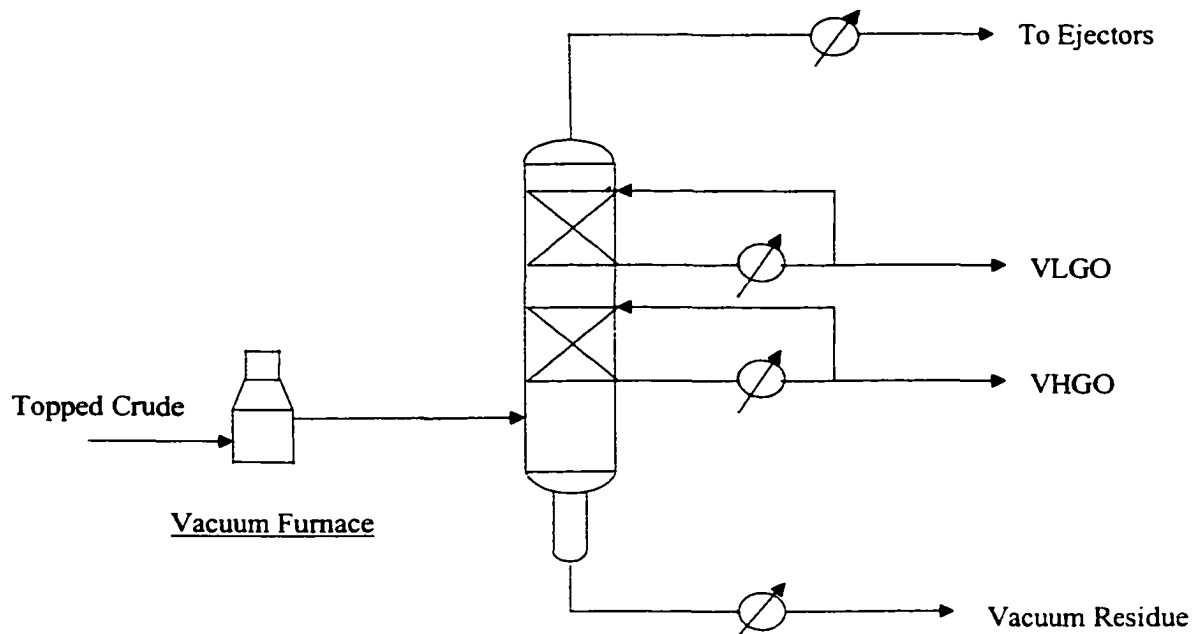


Figure 5.4 Vacuum Distillation (Watkins, 1979)

The HVGO section is the main heat removal zone. HVGO is withdrawn and cooled down in the heat exchanger network and then a portion of HVGO returns to the top of the packing. Although a single cut of VGO (vacuum gas oil) is allowed in some cases, drawing LVGO and HVGO separately is more beneficial from the point of view of

energy savings, because the resultant HVGO draw temperature is 90-120 °C higher than the corresponding draw temperature of a single VGO cut.

The LVGO section is the top zone in the tower where the LVGO is condensed and separated from the non-condensables, cooled and a portion circulated to the top of the packing to remove heat.

The temperature of the steam and non-condensable materials leaving the top of the vacuum tower is determined by setting a 10 to 25 °C approach to the minimum practical cool oil temperature in the top pumparound circuit. The latter temperature is a function of the viscosity properties of the oil processed. Usually a cooling oil temperature of 65 to 95 °C is used. This allows an overhead temperature of 90-135 °C.

The residue section serves two purposes: One is to remove relatively light components, the other is to reduce coke formation. The former is achieved by steam stripping using a steam to net residue ratio of 4-6 lb/bbl. The latter is realized by circulating the partially cooled bottoms to quench the liquid to 365 °C.

The non-condensable gases and steam leave the tower from the top and are ejected from the system by means of the steam jets, thus creating the required vacuum. The non-condensables come from the following sources (Nelson, 1958):

1. Tail of lower-boiling material.
2. Gases produced by cracking of the feedstock.
3. Air dissolved in the feedstock and in the water used in generating steam.
4. Air leakage.

The steam consumption consists of two parts: process steam and vacuum jet steam. The total steam consumption depends on the absolute pressure in the vapor line, the amount of noncondensables, the vaporizer temperature and the temperature of cooling water. Based on the processing of 1000 bpd of a conventional Mid Continent topped crude oil, Nelson showed that the most economical pressure for vacuum tower operation is in the range from 30 to 100 mmHg. The steam consumption at 88 mmHg for different flash zone temperatures is shown in Table 5.1.

Table 5.1 Vacuum distillation steam (process steam + vacuum jet steam) consumption for 1000 bpd topped crude (Nelson, 1958)

Vapor line absolute pressure, mm Hg	Vaporizer temperature, °C	Cooling water temperature, °C	Steam consumption lb/day
88	360	27	58800
88	382	27	23280

The optimum performance depends on the absolute pressure in the flash zone and the maximum non-cracking temperature at the vacuum heater outlet. Figure 5.5, taken from Watkins (1979) shows the ratio of gas oil distilled as a function of the flash zone pressure and temperature.

The system pressure in this figure is the partial pressure of the hydrocarbons instead of the total pressure. In turn, the furnace outlet temperature depends on the boiling range of the feed, the fraction vaporized as well as on the feed coking characteristics. Normally, the maximum flash zone temperatures in the vacuum tower range from 413 to 427 °C (Watkins, 1979).

The absolute pressure in the vacuum tower flash zone is controlled between 25 and 100 mmHg. The effective pressure may be reduced to about 10 mmHg by injecting steam to the furnace and at the bottom of the vacuum tower. The amount of stripping steam used is a function of the boiling range of the feedstock and the fraction vaporized, and generally in the range of 10 -50 lb/bbl. The desired vacuum is maintained by the use of steam ejectors and barometric condensers. The number of ejectors used is determined by the vacuum needed. For a flash zone pressure of 25 mmHg, three ejector stages are required (Nelson, 1958).

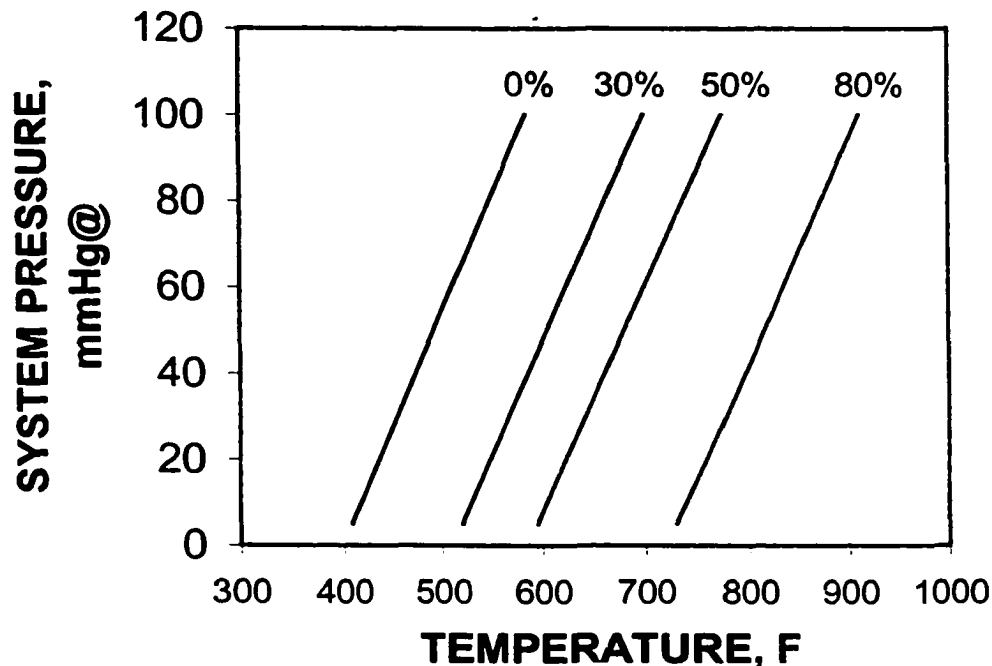


Figure 5.5 Topped crude-vacuum region phase behavior (Watkins, 1979)

Vacuum distillation is widely used to produce catalytic cracking plant feed stocks of low carbon content. It is also used to produce lube oil fractions. In practice, the uses of

vacuum distillates and residue depend on the type of crude oil feed, the type of refinery and its downstream processing capacities. The major specifications for the most common products are (Watkins, 1979):

- *Catalytic cracking feedstocks*: Gas oils for catalytic cracking feedstocks require a strict separation between distillate and residue. The amount of carbon content in these oils should be minimal while not sacrificing gas oil recovery. This is necessary to reduce coke forming on the cracking catalyst. The metals content, particularly vanadium and nickel, should be strictly limited because they are severe catalyst poisons.
- *Hydrotreaters or hydrocrackers Feedstocks*: Feedstocks for hydrotreaters or hydrocrackers can tolerate a slightly higher metal content because the hydrogenation catalysts contain these metals. However, the amount of carbon and asphalt materials should be minimal to prevent coke formation.
- *Distillate fuel oils*: Distillate fuel oils to be used directly are specified by API gravity, viscosity, metal content and flash point. Atmospheric boiling ranges can be used to define the separation.
- *Vacuum residue*: The properties of vacuum residue can be defined in several ways. When distillate production is to be maximized, the amount of gas oil allowed remaining in the bottoms stream must be minimized. The residue is blended into residual fuels. In this operation, one can normally set the volume percent of either the whole crude or the topped crude that is to be yielded as vacuum residuum. This is in effect equivalent to specifying a TBP cut point for vacuum distillates. The goal is to

recover the maximum volume of gas oil, which is free from contaminants by heavier material.

5.5 Vacuum tower specifications

Table 5.2 shows typical specifications which are used in this study. This is a fuel-type tower with two distillate products: light vacuum gas oil (LVGO) and heavy vacuum gas oil (HVGO). In the refining industry, the specification for the LVGO is its flowrate, and it is usually defined to be one third of the total distillate. In this study, however, the same flowrate for LVGO cannot be specified in the three complete plants, because the flowrate of LVGO varies in a wide range. Therefore, D86 95% temperature is used to specify LVGO for all the three designs.

Table 5.2 Vacuum tower specifications

Total trays	7
Flash zone pressure, psia	1.90
LVGO D86 95% temperature, °C	410*
Flash zone temperature, °C	382
Overflash ratio	0.02
Overhead temperature, °C	127
Bottom steam/vacuum residue, lb/bbl	2-3 (2.74)

* Equivalent to 30 % vol percent of total vacuum gas oil.

Products from the vacuum tower are cooled down to recover heat before being sent for further processing. Naturally, one would like to recover as much heat as possible. However, the final temperatures of these products should not be too low, otherwise, they become too viscous to pump. Table 5.3 shows the viscosity of LVGO, HVGO and

vacuum residue at several temperatures. The final temperatures for LVGO, HVGO and vacuum residue are specified at 60 °C, 82 °C and 177 °C, respectively.

Table 5.3 Vacuum Tower Product Temperatures

Product	Temperature, °C	Viscosity, CP
LVGO	104	3.9
	60	14.2
HVGO	104	10.2
	82	20.6
Vacuum Residue	104	1127
	160	60.3
	177	33.8

5.6 Targeting procedure

We now summarize the energy targeting technique for designing complete distillation plants. a conventional-vacuum crude oil distillation plant. For the conventional –vacuum design, the Watkins design method is used to obtain an initial scheme without pump-around circuits. Then a heat demand-supply diagram is constructed, and the direction of heat shifting needed for maximum energy efficiency is determined. This procedure may be repeated for other crudes.

Step 1: Begin with the lightest crude to be processed. As suggested previously, the atmospheric tower does not have any pumparounds at this stage. The vacuum tower, however, needs to have at least one top pumparound because it does not have a condenser.

Step 2: The simulation is performed next. Usually simulation converges without difficulty.

Step 3: Construct the heat demand-supply diagram.

Step 4: Transfer heat from the condenser of the atmospheric tower to the top atmospheric pump-around.

Step 5: If product gaps (difference between 5% ASTM D86 temperature of the heavier product and the 95% ASTM D86 temperature of the lighter adjacent product) becomes smaller than required, the stripping steam flowrate is increased to fix the gap. As long as the steam added has a lower cost than the energy saved, one can continue shifting loads. Otherwise, it is advisable to stop when a trade-off has been reached.

Step 6: If there is heat surplus from the pump-around circuit just added, transfer the heat to the next pump-around circuit between draws in the same way as in step 4. If not, stop.

Step 7: For the vacuum tower, shift heat from the top pump-around to the low pump-around. Check the total energy consumption and the product gap. The heat shifting should stop when either the energy consumption does not decrease or the minimum allowed gap bound is reached.

The energy consumption (E) is calculated using:

$$E = U + 0.7 * \sum H_i^s \quad (5.1)$$

where, U is the minimum heating utility of the system and H_i^s is the enthalpy of each steam used in the column strippers. The weight factor of 0.7 that multiply the steam enthalpies is used because the low-pressure steam is cheaper than the fuel gas used as

heating utility. In turn, the minimum heating utility is assumed to be provided by a furnace and is calculated using the well-known pinch calculation model.

The presence of the vacuum distillation affects the optimal heat load distribution in the atmospheric tower. With the variation of heat distribution in the vacuum tower, the pinch location may change. When Step 7 is completed, one should check the heat demand-supply diagram and see whether the heat distribution in the atmospheric tower is optimal. If not, one has to adjust the heat distribution and go to Step 5 again.

The pre-flash/pre-fractionation case: A special feature of the preflash design is that the heat demand for the crude can be adjusted by changing the temperature of the preflash drum. Because the total heat load in the atmospheric tower depends on the duty of the furnace, which decreases with an increasing preflash temperature, the preflash temperature should be determined prior to distribution of pumparound duties. Therefore, in the case of the preflash design, step 3 is modified as follows:

Step 3: Increase the temperature of the preflash drum until the total energy consumption starts to increase. During this procedure, product gaps are maintained by adjusting the stripping steams.

The stripping-type atmospheric and vacuum case: Instead of having several pumparounds as in the atmospheric tower of the conventional design, the atmospheric tower in the stripping-type design has several heaters. With the knowledge that the conventional design starts with no pumparounds, one can propose a stripping-type design to start with only one heater. However, simulation shows this is not feasible because of the

temperature limits. To overcome this problem, an initial heat distribution among the three heaters is chosen. Thus, step 1 and step 2 are modified as follows:

Step 1: Begin with a stripping-type tower with an initial heat distribution. Set an initial temperature for the feed.

Step 3: Increase the temperature of the feed until the total energy consumption starts to increase.

5.7 Results

It is shown in previous work (Ji and Bagajewicz, 2001) that both preflash and stripping-type designs produce more residue than the conventional design. The higher feed rate to the vacuum tower has two immediate effects. One is the requirement of a higher capacity of the vacuum tower and the other is a higher suction load to the vacuum producing system. From the viewpoint of energy consumption, both preflash design and the stripping-type design have the advantage of reducing the direct heat demand of the crude oil by avoiding overheating of the light components. However, the corresponding vacuum system consumes more steam. The trade-off both the two factors is here investigated with the heat demand-supply diagram.

The feedstock used in this section is a light crude of API 36. The property data for this crude are shown in the Appendix A.

The conventional atmospheric-vacuum distillation design: Basically, there are two rules to determine if a new pump-around is needed (Step 6). One is the existence of heat surplus in the pump-around last added and the other is that the addition of a new pump-around should reduce the total energy consumption. For the vacuum tower, the two

pump-arounds already exist at the beginning of the procedure. The problem is then to minimize the objective function without violating the product gap.

Table 5.4 shows the resulting energy consumption after the corresponding steps in the targeting procedure are implemented. The energy consumption decreases constantly with the addition of a new pump-around. The resulting heat demand-supply diagram is shown in Figure 5.6.

Table 5.4. The variation of the energy consumption with the addition of each pump-around in the case of the conventional-vacuum design (Vacuum jet steam consumption not included)

	Energy consumption (MW)
No pumparound (Step 3)	97.29
With PA1 (Step 4)	95.33
With PA1 and PA2 (Step 6)	86.46
With PA1, PA2 and PA3 (Step 6)	76.94
With VPA2 optimized (Step 7)	75.13

$\Delta T_{\min} = 22.2 \text{ } ^\circ \text{C}.$

The installation of PA1 or VPA2 only results in a small reduction of energy consumption. This is because the temperature of the heat provided by PA1 is still low and in the heat demand-supply diagram, most of this heat is in the region of the condenser, where heat supply is already in surplus. The reason why VPA2 results in a small decrease is that the duty of the VPA2 is relatively small compared to the duties of atmospheric pump-arounds.

Although the heat loads provided by vacuum pump-arounds and products are not as large as those of the atmospheric counterparts, they affect the heat distribution in the atmospheric pump-around circuits. With additional heat sources available in the intermediate temperature region (PA2 region), it is beneficial for the complete design to shift more heat from PA2 to PA3. Table 5.5 compares the heat distribution in the atmospheric tower with the conventional design (Bagajewicz and Ji, 2001).

Table 5.5. Comparison of pump-around loads in the atmospheric tower
(Units: MW)

Pump-around circuit	Conventional design*	Atmospheric-vacuum design
PA1	22.28	23.07
PA2	33.71	12.87
PA3	8.79	22.69

* Taken from Bagajewicz and Ji (2001).

The complete plant has a lower duty in the middle pump-around (PA2) and a higher duty in the lower pump-around (PA3). This can be explained as follows. In the atmospheric conventional distillation only (see Figure 5.7), when the PA3 duty reaches 8.79 MW, the surplus in the PA2 region vanishes. Therefore, further heat shift to PA3 does not reduce the net heat demand and worsens the separation between diesel and gas oil.

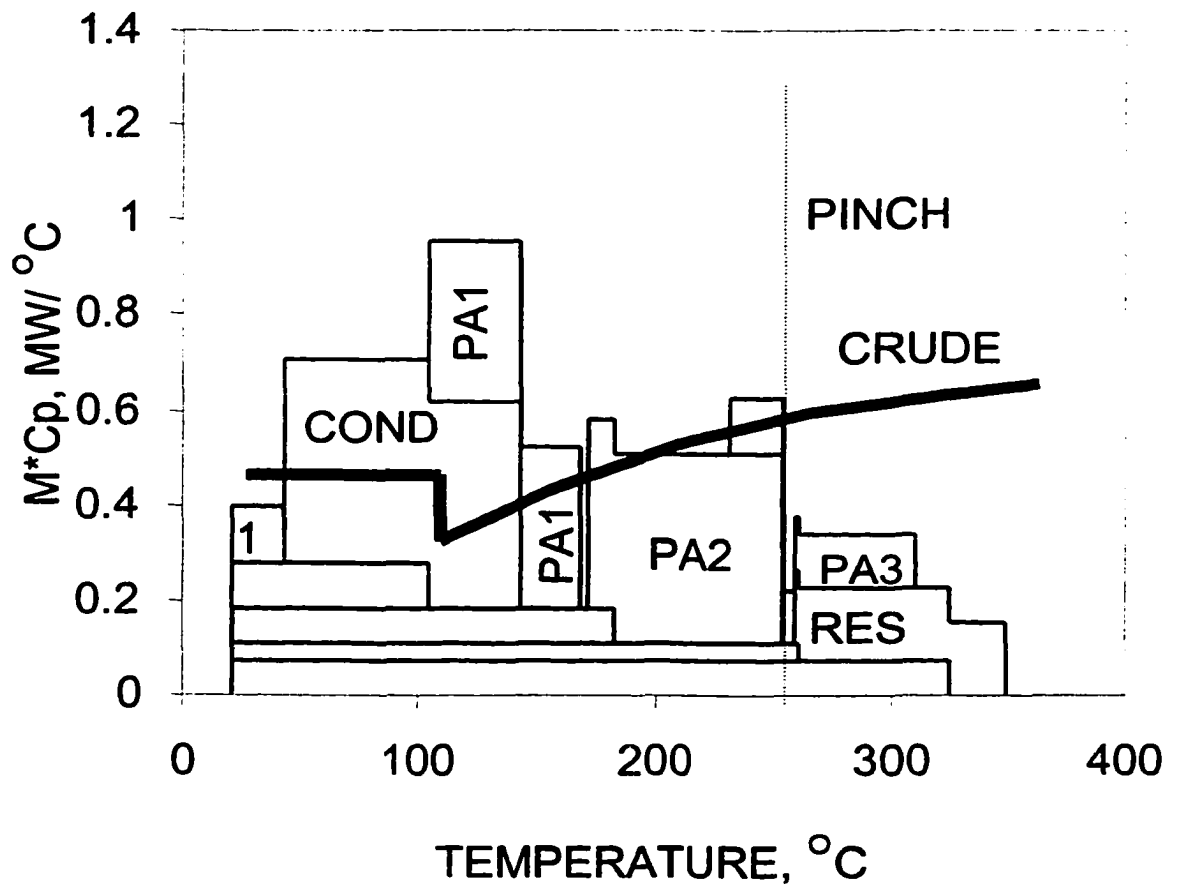


Figure 5.7 Atmospheric conventional distillation

In the complete atmospheric-vacuum plant, however, vacuum products and pump-arounds provide new heat sources in the PA2 region (Figure 5.6), which contribute to a larger heat surplus in the PA2 region and allows more heat to be shifted from PA2 to PA3. The duty of PA3 increases until the trade-off between the reduced energy consumption and the increased steam consumption is not favorable.

Comparison: A comparison among the three complete plants is shown in Table 5.6. In this table from the left to right are the conventional design, the preflashing design and the stripping-type design. The preflash design has the lowest energy consumption, but its difference with the conventional is small, indicating that the conventional design is competitive. The difference is because the atmospheric heater in the preflash design has a lower duty than in the conventional design.

Figure 5.8 shows the heat demand-supply diagram for the preflash type crude distillation. In this figure, the heat demand for the crude without preflashing is shown as dashed line.

The Stripping-type design consumes 40% more energy than the conventional design. Both the steam consumption and the minimum heating utility are higher than that of the conventional design. The larger vacuum steam consumption is incurred by the larger amount feed to the vacuum tower. The vacuum steam consumption of the stripping-type design is 48.5% higher than the conventional design. The large increase in the duty of the atmospheric tower is due to the requirement of heat at higher temperature levels where less recoverable heat is available. The requirement for higher temperature heat makes a large part of the heat from the products and the pump-arounds unusable, and more cooling water has to be used to remove the unusable heat.

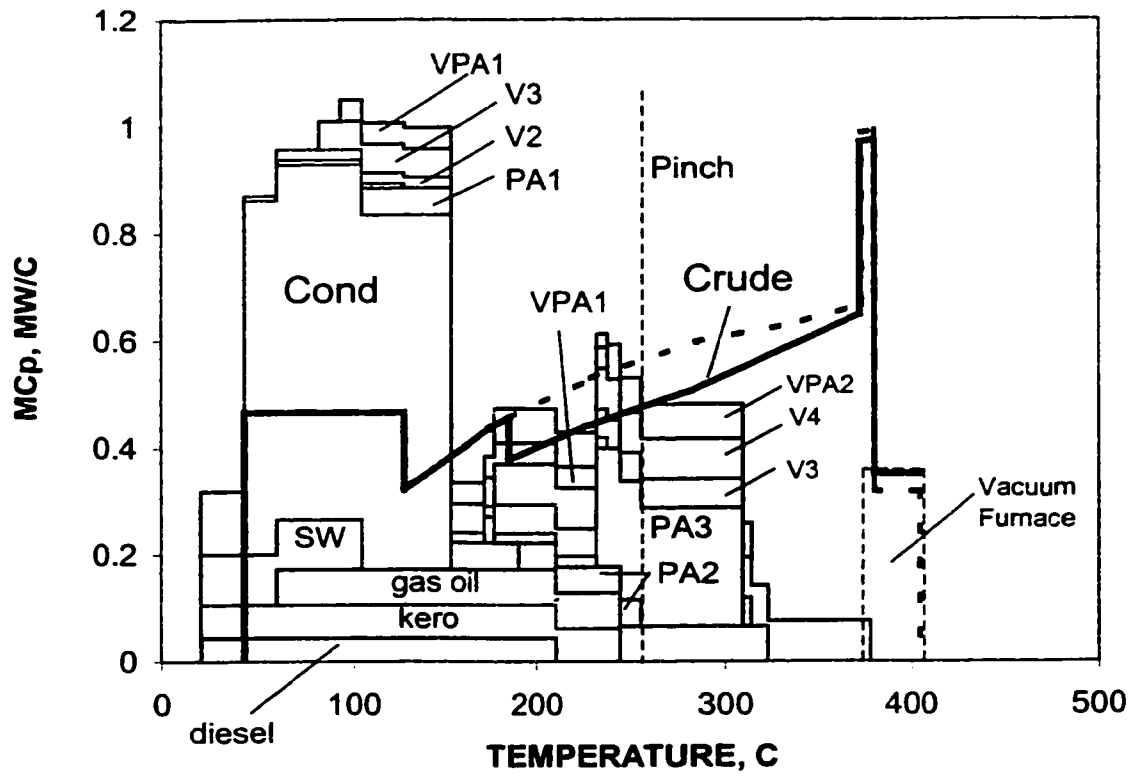


Figure 5.8 Heat demand-supply diagram for preflash type distillation (light crude)

Table 5.6. Comparison of the optimal designs of three complete plants

	Conventional	Preflashing	Stripping-type
Steam enthalpy, MW			
Atmospheric	15.74	13.08	16.38
Vacuum*	11.55	12.35	17.15
Total steam	27.28	25.43	33.53
Product Gap, °C			
Naphtha-kerosene	16.6	16.7	18.8
Kerosene-diesel	0.0	0.0	0.7
Diesel-gas oil	-4.0	-4.5	-25.8
LVGO-HVGO	-30.4	-29.7	-30.2
Yield, M³/hr			
Naphtha	244.39	244.92	244.81
Kerosene	144.76	145.15	141.03
Diesel	71.82	69.95	51.84
Gas oil	124.25	110.40	45.44
LVGO	22.92	34.92	115.09
HVGO	81.43	86.09	92.24
Vacuum residue	105.53	103.58	104.37
Vacuum overhead, kg/hr	171.95	219.04	92.08
HDBR**, MW	195.81	191.58	
HU, MW	62.57	62.10	80.48
Energy, MW	81.67	79.90	114.01

* Steam consumption 23.28 lb per bbl feed.

** Total heat demand before recovery

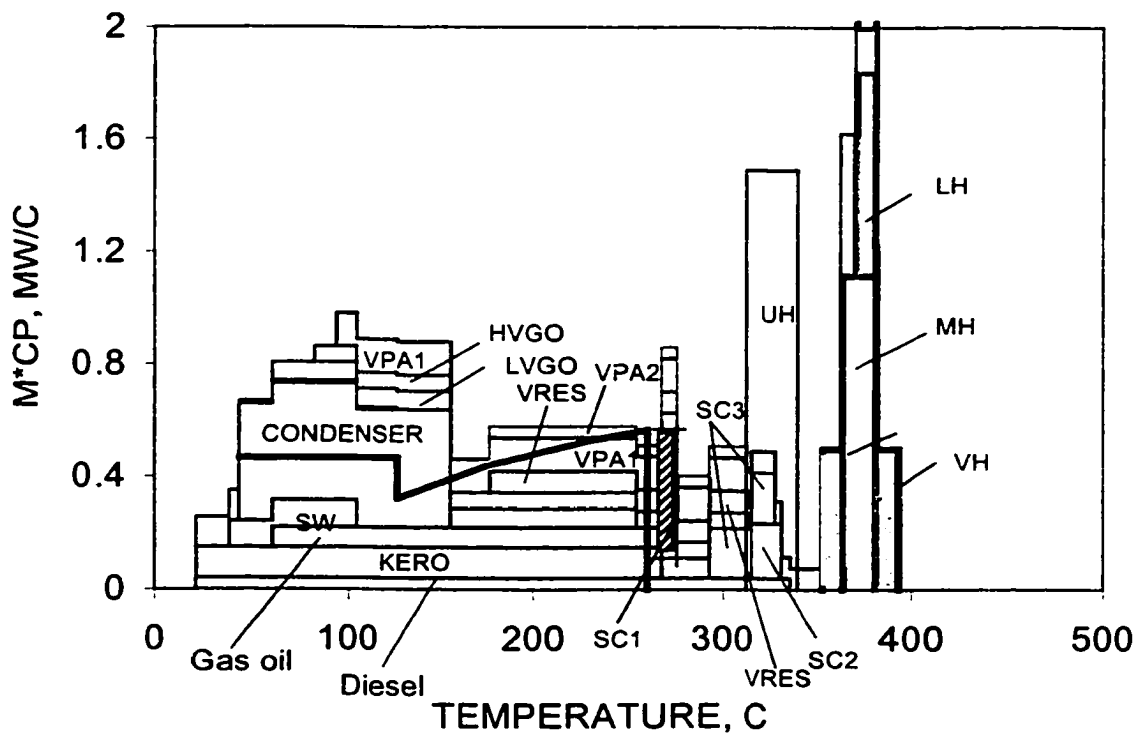


Figure 5.9 Stripping-type crude distillation (light crude)

It is also seen that both the stripping-type design and the preflash design produce less atmospheric gas oil, but the loss is picked up by the vacuum tower in terms of more LVGO. The product gaps are similar among the three designs except for the diesel-gas oil gap in the stripping-type design, where some diesel is not vaporized in the mid heater and is carried out in the gas oil stream.

Figure 5.9 shows the heat demand-supply diagram for stripping-type crude distillation. The addition of the vacuum tower does not have significant effect on the topology of the heat demand-supply diagram. This is because the heat demand takes place at high temperatures. The heat from vacuum products and vacuum pump-arounds appears on the left of these heaters, where the heat can only be used to preheat the crude. While the heat from the vacuum section can be utilized to a large extent in both the conventional design and the preflash design, it is almost of no use in the stripping-type design. This explains why the energy efficiency for the stripping-type design in a complete plant is even worse than in the stripping-type atmospheric distillation plant.

5.8 Results for a heavy crude

As mentioned before, both the preflash design and the stripping-type design aim at light crudes. In terms of energy efficiency, the possible gain from both designs is that the heat demand for the light components can be lowered (Ji and Bagajewicz, 2002a, b). Because the amount of light components in a heavy crude is low, it does not make sense to use the preflash design or the stripping-type design for a heavy crude. Therefore, only the conventional-vacuum design will be studied for the heavy crude. The heavy crude of 20.0 API is used in this study. Property data of this crude are shown in the appendix.

The heating utility for a complete conventional plant processing a heavy crude is 51.35 MW. The heat demand-supply diagram and the operation variables for a scheme with three pump-around circuits are shown in Figure 5.10. Compared with the conventional design without vacuum distillation (Figure 5.11), the heat deficit in the low to medium temperature range is improved but still prevails. The heat surplus in the PA2 region can be used to cover the heat deficit in the condenser region. Similar to the atmospheric design, the total energy consumption is not sensitive to the atmospheric tower heat distribution. This is an added flexibility for the heat exchanger network design.

5.9 Conclusion

Rigorous targeting procedures have been developed for three types of complete crude distillation plants. It has been found that the introduction of vacuum tower changes the topologies for both the conventional design and the preflash design, and thereby changes the heat distribution among the pumparounds. In the stripping-type design, however, the heat provided by the vacuum products cannot be utilized. The comparison shows that energy consumption for the preflash-vacuum design is slightly smaller than the conventional-vacuum design. Because the energy consumption difference is very small, it should not be concluded that the preflash-vacuum design is better. The energy targets obtained above are used in Part II to develop a heat exchanger network for a complete distillation plant.

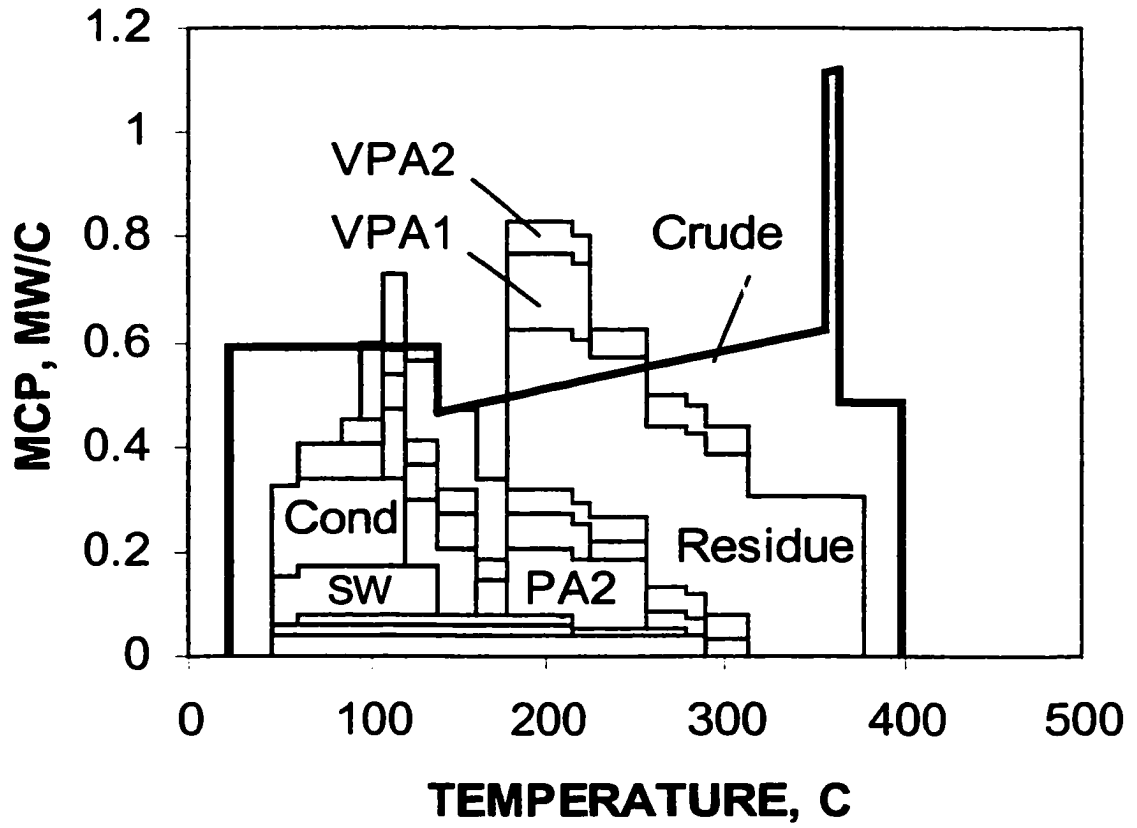


Figure 5.10 The conventional-vacuum crude distillation (heavy crude)

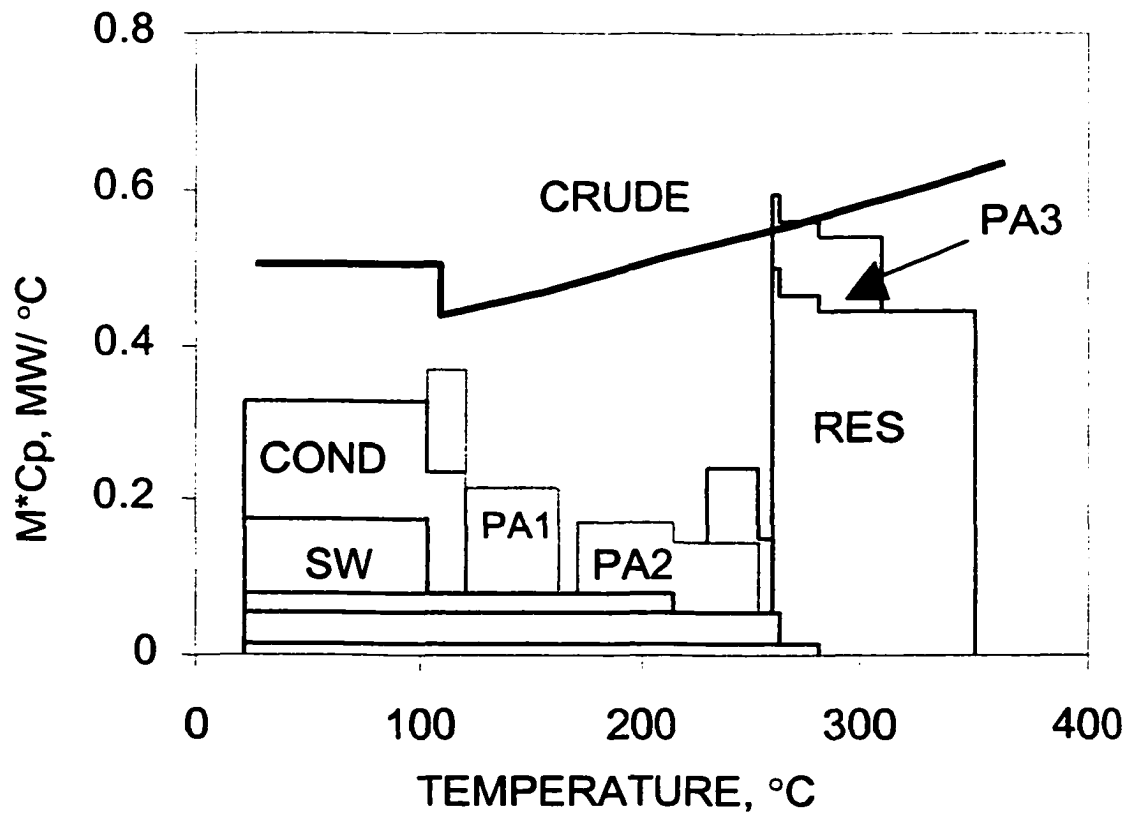


Figure 5.11 The conventional crude distillation for the heavy crude
(without vacuum tower)

5.10 References

1. Bagajewicz M., On the design flexibility of atmospheric crude fractionation units, *Chemical Engineering Communication*, Vol. 166, 1998.
2. Bagajewicz M. and Ji S., Rigorous Procedure for the Design of Conventional Atmospheric Crude Fractionation Units, Part 1: Targeting, *Industrial and Engineering Chemistry Research*, 40(2), 2001.
3. Edminister, W.C., *Applied Hydrocarbon Thermodynamics*, Houston, Gulf Publishing Company, 1964.
4. Gary, James H., Handwerk, Glenn E., *Petroleum Refining: technology and economics*, Marcel Dekker Inc., New York, 1994.
5. Golden, S., Prevent Pre-flash Drum Foaming, *Hydrocarbon Processing*, May 1997, pp141-153.
6. Harbert, W. D., Preflash saves energy in crude unit, *Hydrocarbon Processing*, July, 123-125, 1978.
7. Ji, Shuncheng and Bagajewicz, M., Rigorous targeting procedure for the design of crude fractionation units with pre-flashing or pre-fractionation, *Industrial and Engineering Chemistry Research*, 2002a, Submitted.
8. Ji, Shuncheng and Bagajewicz, M., On the energy efficiency of stripping-type crude distillation, *Industrial and Engineering Chemistry Research*, 2002b, to be submitted.
9. Liebmann, K., *Integrated crude oil distillation design*, Ph.D. dissertation, University of Manchester Institute of Science & Technology, 1996.
10. Liebmann, K., and Dhole, V. R., *Integrated Crude Distillation Design*. *Computers & Chemical Engineering*, 19, Supplement ,S119, 1995

11. Liebmann, K.; Dhole, V. R. and Jobson, M., *Integration Design Of A Conventional Crude Oil Distillation Tower Using Pinch Analysis*. Institution of Chemical Engineers, 76(3), part A, 335-347, 1998.
12. Maxwell, J.B., *Data Book on Hydrocarbon*, Princeton, N.J., D. van Nostrand Co., 1965.
13. Nelson, W. L., *Petroleum Refinery Engineering*, 4th ed., New York, 1958.
14. Packie, J.W. *Distillation Equipment in the Oil Refining Industry*. *AIChE Transactions*. 1941, 37, 51.
15. Bagajewicz, M. and Soto, J., *Rigorous Procedure for the Design of Conventional Atmospheric Crude Fractionation Units. Part III: Trade-Off Between Complexity And Energy Savings*. Submitted. *Industrial and Engineering Chemistry Research*.
16. Watkins, R. N., *Petroleum Refinery Distillation*. Gulf Publishing Company, 1979.

5.11 Appendix

Appendix A

The crude oils used in this paper are summarized in Table 5A.1. The process rate is 5000 bbl/hr. The TBP data and light ends composition are shown in Table 5A.2 and Table 5A.3.

Table 5A.1 Feedstock Used for the Design

Crude	Density (kg/m ³)	Throughput (m ³ /hr)
Light Crude	845 (36.0 API)	795
Heavy Crude	934 (20.0 API)	795

Table 5A.2 TBP Data (°C)

Vol. %	Light Crude	Intermediate Crude	Heavy Crude
5	45	94	133
10	82	131	237
30	186	265	344
50	281	380	482
70	382	506	640
90	552	670	N/A

Table 5A.3 Light-ends Composition of Crude

Compound	Light crude	Heavy crude
	Vol. %	Vol. %
Propane	0.78	0.04
Isobutane	0.49	0.04
n-Butane	1.36	0.11
Isopentane	1.05	0.14
n-Pentane	1.30	0.16
Total	5.11	0.48

Appendix B

Table 5A.4 lists the operating conditions of the designs reported by Liebmann (1996). The designs were carried out using ASPEN plus release 8.5-6. Column 1 is the stripping-type design. Column 2 is the conventional design.

Table 5A.4 Comparison of Operating conditions in two types of designs

	Liebmann-D-2	Base-Liebmann***
Flash zone in, C		343
FZT,C		340
FZP,kpa		261
Heaters:		
Heater-12 (UH)	195.2-248.5 C	
Heater-23 (MH)	202.5-370 C	
Heater-34 (LH)	340.6-370 C	
*Reboiler	** Crude 100,000 BBL/day	

Chapter 6 Design of Crude Distillation Plants with Vacuum

Units. II. HEN Design

6.1 Overview

In this chapter, the design of the heat exchanger network is presented. A multi-period heat exchanger network design model is proposed to handle two different crudes -- a light crude and a heavy crude. This model considers the existence of a preflash drum, which is only used for the light crude period. Part of this multi-period model contains a topological constraint through which all periods share the same heat exchange “matching pattern” but not necessarily at the same temperature levels.

6.2 Introduction

In Chapter 5, rigorous targeting procedures have been developed for three types of complete crude distillation plants. It was found that the introduction of vacuum tower changes the topologies for both the conventional design and the preflash design, and thereby changes the heat distribution among the pumparounds. Comparisons show that energy consumption for the preflash-vacuum design is slightly smaller than the conventional-vacuum design. It was concluded that the stripping-type design cannot compete with the conventional design in both the operating cost and the capital investment. The energy targets obtained above are used in this part to develop a heat exchanger network for a complete distillation plant.

Bagajewicz and Soto (2001a) presented heat exchanger networks for atmospheric distillation featuring maximum energy efficiency. The problem with such a design is that it requires extensive splitting of the crude stream. Such high splitting reduces the controllability of the preheat train. In another paper by the same authors (Bagajewicz and Soto, 2001b), heat exchanger network for the atmospheric distillation using two, three and four branches, respectively, were studied and showed the total cost is not sensitive to the number of branches. This is because the HEN with less number of matches includes less exchanger shells and therefore less investment cost. It was concluded that when the branching is reduced, the trade-off between heat utility and capital cost breaks even.

The model proposed in the above paper (Bagajewicz and Soto, 2001b) uses binary variables to count heat exchangers and these binary variables are shared by both operation periods. The sharing of binary variables forces the the same matches for a given pair of streams in the same intervals. This paper extends the model to cases where a match between a given pair can take place in different intervals in different periods. The heat exchanger network also takes into account the flexibility of using preflashing units for light crude processing.

Although many heat exchanger network (HEN) design techniques are available, their ability to address rigorous industrial problems with large number of streams and at the same time controlling branching is limited. For example, Nielsen (1997) noted that most HEN problems in the literature had less than 10 process streams. Papalexandri (1998) and his coworkers noted that “industrial applicability of the proposed methods (for HEN) has been limited, as important features of industrial HEN can not be efficiently account for”. For example, too complex heat exchanger networks with many branches

and complex piping should be avoided because of process operability and reliability concerns.

Besides the main objective of the maximum heat utilization, the HEN should also have the flexibility to accommodate varying operating conditions (Papalexandri, 1993). In this regard, Bagajewicz (1998) and Bagajewicz and Ji(2001) showed that operating conditions (process stream temperatures and flowrates) in a crude distillation plant vary with the crude oil processed and the product specifications.

The problem of multiperiod HEN has been addressed by several authors. Floudas and Grossmann proposed a procedure based on a superstructure representation that embeds all possible structural options for different time periods (Floudas and Grossmann, 1986, 1987). Papalexandri and Pistikopoulos (1993, 1994) proposed a unified hyperstructure representation of mass and heat exchange alternatives to account for all mass and heat integration possibilities.

The HEN design problem for a complete crude distillation plant discussed in Chapter 5 has at least 18 process streams (15 hot and 3 cold). Compared with that of chemical plants, the flexibility issue is much more challenging. Depending on the difference of crude oils to be processed, the stream flowrates and temperatures can vary in such a wide range that a HEN for one crude oil is not even feasible for another crude oil. With atmospheric distillation, Bagajewicz and Soto (2001) showed the optimal topology for a light crude HEN departs substantially from that for a heavy crude. In fact, the former is pinched while the latter is not.

This chapter addresses the design of a heat exchanger network for a complete crude distillation unit that uses a vacuum column for both crudes and a preflash unit for a

light crude. A new concept of “match pattern” is presented and its mathematical representation is given. This representation is based on the same interval transshipment model as in Bagajewicz and Soto (2001) and extends this model to allow the crude to match the same set of hot streams in different intervals and be considered the same topology. A MILP model for such multi-period HEN design is proposed.

6.3 Energy Targets

Figure 6.1 shows the diagram for a complete crude distillation plant. Note that the preflash drum is bypassed in the heavy crude period. The energy targets are used to design the heat exchanger network are determined by the procedure proposed in Part I (Ji and Bagajewicz, 2001).

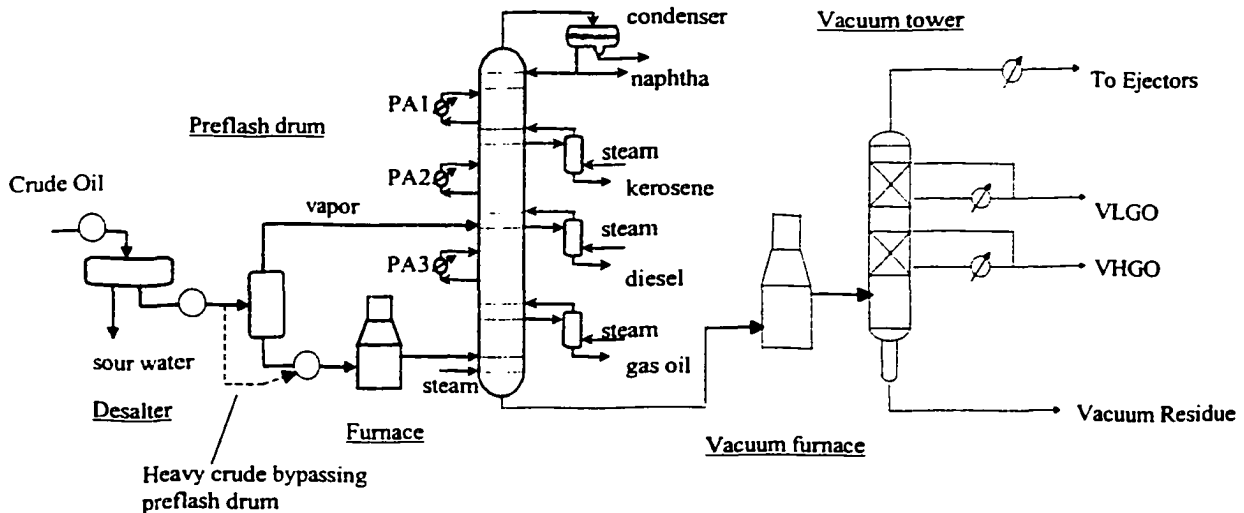


Figure 6.1 Complete crude distillation plant

The design procedure of the distillation column starts by assuming a minimum temperature difference for the heat integration or heat recovery approximation temperature (HRAT). First, the Watkins design method is used to obtain an initial scheme without pump-around circuits. Then a heat demand-supply diagram is constructed, and the direction of heat shifting needed for maximum energy efficiency is determined. This procedure may be repeated for other crudes processed.

With this procedure and a HRAT value of 22.2 °C, the energy target for light crude oil is obtained from Figures 2. The same procedure is applied for the heavy crude case (Figure 6.3) and two sets of conditions can be obtained: product and pump around flowrates, supply and target temperatures, and energy consumption for the light and heavy crude. The data that constitute the starting point of the design are shown in Tables 6.1 and 6.2.

It can be seen from the heat demand-supply diagrams that a heat exchanger network featuring the minimum utility should be complex. For example, the pinch point for the light crude (Figure 6.2) is 254 °C. Above the pinch, five hot streams are found in the region between 254 °C and 310 °C. In order to completely use the heat from all the five streams, the crude stream has to be split into five branches.

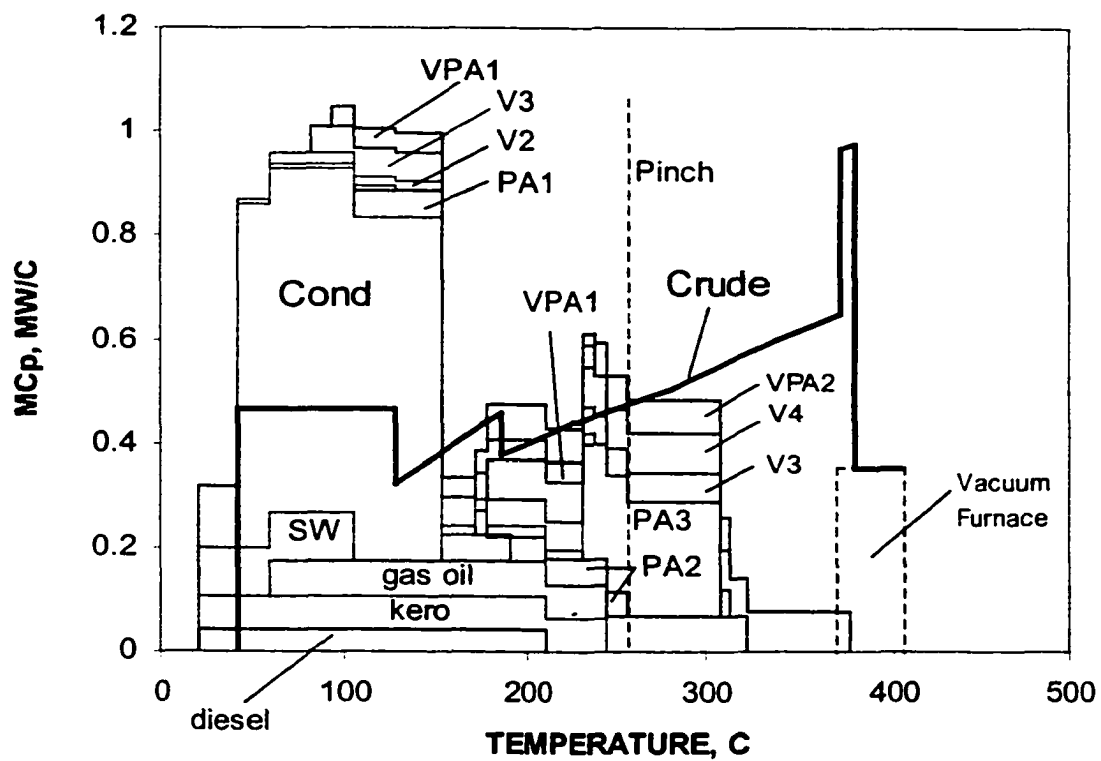


Figure 6.2 Heat demand-supply diagram for the light crude distillation

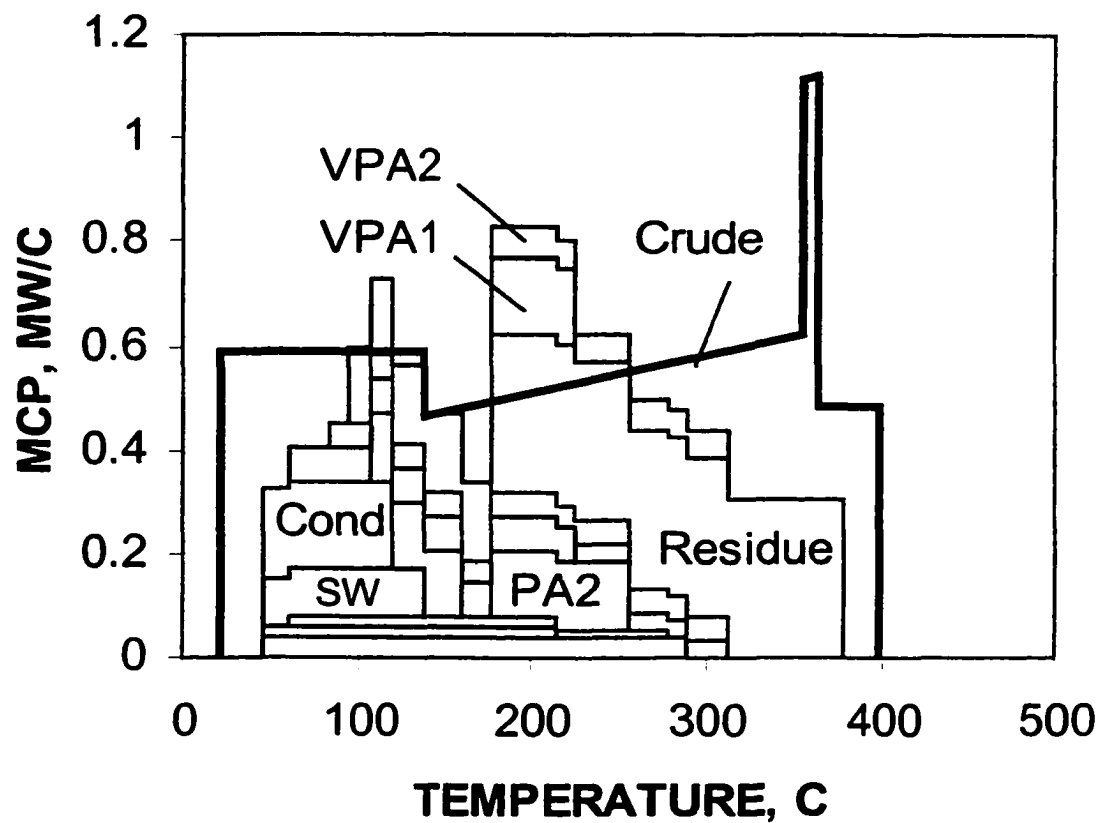


Figure 6.3 The conventional-vacuum crude distillation (heavy crude)

Table 6. 1 Stream data for light crude distillation with preflashing

Stream	Description	Ts, C	Tt,C	Q, MW	MCP, MW/C
J1	crude before desalter	21.1	104.4	-38.83	-0.4658
J2	crude between desalter and preflash drum	162.8	383.4	-111.58	Vary
J3	topped crude	348.9	413.4	-11.56	-0.1793
J4	crude between desalter and preflash drum	104.4	162.8	-26.61	-0.4560
I1	Saline water	104.4	43.3	5.73	0.0938
I2	Atmospheric condenser	144.8	43.3	53.71	0.5290
I3	Atmospheric PA1	176.7	104.4	17.59	0.2434
I4	Atmospheric PA2	246.9	176.7	11.72	0.1670
I5	Atmospheric PA3	306.1	232.2	20.52	0.2775
I6	kerosene	185.0	43.3	10.52	0.0742
I7	diesel	232.2	43.3	7.19	0.0380
I8	Atmospheric gas oil	312.8	60.0	17.34	0.0686
I9	Vacuum PA1	232.2	93.3	7.20	0.0518
I10	Vacuum PA2	312.8	176.7	7.33	0.0538
I11	LVGO	232.2	60.0	3.21	0.0186
I12	HVGO	312.8	82.2	12.56	0.0545
I13	Vacuum residue	371.1	176.7	15.20	0.0781

Table 6. 2 Stream data for heavy crude distillation

Stream	Description	Ts, C	Tt,C	Q, MW	MCP, MW/C
J1	crude before desalter	21.1	137.8	-68.99	-0.5912
J2	crude between desalter and preflash drum	137.8	363.1	-123.51	Vary
J3	topped crude	354.4	399.7	-22.06	-0.4872
I1	Saline water	137.8	43.3	8.74	0.0925
I2	Atmospheric condenser	119.1	43.3	12.83	0.1693
I3	Atmospheric PA1	160.0	104.4	7.33	0.1319
I4	Atmospheric PA2	256.5	176.7	10.26	0.1285
I5	Atmospheric PA3	312.8	225.6	2.93	0.0336
I6	kerosene	214.2	43.3	3.91	0.0214
I7	diesel	288.6	43.3	10.00	0.0407
I8	Atmospheric gas oil	278.8	60.0	3.23	0.0148
I9	Vacuum PA1	225.6	93.3	19.69	0.1489
I10	Vacuum PA2	312.8	176.7	7.33	0.0538
I11	LVGO	225.6	60.0	10.93	0.0660
I12	HVGO	312.8	82.2	10.29	0.0446
I13	Vacuum residue	376.7	176.7	61.39	0.3069

6.4 Heat exchanger network

The objective is to design a multi-period HEN with limited number of branches. As mentioned before, the penalty for limited number of branches is that the HEN requires higher utilities. The requirements and assumptions are the following:

- Each cold stream can be split into at most 2 branches.
- Each heat exchanger can handle variable heat loads.
- Each cold stream exchanges heat with a fixed set of hot streams in the same order in all operation periods.
- HEN should have the ability to handle different number of process streams in different period.

In the case of light crude processing, a preflash drum is used to flash off light ends to avoid two-phase flow in the preheat heat exchanger train. The preflash drum is bypassed in the case of heavy crude processing. Therefore, the light crude oil period has one more cold stream.

The classical transshipment model (Papoulias and Grossmann, 1983) uses one integer per pair of streams to determine the existence of a match. This leads to many streams transferring heat in the same interval and as a result, one cannot control splitting. Bagajewicz and Soto (2001b) used integers as in the original transshipment model, but they defined these integers in each interval. To count exchangers, they used a special set of constraints (Bagajewicz and Rodera, 1998).

Although the model presented by Bagajewicz and Soto (2001) renders good control of branching, the model forces the two periods to share the same matches *in the same intervals*. Figure 6.4 illustrates a cold stream C_1 matching with hot streams H_1 and H_2 in two periods. The two topologies are apparently the same, that is, C_1 received heat first from H_2 and then from H_1 . Only two heat exchangers are needed. However, the above model can not handle this situation because in the second interval, the constraint of single match in each interval is violated, even though the cold stream can cascade heat up.

This paper uses two independent sets of binary variables to count matches in each period separately. A constraint is then applied which requires both periods share the same topology. The topology is expressed in terms of matching patterns, which are defined in the following section.

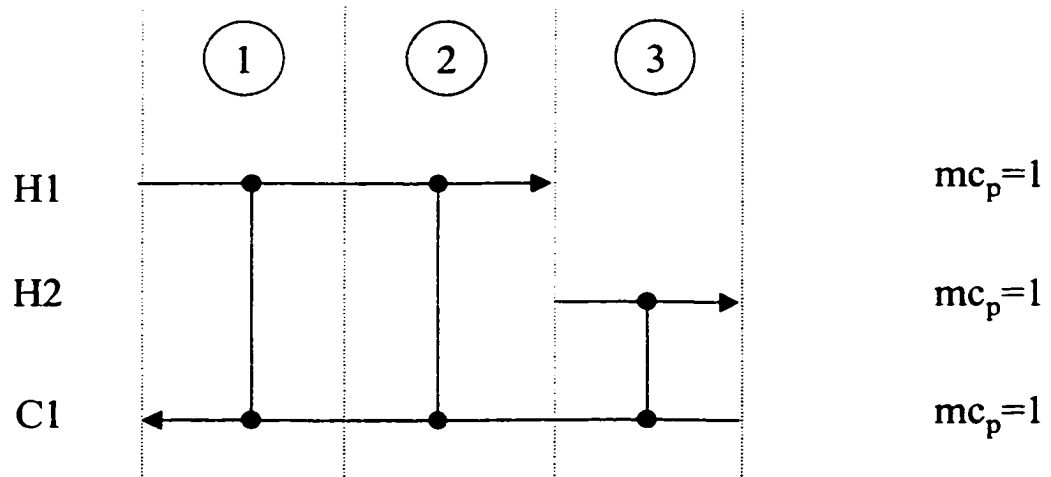
6.5 Stream matching pattern and its representation

Each cold stream is required to exchange heat with the same hot streams and in the same order in all operation periods. An algorithm to represent the matching pattern for each cold stream in each period is needed. Such representation should be unique for each match pattern and be *independent of the intervals*.

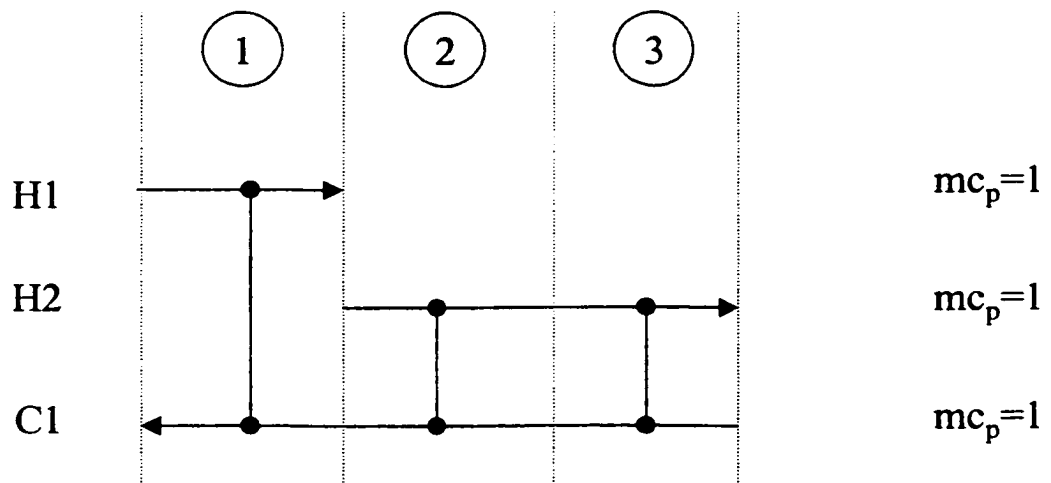
Bagajewicz and Rodera (1998) proposed to count heat exchangers using the following constraint.

$$K_{i,j,T} = \max(y_{i,j,T} - y_{i,j,T-1}, 0) \quad (6.1)$$

In this constraint, $y_{i,j,T}$ represents a match between hot stream i and cold stream j in interval T . This model count continuous matches as a single exchanger.



Period I



Period II

Figure 6.4 The above figures show the same matching sequence between C1 and hot streams H1 and H2.

Now, consider three hot streams H₁, H₂ and H₃ matching with cold stream J₁ as shown in Figure 5. A parameter a_i is associated to each hot stream.

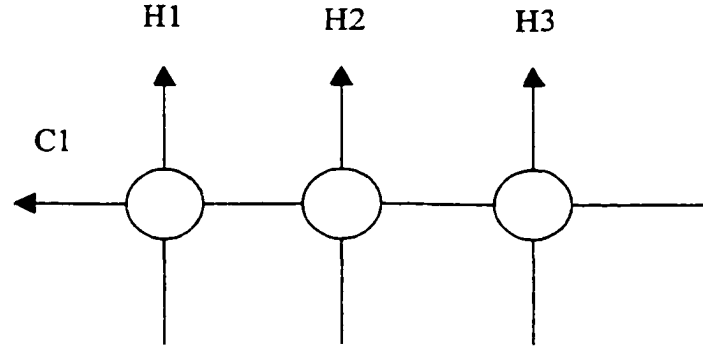


Figure 6.5 A cold stream matching with three hot streams

Next another parameter $PA_{j,T}$ is used to capture the information as to which hot stream matches with cold stream j in interval T .

$$PA_{j,T} = \sum_i K_{i,j,T} \cdot a_i \quad (6.2)$$

If there is no match in an interval T , then $PA_{j,T}$ equals to zero. Next, define an auxiliary variable $PB_{j,T}$ as follows:

$$PB_{j,T} = \max\{(PA_{j,T} \cdot C - \sum_{k \leq T-1} PA_{j,k}), 0\} \quad (6.3)$$

where C is a number large enough to ensure that $PB_{j,T}$ is non-negative. Further, define a matching pattern identification number (MPI_j) for a specific sequence of hot streams as follows:

$$MPI_j = \sum_T PB_{j,T} \quad (6.4)$$

Under certain choices of a_i , MPI_j is unique for each matching sequence. Table 6. 3 shows the details corresponding to an example where J_1 matches with 3 hot streams H_1 , H_2 and H_3 .

Table 6. 3 Parameters representing a matching pattern

	T1	T2	T3	T4	T5	T6
$K_{H_1, J_1, T}$	0	1	0	0	0	0
$K_{H_2, J_1, T}$	0	0	0	1	0	0
$K_{H_3, J_1, T}$	0	0	0	0	1	0
$PA_{J_1, T}$	0	a_{H_1}	0	a_{H_2}	a_{H_3}	0
$PB_{J_1, T}$	0	$a_{H_1} \cdot C$	0	$a_{H_2} \cdot C - a_{H_1}$	$a_{H_3} \cdot C - a_{H_2} - a_{H_1}$	0
MPI_j	$C \cdot \{a_{H_1} + a_{H_2} + a_{H_3}\} - 2 \cdot a_{H_1} - a_{H_2} = C - 2 \cdot a_{H_1} - a_{H_2}$					

The maximum operator in equation (3) can be represented in a linear form by using the following equivalent constraints (Bagajewicz and Manousiiothakis, 1992)

$$B = \text{Max}(A_1, A_2) \Leftrightarrow \begin{cases} A_1 + \lambda \Omega \geq B \\ B \geq A_1 \\ A_2 + (1 - \lambda) \Omega \geq B \\ B \geq A_2 \end{cases} \quad (6.5)$$

where λ is binary and Ω is a sufficiently large number.

For matches between cold stream j and N hot streams, the possible number of matching patterns can be computed as follows:

Parent pattern and children patterns

Suppose a matching pattern for a cold stream involves K hot streams in sequence. If a matching pattern is obtained by removing one or more hot streams without changing the order of the remaining hot streams, then the resulting pattern is called a child pattern. Figure 6.6 shows an example of a parent matching pattern and its six children patterns.

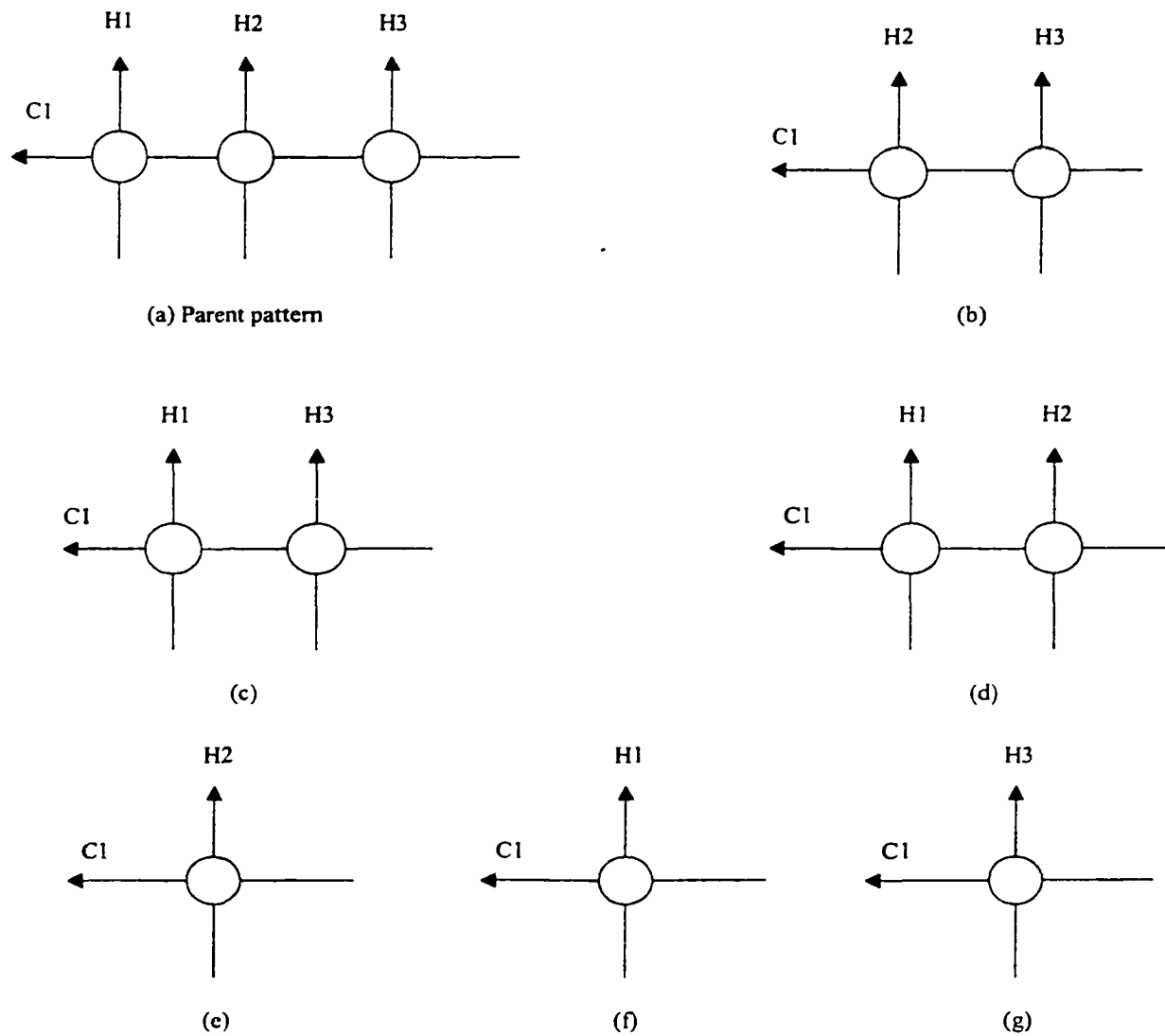


Figure 6.6 Parent pattern and its children patterns

Thus, for any given cold stream, the matching pattern for one period and has to be either identical or a parent pattern of the other periods.

Let $MP(N, m)$ represent the number of matching patterns for a cold stream to match with m hot streams which are picked from a hot stream pool of N hot streams.

Thus,

$$MP(N, m) = \frac{N!}{m!} \quad (6.6)$$

Let $CP(K, i)$ be the number of children patterns generated by removing i streams from a parent pattern with K hot streams. $CP(K, i)$ is given by:

$$CP(K, i) = \binom{K}{i} \quad (6.7)$$

Then the total number of children patterns CP , is

$$CP = \sum_{i=1}^{K-1} \binom{K}{i} \quad (6.8)$$

Conditions for a unique MPI

Consider a cold stream j matching sequentially with N hot streams $I_1, I_2, I_3, \dots, I_{N-1}, I_N$, from high temperature to low temperature. Therefore,

$$MPI_j = C \cdot \sum_{i=1}^N a_i - \sum_{j=1}^{N-1} (N-j) \cdot a_j \quad (6.9)$$

Different cases are now considered to infer the values of parameters a_i to make the sequence unique. Consider switching stream I_k and I_m ($k < m$).. Then,

$$MPI'_j - MPI_j = -(N-k) \cdot a_m - (N-m) \cdot a_k + (N-k) \cdot a_k + (N-m) \cdot a_m \quad (6.10)$$

where MPI'_j is the new pattern. After some manipulation, one obtains:

$$MPI'_j - MPI_j = (m - k) \cdot (a_k - a_m) \quad (6.11)$$

Thus, the condition for $MPI'_j = MPI_j$ is $a_k = a_m$.

Consider now altering the order of three arbitrary hot streams I_k, I_l and I_m ($k < l < m$) to a new order, say I_m, I_k, I_l , keeping the positions of the other matches unchanged. Then

$$MPI'_j - MPI_j = -(N - k) \cdot a_m - (N - l) \cdot a_k - (N - m) \cdot a_l + (N - k) \cdot a_k + (N - l) \cdot a_l + (N - m) \cdot a_m \quad (6.12)$$

Thus, the condition for $MPI'_j = MPI_j$ is:

$$a_m = \frac{(l - k) a_k + (m - l) a_l}{m - k} \quad (6.13)$$

In a similar fashion one can obtain the condition for $MPI'_j = MPI_j$ when 4 hot streams (I_x, I_y, I_z, I_u) are exchanged is:

$$a_m = \frac{i \cdot a_x + j \cdot a_y + k \cdot a_z + l \cdot a_u}{i + j + k + l} \quad (6.14)$$

where i, j, k, l are positive integers that represent differences between the exchanged positions. In view of the above, to make the value of MPI_j unique, parameters a_i should satisfy the following conditions

- Be positive.
- Be different.
- No parameter can be equal to the average of any other numbers of parameters.

Table 6. 4 lists parameters a_i used in this study. It has been chosen to make a_i as hot stream number plus a decimal number. The purpose of picking such values is to expedite data analysis.

Table 6. 4 Parameter a_i in this work

Stream	a_i	Stream	a_i
I1	1.21	I8	8.05
I2	2.03	I9	9.13
I3	3.27	I10	10.33
I4	4.53	I11	11.16
I5	5.04	I12	12.24
I6	6.07	I13	13.41
I7	7.31	S1	20

6.6 Multi-period model

In this paper, most of the constraints by Bagajewicz and Soto (2001) are used. However, instead of requiring the same matches interval by interval for different periods, the matching pattern constraints are used. Following, the sets, variables and constraints are listed.

Sets:

- Cold streams before splitting: JO
- Cold streams after splitting: J (including cooling water, which is placed at the last)

Subsets

JA=[J_1, J_2] J_1 and J_2 are two branches of JO1(crude before the desalter)

JB=[J_3, J_4] J_3 and J_4 are two branches of JO2 (crude after the desalter)

JC=[J_5, J_6] J_5 and J_6 are two branches of JO3 (crude after the preflash drum)

- Hot streams including furnace: H (furnace appears last)

H1 = {Kerosene, Diesel, AGO, Residue, Naphtha, Sour-Water, Condenser,
PA1, PA2, PA3}

- Intervals $T = \{T_0, T_1, \dots, T_N\}$

Variables:

Let $\theta(J)$ be split ratio of branch J. For each period, the following equations hold:

$$\sum_{JA} \theta(ja) = 1 \quad (6.15)$$

$$\sum_{JB} \theta(jb) = 1 \quad (6.16)$$

$$\sum_{JC} \theta(jc) = 1 \quad (6.17)$$

$$QC_{ia,t} = \theta_{ia} \cdot QCO_{io1,t} \quad (6.18)$$

$$QC_{jb,t} = \theta_{jb} \cdot QCO_{jo2,t} \quad (6.19)$$

Heat balance for hot streams:

$$R_{S,T} - R_{S,T-1} + \sum_j Q_{S,j,T} = HU_T \quad (6.20)$$

$$R_{i,T} - R_{i,T-1} + \sum_j Q_{i,j,T} - QH_{i,T} = 0 \quad (6.21)$$

Heat balance for cold streams:

$$\sum_i Q_{i,j,T} - QC_{j,T} = 0 \quad (6.22)$$

Upper bounds for heat exchange in interval T:

$$Q_{i,j,T} - y_{i,j,T} \cdot U_{i,j,T} \leq 0 \quad (6.23)$$

$$Q_{i,j,T} - \varepsilon_{i,j,T} \cdot y_{i,j,T} \leq 0 \quad (6.24)$$

$U_{i,j,T}$ and $\varepsilon_{i,j,T}$ are positive constants. For simplicity, the same value can be used for all i, j, T .

A cold branch can only match with one hot stream (except heating utility) in each interval.

$$\sum_{i \neq S} y_{i,j,T} \leq 1 \quad (6.25)$$

$$\begin{cases} K_{i,j,T} \geq y_{i,j,T} - y_{i,j,T-1} & T > T_1 \\ K_{i,j,T_1} = y_{i,j,T_1} \end{cases} \quad (6.26)$$

In this constraint, $K_{i,j,T}$ is a binary variable used to count heat exchangers. Note that $K_{i,j,T}$ can be one in a period even if the heat duty in that interval is zero. This stands for a heat exchanger that is in use in one period and idle in another period.

Bound on the number of heat exchangers:

$$\sum_{i,j,T} K_{i,j,T} \leq N \quad (6.27)$$

Equality of matching patterns:

$$MPI_j^I = MPI_j^{II} \quad (6.28)$$

To reduce computational time, this problem is decomposed into two subproblems: design above and design below the preflash drum temperature level. The objective function for the subproblem above the preflash drum is to minimize the heating utility. The number of exchangers N is initially given a large number, say 50, and reduced step-by-step until the utility consumption starts to increase. In addition, in this subproblem residue heats in the last interval can be non-zero, allowing in this way to cascade down

heat to the other subproblem. As no heating utility is required below the preflash drum, the number of heat exchangers below the preflash drum is minimized.

6.7 Results and Discussion

Because the heavy crude bypasses the preflash drum, there is one less cold streams in the heavy crude period than in the light crude period. In order to make the number of cold streams the same, the heavy crude is regarded as going through a dummy preflash drum. This dummy preflash drum has neither temperature constraint nor vapor effluent. By doing so, the heavy crude (after the desalter and before the furnace) is divided into two segments: before and after the preflash drum (Figure 6.7).

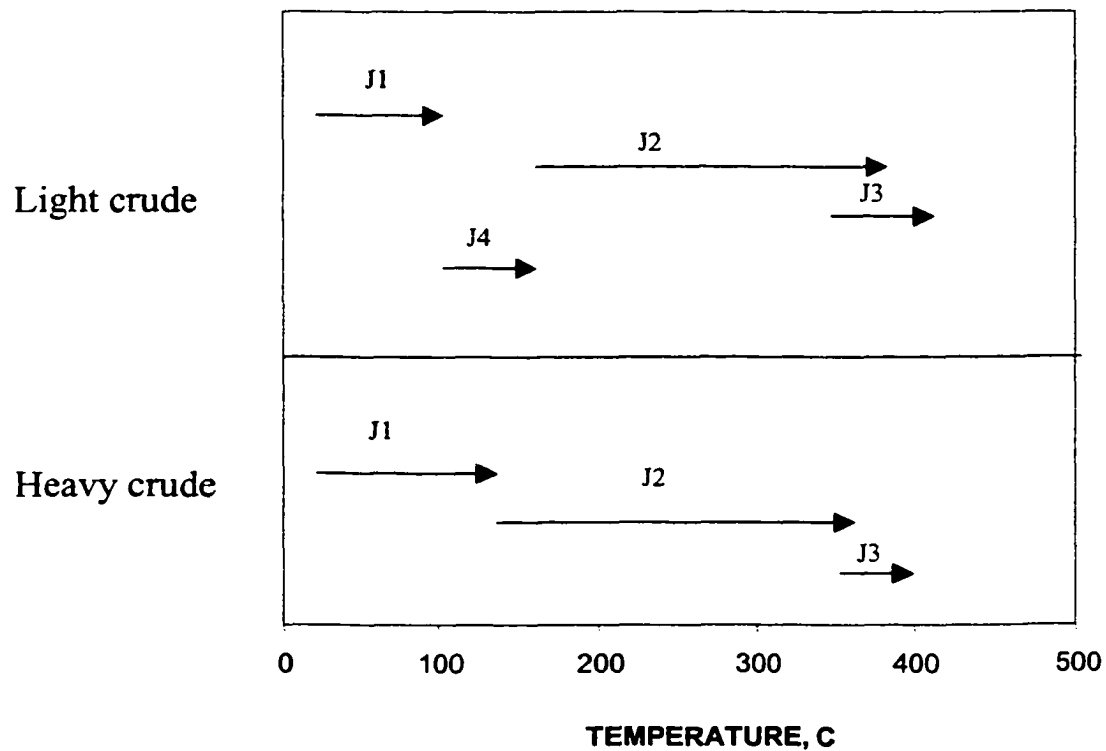


Figure 6.7 The starting and targeting temperatures of colds streams in two periods

Using the original intervals, heating utility would be required below the preflash drum for the heavy crude. Table 6. 5 shows the interval heat balances. Although the heat balance for interval T₁ is positive, cold stream C₄ has to split into at least 3 branches in order to meet its heat demand.

Table 6. 5 Heat balance for the heavy crude in the first interval below the preflash drum

	Interval T1 MW	Heat cascaded from design above the preflash drum, MW
C1	0.00	0.00
C4	24.20	0.00
I1	0.00	0.00
I2	0.00	0.00
I3	0.00	0.00
I4	6.28	0.00
I5	1.79	1.79
I6	1.05	0.00
I7	4.56	2.57
I8	1.51	0.79
I9	7.31	0.03
I10	6.03	3.40
I11	3.26	0.03
I12	3.56	1.38
I13	15.01	0.00
Interval heat from hot streams	26.16	

Table 6. 6 compares the targeted furnace duty and the actual duty. The duties for both the light crude and the heavy crude increase as expected. There are 8 exchangers (including the furnace) above the preflash drum and 17 exchangers below, totaling 31 exchangers. In the light crude period, hot streams H1, H6, H7, H8 and H11 are not used. Some of these streams are hot enough to heat the crude above the pinch.

Table 6. 5 Comparison of targeted furnace duty and actual furnace duty

	Light crude	Heavy crude
Targeted furnace duty, MW	68.02	57.26
Actual furnace duty, MW	71.55	57.94

HRAT/EMAT=33.3 °C/22.2 °C

However, they are not selected before in the same temperature interval there are other hot streams with larger heat capacities. As the cold streams are limited to split into two branches, the model picks two hot streams with the largest heat capacities. These streams cannot be used below the desalter because the heat from the condenser is enough to heat the crude. The situation changes with the heavy crude, where the aforementioned hot streams are used to heat the crude below the desalter, because the condenser heat is not enough (see Figure 6.3). The different heat supply scenarios below the desalter increase the complexity of the heat exchanger network. As shown in Figure 6.10, nine exchangers are required to heat the heavy crude, while only one is used for the light crude (Figure 6.10). The situation is similar to that found by Bagajewicz and Jose (2001) with the atmospheric distillation.

6.8 Conclusion

The paper addresses the design of a heat exchanger network for complete crude distillation plants. A multi-period heat exchanger network design model was proposed to handle two radically different crudes. In order to reduce the complexity of the heat exchanger network, an assumption is made that crude streams can be split to no more than two branches. This model also takes into account the flexibility of using preflash drum for the light crude only. Part of this multi-period model contains a topological constraint through which all periods share the same heat exchange “matching pattern” but not necessarily at the same temperature levels.

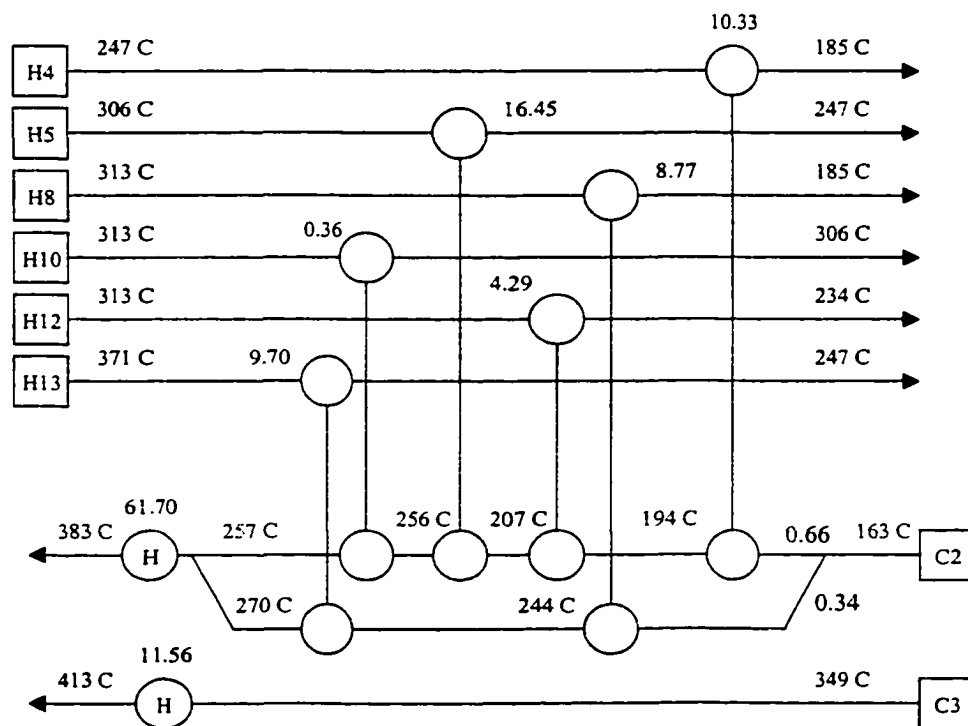


Figure 6.8 Heat exchanger network above the preflash drum for the light crude

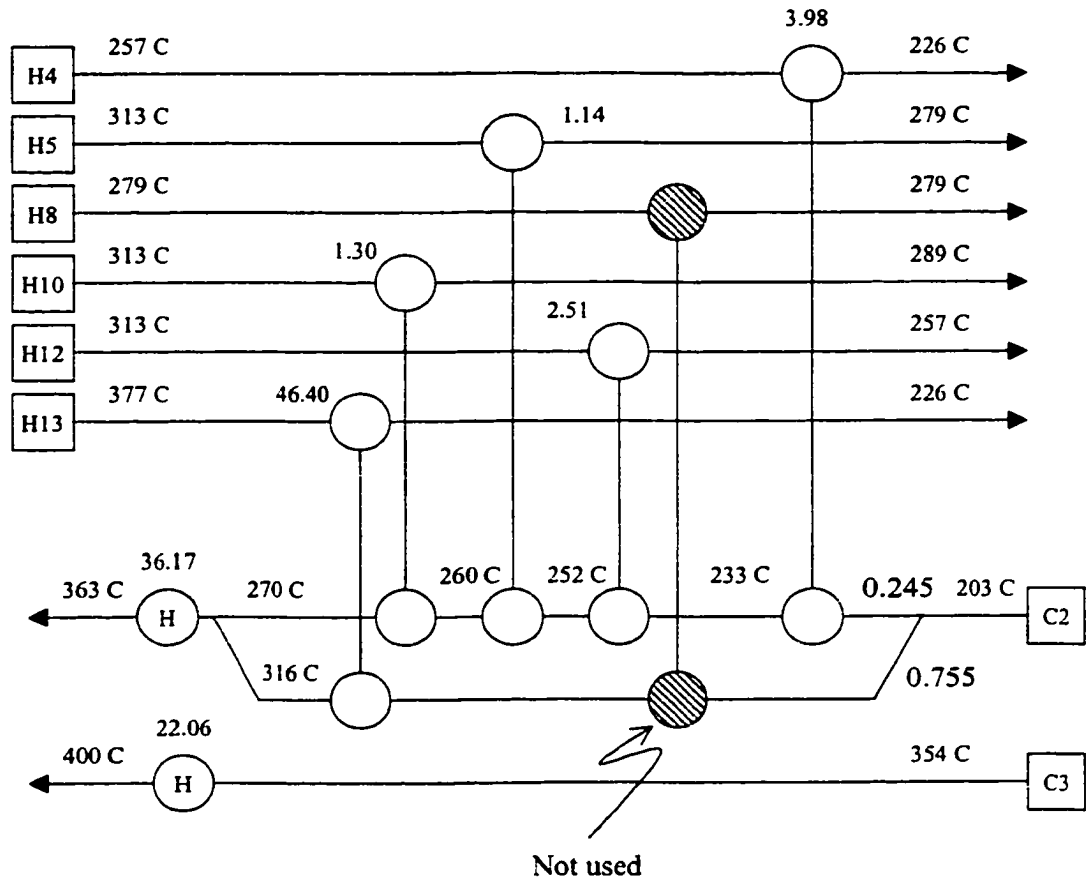


Figure 6.9 Heat exchanger network above the preflash drum for the heavy crude

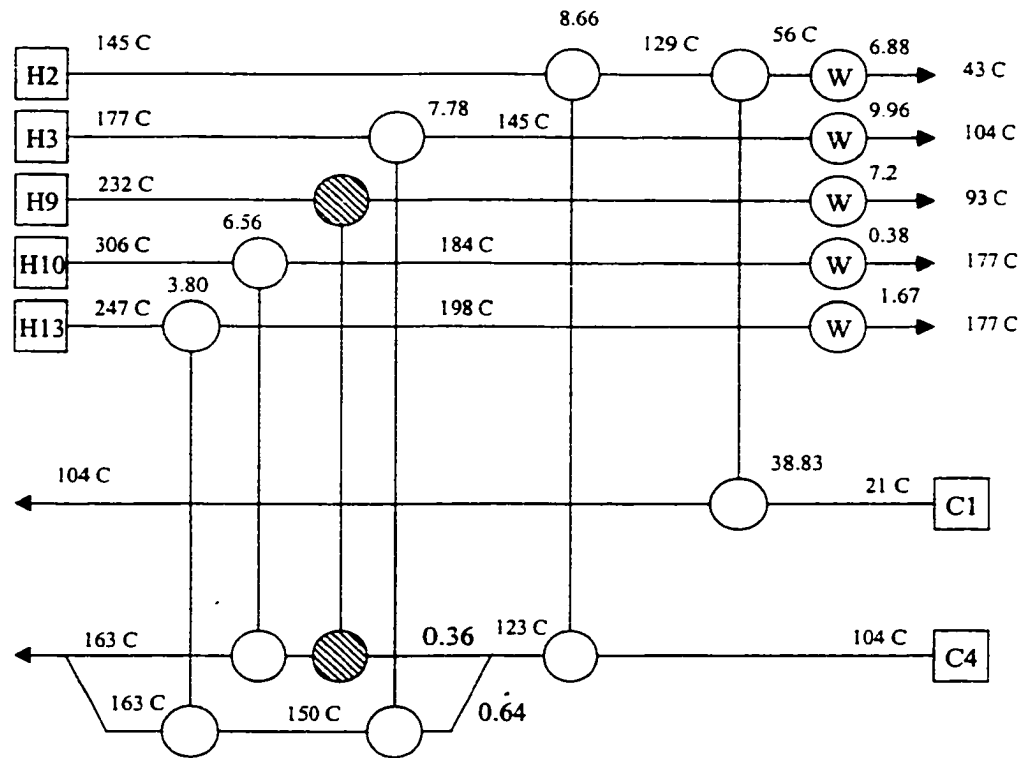


Figure 6.10 Heat exchanger network below the preflash drum for the light crude

(Coolers for H1, H6, H7, H8, H11 and H12 are not shown, idle exchangers on stream C1 can be found in Figure 6.9)

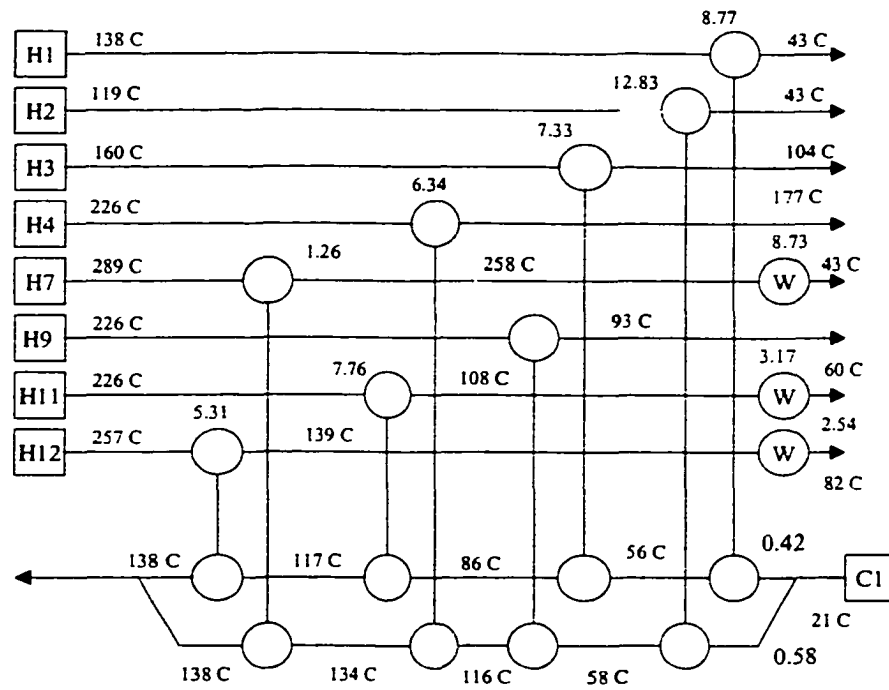


Figure 6.11 Heat exchanger network for heavy crude (C1) below the desalter

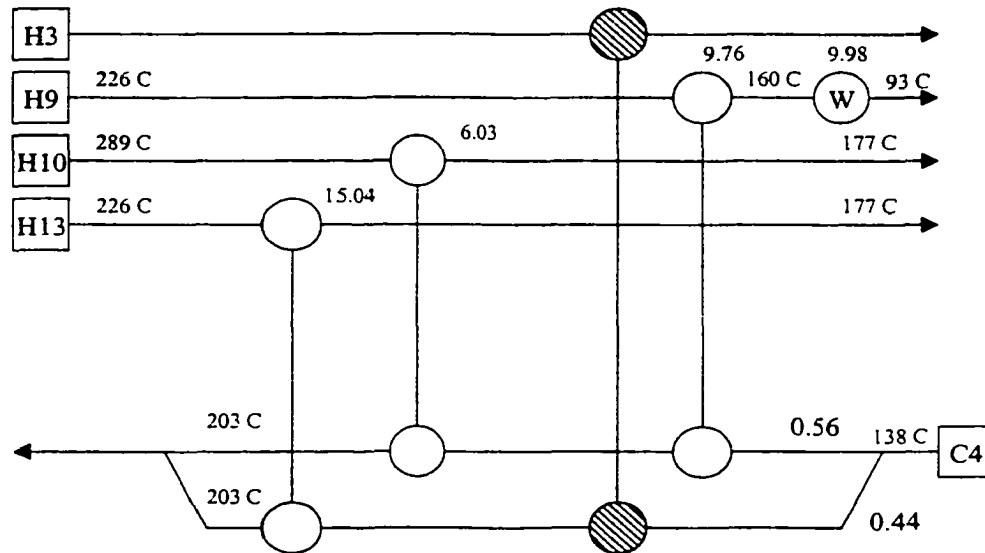


Figure 6.12 Heat exchanger network for heavy crude (C4) below the preflash drum

6.9 Nomenclature

$\varepsilon_{i,j,T}$ = positive number used in the logical inequality

$\theta(J)$ = split ratio of branch J

$CP(K, i)$ = the number of child patterns generated by removing i streams

E = total energy consumption

H_i^s = enthalpy of steam i

HU_T = heat from the hot utility in interval T

I = hot stream

J = cold stream

$MP(N, m)$ = the number of matching patterns

$K_{i,j,T}$ = variable used to count heat exchangers

$PA_{j,T}$ = parameter representing a match between a cold stream j and hot stream i in interval T

$PB_{j,T}$ = auxiliary variable for representing a heat exchange match pattern

$Q_{i,j,T}$ = heat transfer between hot stream i and cold stream j in interval T

$QH_{i,T}$ = heat available from hot stream i in interval T

$QC_{j,T}$ = heat demand for cold stream j in interval T

$Q_{S,j,T}$ = heat transfer between hot utility S and cold stream j in interval T

$R_{S,T}$ = residue heat of hot utility in interval T

$R_{i,T}$ = residue heat of hot stream i in interval T

T = interval

U = minimum heating utility

$U_{i,j,T}$ = positive number used in the logical inequality

$y_{i,j,T}$ = binary variable for heat transfer between stream i and cold stream j in interval T

6.10 References

1. Andrecovich, M., and Westerberg, A., A Simple Synthesis Method Based on Utility Bounding for Heat-integrated Distillation Sequences. *AIChE Journal*, 31(3), 363-375, (1985).
2. Bagajewicz M. and S. Ji. Rigorous Procedure for the Design of Conventional Atmospheric Crude Fractionation Units Part I: Targeting. *Industrial and Engineering Chemistry Research*. 40 (2), pp. 617-626 (2001).
3. Bagajewicz M. and J. Soto., Rigorous Procedure for the Design of Conventional Atmospheric Crude Fractionation Units Part II: Heat Exchanger Networks. *Industrial and Engineering Chemistry Research*. 40 (2), pp. 627-634 (2001a).
4. Bagajewicz M. and Soto. J., Rigorous Procedure for the Design of Conventional Atmospheric Crude Fractionation Units. Part III: Trade-Off between Complexity and Energy Savings. Submitted. *Industrial and Engineering Chemistry Research*.(2001b)
5. Bagajewicz, M., On the Design Flexibility of Crude Atmospheric Plants. *Chemical Engineering Communications*, 166, 111-136, (1998).
6. Bagajewicz, M. and Manousiouthakis, V. Mass/Heat-Exchange Network Representation of Distillation Networks. *AIChE Journal*, 38(11), 1769 (1992).

7. Bagajewicz M. and H. Rodera. *A New MILP Model For Heat/Mass Exchanger Networks Featuring Minimum Number Of Units*. AIChE Annual Meeting, Miami (1998).
8. Floudas, C. and Grossmann, I., Automatic generation of multiperiod heat exchanger network configurations, *Computers and Chemical Engineering*, 11(2), 123-142 (1987).
9. Floudas, C. and Grossmann, I., Synthesis of flexible heat exchanger networks for multiperiod operation, *Computers and Chemical Engineering*, 10 (1), 153-168(1986)
10. Golden, S., Prevent Pre-flash Drum Foaming, *Hydrocarbon Processing*, May 1997, pp141-153.
11. Gundersen T. and I. E. Grossmann, Improved Optimization Strategies for Automated Heat Exchanger Network Synthesis Through Physical Insights. *Comput. Chem. Engng.* 14, 9, pp. 925-944 (1990).
12. Ji, S. and Bagajewicz M., Rigorous targeting procedure for the design of crude fractionation units with pre-flashing or pre-fractionation, *IECR*, submitted.
13. Liebmann, K.; Dhole, V. R. Integrated Crude Distillation Design. *Comput. Chem. Eng.* 1995,19, S119.
14. Liebmann, K.; Dhole, V. R.; Jobson, M. Integration Design Of A Conventional Crude Oil Distillation Tower Using Pinch Analysis. *Institution of Chemical Engineers*, 1998, 76(3), part A, 335.
15. Nielsen, J., et al, Retrofit and optimization of industrial heat exchanger networks: a complete benchmark problem, *Computers and Chemical Engineering*, 21, S469-474 (1997).

16. Papalexandri K, et al, Heat integration aspects in a crude preheat refining section, *Computers and Chemical Engineering*, 22, S141-148, 1998.
17. Papalexandri, K. and Pistikopoulos, E., a multiperiod MINLP model for improving the flexibility of heat exchanger networks, *Computers and Chemical Engineering*, 17, S111-116 (1993).
18. Papalexandri, K. and Pistikopoulos, E., a multiperiod MINLP model for the synthesis of flexible heat and mass exchange networks, *Computers and Chemical Engineering*, 18(11-12), 1125-1139, 1994.
19. Papoulias S. and I. E. Grossmann. *A Structural Optimization Approach in Process Synthesis-II: Heat Recovery Networks*. *Comput. Chem. Engng.* 7, 707 (1983).
20. Sharma, R.; Jindal, A.; Mandawala, D.; Jana, S. K. Design/Retrofit targets of Pump-around Refluxes for Better Energy Integration of a Crude Distillation Column. *Ind. Eng. Chem. Res.* 1999, 38, 2411.
21. Soto, J., Multipurpose heat exchanger network for maximum energy efficiency of crude fractionation units, Master Thesis, University of Oklahoma, 2000.
22. Stichlmair, J.G, and Fair J. R, *Distillation Principles and Practices*, Wiley-VCH, New York, 1998.p76.
23. Terranova, B., and Westerberg, A., Temperature-Heat Diagrams for Complex Columns. 1. Intercooled/Interheated Distillation Columns. *Ind. Eng. Chem. Res.* 28, 1374-1379, (1989).

Chapter 7 New Flowsheets for Crude Distillation

7.1 Introduction

In previous chapters, systematic methods were presented and applied to crude distillation design. Rigorous procedures were proposed for the design of both the atmospheric plant and the complete plant. The procedures take into account the flexibility of processing different crudes year around. In addition, the role of light components in crude fractionation known as the carrier effect or the carrier design was first given a rigorous definition. In view of this, two typical design alternatives, the preflashing design and the stripping-type design were analyzed focusing on energy efficiency and compared to the conventional design.

In addressing the aforementioned methods, a multi-period heat exchanger network design model (Chapter 6) was proposed to handle two radically different crudes --- a light crude and a heavy crude. Part of this multi-period model contains a topological constraint through which all periods share the same heat exchange “matching pattern” but not necessarily at the same temperature levels.

This chapter explores possible new flowsheets for future study. Two tools are used: the heat demand-supply diagram and distillation sequencing.

7.2 Use of the heat demand-supply diagram

The heat demand-supply diagram provides a straightforward view of the energy recovery scenario. Figure 7.1 shows the diagram for the conventional atmospheric crude

distillation. Efforts on reduction of energy consumption should be made in the following two directions:

- Increase the quantity or quality of the heat supply
- Decrease the quantity or quality of the heat demand

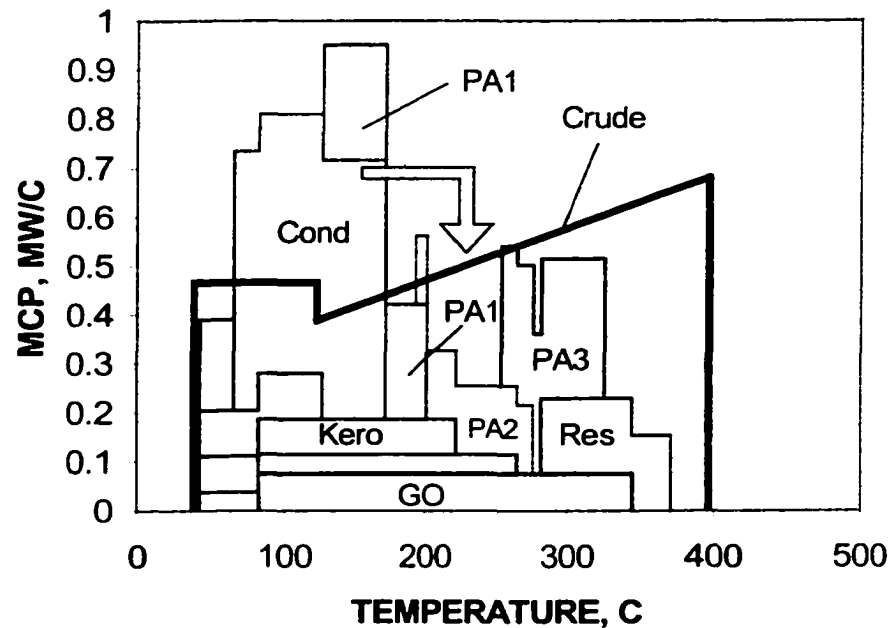


Figure 7.1 Atmospheric Distillation (light crude oil, $\Delta T_{\min} = 22.2 \text{ }^{\circ}\text{C}$)

The properties of the crude can be found in Tables 2.1, 2.2 and 2.3.

Cond: condenser. Kero: kerosene. GO: gas oil. Res: residue. PA: pump-around.

The first case was discussed in Chapter 3. In the second case, one wants to vary the heating pattern of the crude, as in the case of the preflash design. In trying to obtain an alternative, focus is shifted to the utilization of heat from the condenser. The major hurdle preventing the use of the condenser heat is its low temperature level. The most

convenient way to overcome this hurdle is to shift heat from condenser to the pump-arounds (Bagajewicz, 1998, Bagajewicz and Ji, 2001). However, this effort is limited by material and heat balance. Specifically, as heat is shifted, the liquid flowrate in the tray above the pump-around is reduced. When this reaches zero, the maximum transferable heat is also reached. Now ways to break this limit are explored.

One way to shift the condenser heat to higher temperatures is by using a heat pump (Figure 7.2).

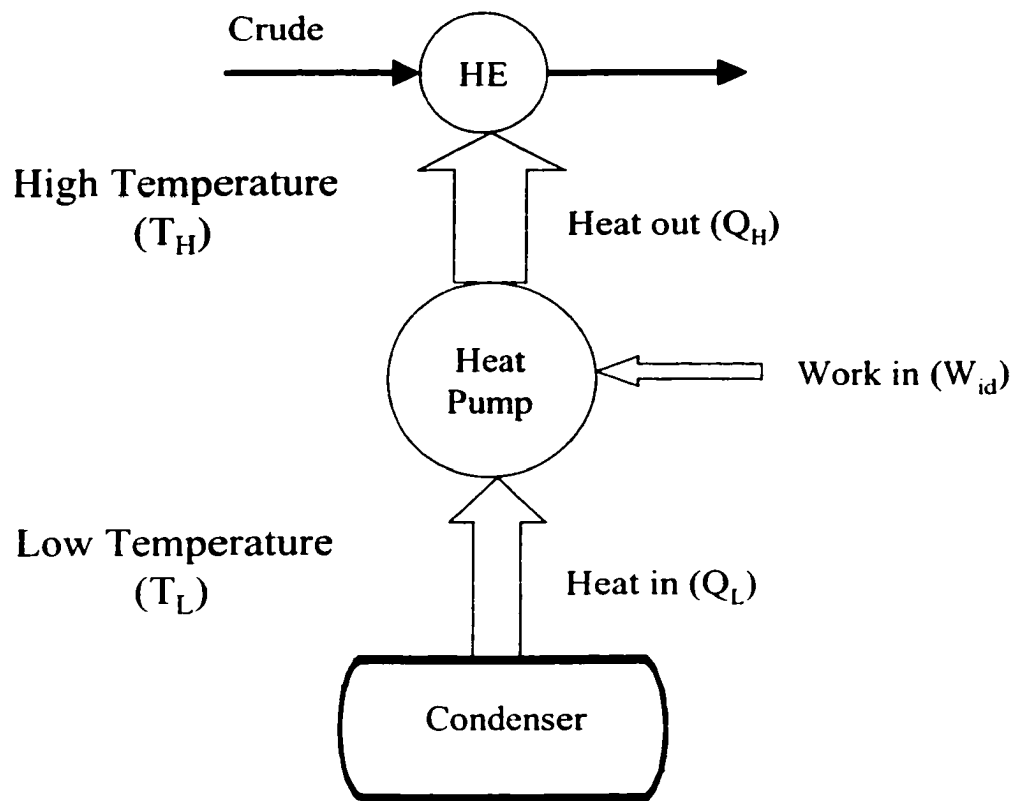


Figure 7.2 Reducing heat consumption using heat pump

This alternative does not alter the operating conditions of the column, but is expensive. Table 7. 1 shows the relative cost for shifting heat from the condenser and

PA1 to the targeted region (Figure 7.3). Note that the heat is transferred through the pinch.

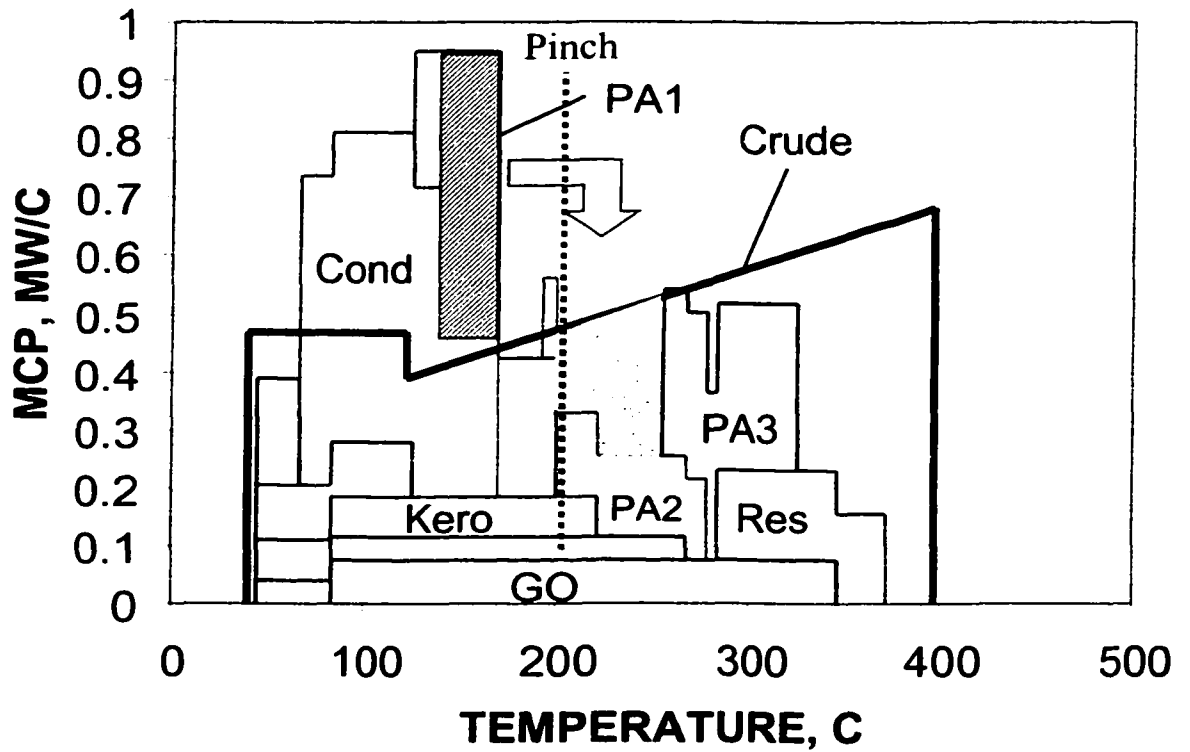


Figure 7.3 Shifting heat to a high temperature region using heat pump

The properties of the crude can be found in Tables 2.1, 2.2 and 2.3.

The pinch location is shown by a dash line

In order to estimate the cost, the electricity consumption needs to be estimated. The theoretical minimal work (ideal work) needed for transferring the heat can be computed using equation (1):

$$W_{id} = Q_H \left(1 - \frac{T_L}{T_H}\right) \quad (7.1)$$

where W_{id} is the amount of ideal work consumed

T_L is the source temperature at which the heat pump extracts heat.

T_H is the target temperature at which the heat pump discharges heat.

Q_H is the amount of heat the heat pump provides at T_H .

The actual electricity consumption can be computed by equation (2).

$$W_r = W_{id} \cdot \eta \quad (7.2)$$

where

W_r is the actual (real) work consumption.

η is the heat pump efficiency.

In Figure 7.1, it is intended to transfer 13.25 MW heat from the condenser through the pinch. The temperature range of the heat available is 144.1 –170.6 °C (417.3-443.7 °K) and the targeted temperature range is 201.5-254.4 °C (474.7-527.6 °K). Assume two heat pumps are used, each transferring 6.625 MW heat from the condenser. The first heat pump operates between 144.1 C and 227.9 C, and the second heat pump operates between 157.4 C and 254.4 C. The heat pumps have an efficiency of 60% (Table 7.1). Based on the prices provided by Douglas (1988, fuel \$4.00/MMbtu, electricity \$0.04/kwhr), the annual saving in operating cost is \$245,406 per year.

Table 7. 1 Relative operation cost for shifting heat to the targeted region

	Heat pump A	Heat pump B
T_H , K	501.1	527.6
T_L , K (condenser)	417.3	430.5
W_{id}/Q_H	0.17	0.18
Heat pump efficiency	0.60	0.60
W_r/Q_H	0.28	0.31
Q_L , MW	6.625	6.625
Q_H , MW	7.96	8.12
W_r , MW	2.22	2.49
Annual savings in fuel*, \$	859733	877357
Annual cost for the electricity, \$	702785	788899
Net annual savings, \$	156947	88458

* 330 days/year

** fuel \$4.00/MMbtu, electricity \$0.04/kwhr

7.3 Distillation sequencing

Distillation sequencing is another useful tool for developing new design schemes. The problem of crude distillation can be viewed as to be similar to separating 5 components. The conventional design is virtually an indirect sequence, as it is shown in Figure 7.4. The bottom parts of columns 1, 2 and 3 correspond to the side strippers in the conventional design (Figure 7.5). The stripping-type design is a direct sequence (Figures 7.6 and 7.7).

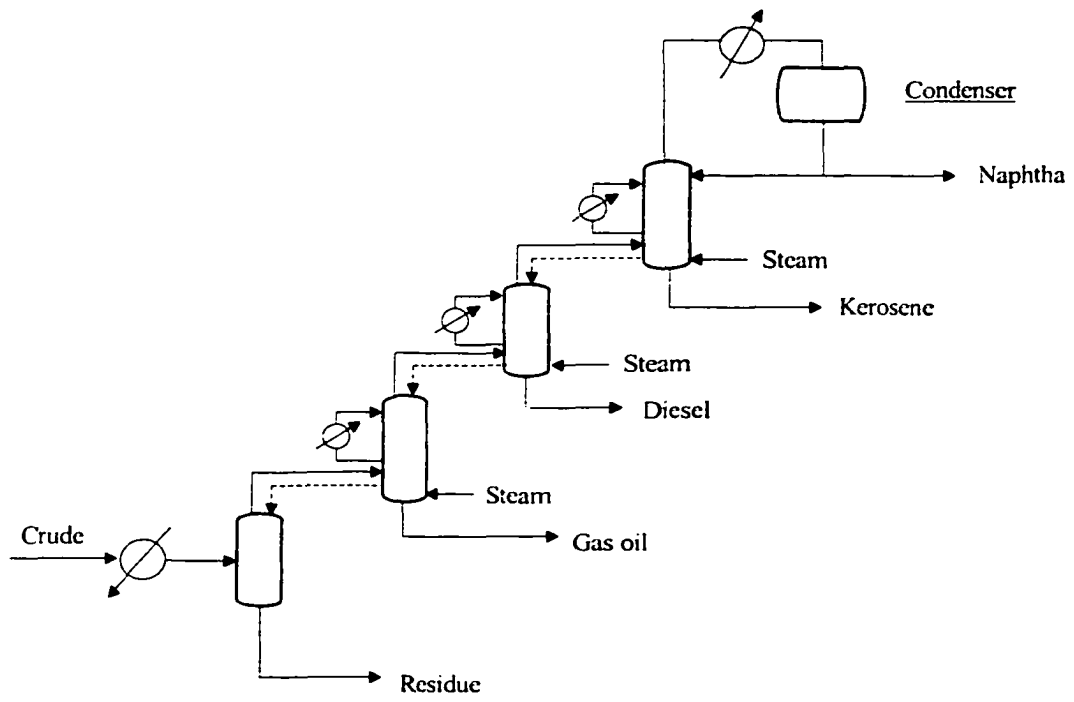


Figure 7.4 Indirect sequence

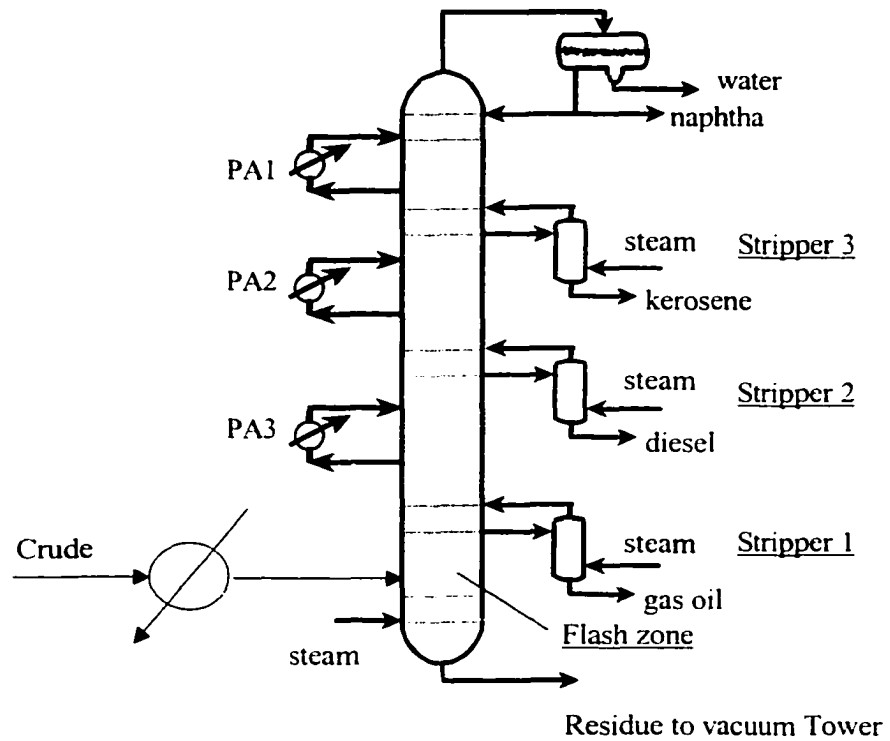


Figure 7.5 Conventional design

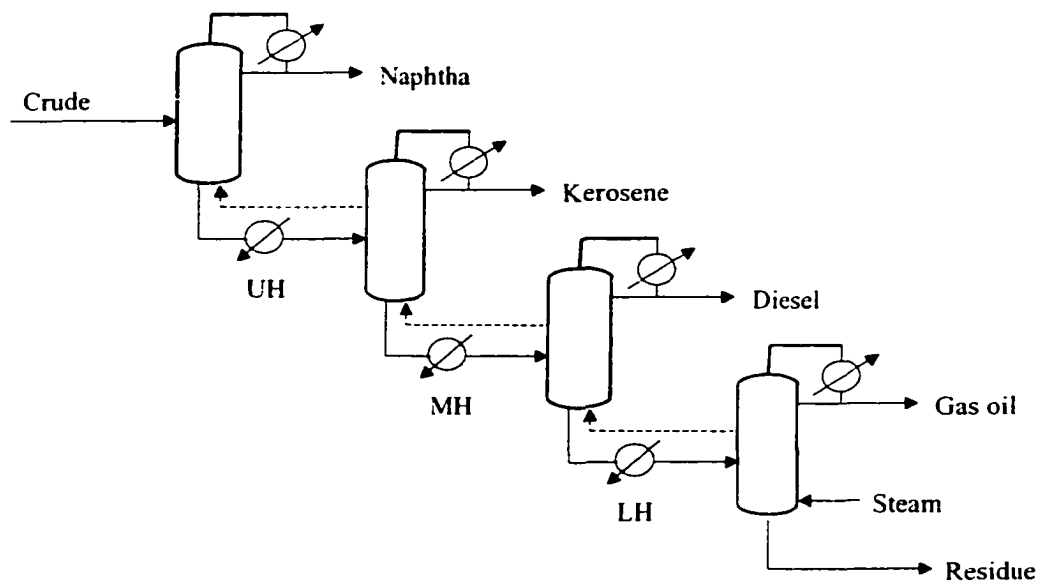


Figure 7.6 Direct sequence

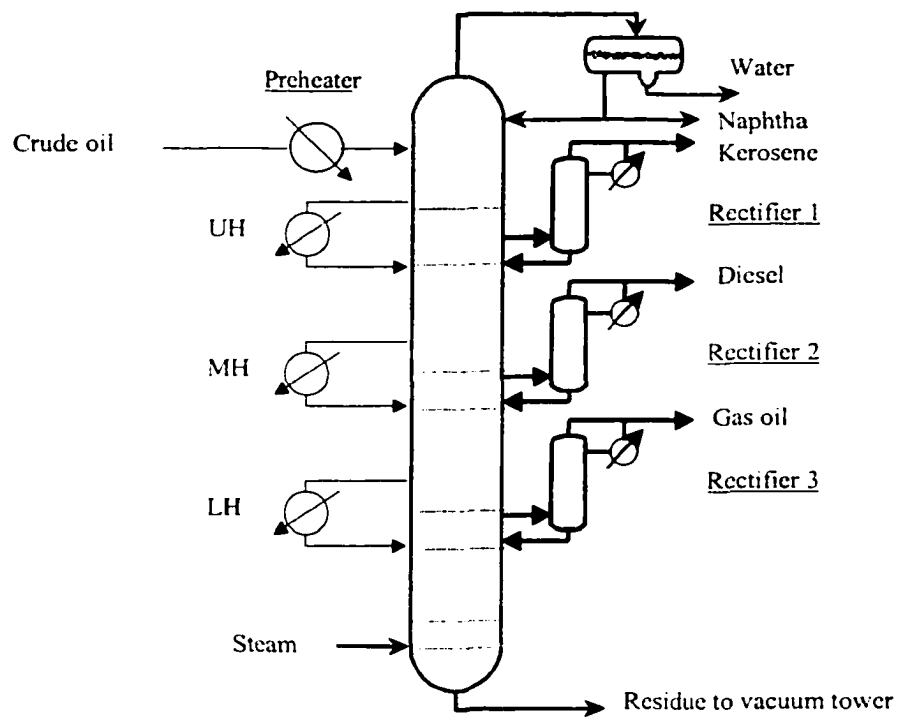


Figure 7.7 Stripping-type design

Preflashing and Prefractionation designs are other sequences (Figure 7.8, 9). Note that in the preflash design the sloppy separation of the first flash produces a top vapor that needs further separation. In this regard, this scheme departs from the traditional sharp sequence proposed as framework for the analysis. The complete list of possible sequences is depicted in Figure 7.10.

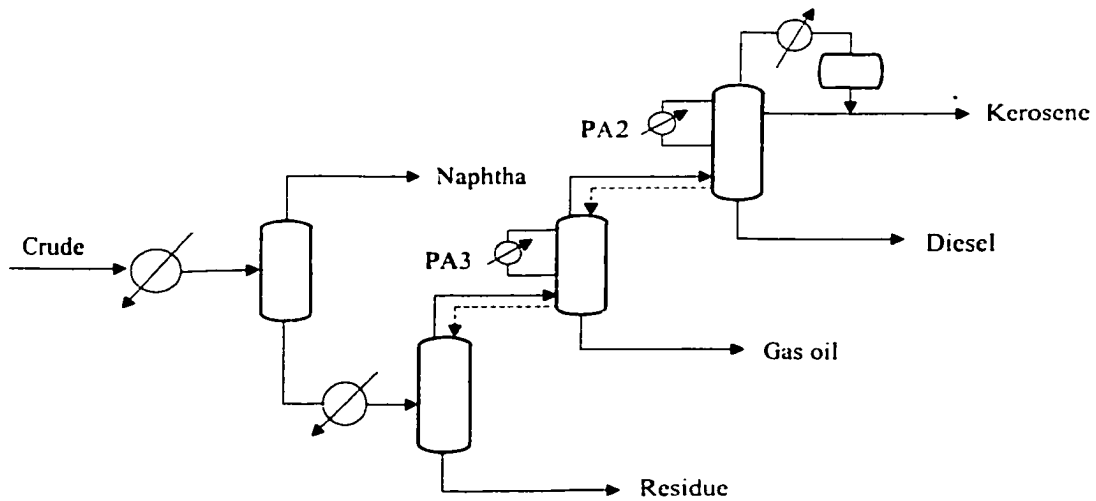


Figure 7.8 Prefractionation design

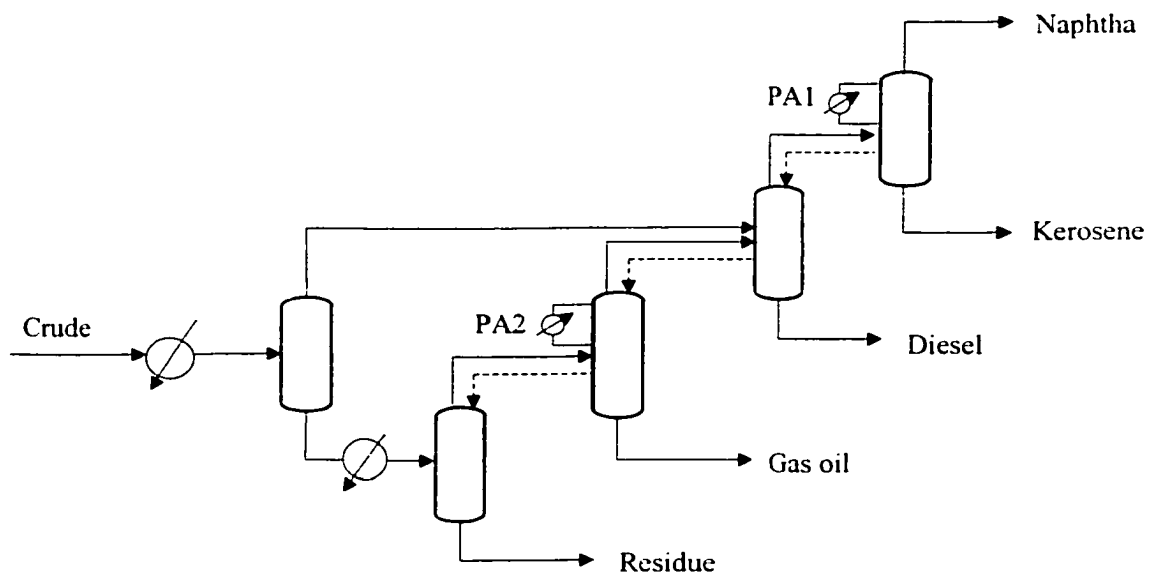


Figure 7.9 Preflashing design

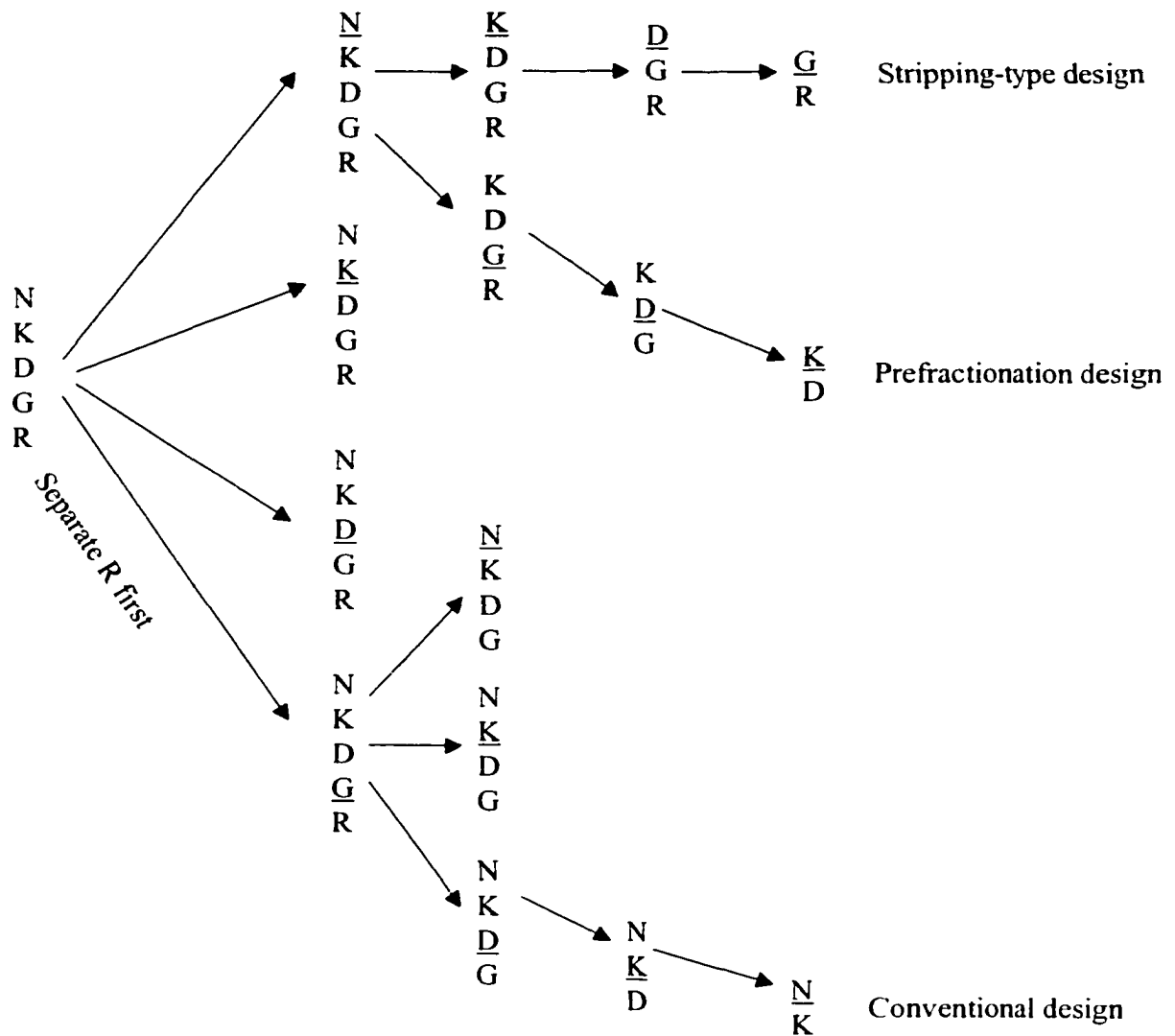


Figure 7.10 Distillation sequences for crude separation

N-naphtha, K-kerosene, D-diesel, G- gas oil, R-residue.

In screening the potential sequence, one has to take account of the following constraints

1. The maximal allowable temperature
2. The allowable residue yield

3. Non-sharp split between distillates

These constraints can be used to eliminate some sequence. For example, the first and the second constraints exclude the stripping-type design. A previous study (Ji and Bagajewicz, 2001) shows that early separation of stripping components increases the yield of the residue, which is not a desired effect. The stripping components include all compounds in naphtha and kerosene as well as some components in diesel. Therefore, the residue has to be separated first in order to maintain the stripping effect as in the bottom branch which eventually leads to the conventional design but renders others too. The remaining sequences are meaningful and deserve to be explored.

7.4 Vacuum distillation

Vacuum distillation is used to vaporize those components that cannot be flashed using atmospheric pressure. The current crude vacuum distillation only uses one column operating at about 10 mmHg. Because the vacuum jet steam consumption increases with the decrease of the distillation pressure, it is natural to think about an alternative of using two vacuum towers, one operating at low vacuum, say 100 mmHg, and the other operating at 10 mmHg (Figure 7.11). If a significant amount of vacuum gas oils can be at the low-vacuum tower, the feed to the second vacuum tower can be reduced and accordingly the total vacuum jet steam will be reduced. The disadvantage is the extra investment cost of the low-vacuum tower. Hopefully, the cost is not high. As the vapor volume is inversely proportional to the operating pressure, the diameter of the low-vacuum tower will be only one tenth of the 10 mmHg tower.

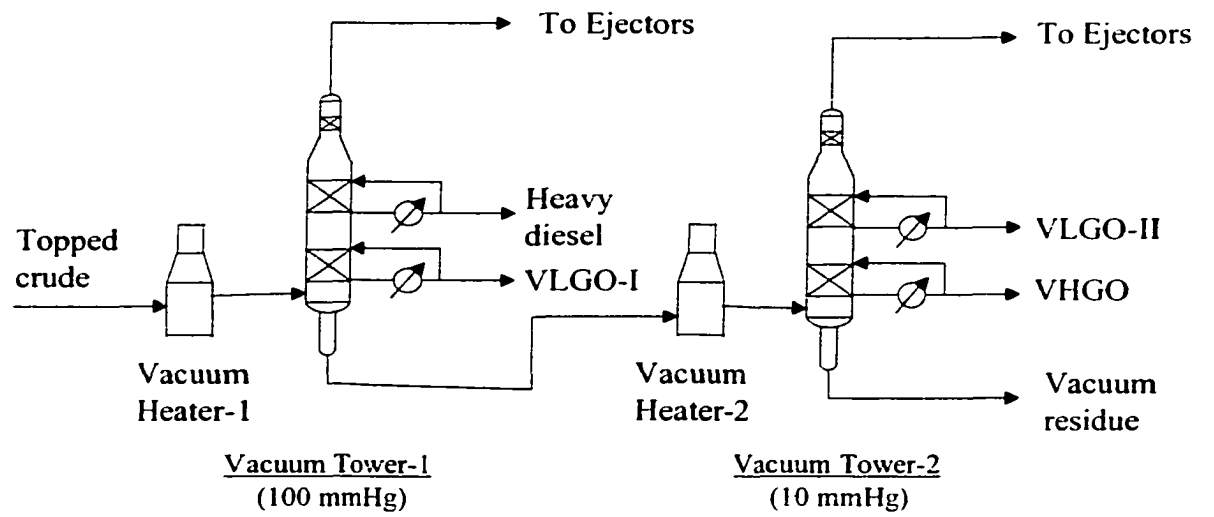


Figure 7.11 Vacuum distillation with two towers

Other separation technologies, such as membrane separation, could be incorporated with distillation. This is part of the future work.

7.5 References

1. Bagajewicz, M. On the Design Flexibility of Crude Atmospheric Plants. *Chemical Engineering Communications*. 1998, 166, 111.
2. Bagajewicz M. and S. Ji. Rigorous Procedure for the Design of Conventional Atmospheric Crude Fractionation Units Part I: Targeting. *Industrial and Engineering Chemistry Research*. 40 (2), pp. 617-626 (2001).
3. Douglas, J. M., *Conceptual design of chemical processes*, p569, McGraw-Hill, 1988.
4. Ji Shuncheng and Bagajewicz, M., Rigorous targeting procedure for the design of crude fractionation units with pre-flashing or pre-fractionation, *Industrial and Engineering Chemistry Research*. Submitted.
5. Liebmann, K., and Dhole, V. R., Integrated Crude Distillation Design. *Computers & Chemical Engineering*, 19, Supplement, S119, (1995)
6. Stichlmair, J.G, and Fair J. R, *Distillation Principles and Practices*, Wiley-VCH, New York, 1998.